

# The climate and vegetation of Europe, North Africa and the Middle East during the Last Glacial Maximum (21,000 years BP) based on pollen data

Basil A.S. Davis<sup>1</sup>, Marc Fasel<sup>2</sup>, Jed O. Kaplan<sup>3</sup>, Emmanuele Russo<sup>4</sup>, Ariane Burke<sup>5</sup>

<sup>1</sup>Institute of Earth Surface Dynamics, University of Lausanne, Lausanne, 1015, Switzerland

<sup>2</sup>enviroSPACE lab, Institute for Environmental Sciences, University of Geneva, Geneva, 1211, Switzerland

<sup>3</sup>Department of Earth Sciences, The University of Hong Kong, Hong Kong, Peoples Republic of China

<sup>4</sup>Department of Environmental Systems Science, ETH Zurich, Zurich, 8092, Switzerland

<sup>5</sup>Laboratoire d'Ecomorphologie et de Paleoanthropologie, Departement d'Anthropologie, Universite de Montreal, Montreal, Quebec, H3C 3J7, Canada

*Correspondence to:* Basil A. S. Davis ([basil.davis@unil.ch](mailto:basil.davis@unil.ch))

**Abstract.** Pollen data represents one of the most widely available and spatially-resolved sources of information about the past land cover and climate of the Last Glacial Maximum (21,000 years BP). Previous pollen data compilations for Europe, the Mediterranean and the Middle East however have been limited by small numbers of sites and poor dating control. Here we present a new compilation of pollen data from the region that improves on both the number of sites (63) and the quality of the chronological control. Data has been sourced from both public data archives and published (digitized) diagrams. Analysis is presented based on a standardized pollen taxonomy and sum, with maps shown for the major pollen taxa, biomes and total arboreal pollen, as well as quantitative reconstructions of forest cover and winter, summer and annual temperatures and precipitation. The reconstructions are based on the modern analogue technique (MAT) with a modern pollen dataset taken from the latest Eurasian Modern Pollen Database (~8000 samples). A site-by-site comparison of MAT and Inverse Modelling methods shows little or no significant difference between the methods for the LGM, indicating that no-modern-analogue and low CO<sub>2</sub> conditions during the LGM do not appear to have had a major effect on MAT transfer function performance. Previous pollen-based climate reconstructions using modern pollen datasets show a much colder and drier climate for the LGM than both Inverse Modelling and climate model simulations, but our new results suggest much greater agreement. Differences between our latest MAT reconstruction and those in earlier studies can be largely attributed to bias in the small modern dataset previously used. We also find that quantitative forest cover reconstructions show more forest than that previously suggested by biome reconstructions, but less forest than that suggested by simple percentage arboreal pollen, although uncertainties remain large. Overall, we find that LGM climatic cooling/drying was significantly greater in winter than in summer, but with large site to site variance that emphasizes the importance of topography and other local factors in controlling the climate and vegetation of the LGM.

## 44 **1 Introduction**

45

46 During the Last Glacial Maximum (LGM) ~21,000 years BP (Mix et al., 2001), the climate,  
47 vegetation and landscape of Europe and its surrounding regions were very different than  
48 today. Scandinavia and a large part of the British Isles were covered by a single ice sheet,  
49 with separate ice sheets covering the Alps and Pyrenees, while many smaller and lower  
50 mountainous areas were also glaciated (Ehlers et al. 2011). As a result of this global build-up  
51 of ice on land, sea levels were around 120 meters lower than today, resulting in the retreat of  
52 Atlantic and Mediterranean coastlines and the emergence on land of the English Channel and  
53 North Sea basin. Falling sea levels also led to the disconnection of the Black Sea from the  
54 Mediterranean, and a subsequent drop in Black Sea water levels as evaporation exceeded  
55 inflow (Arslanov et al. 2007). On land, permafrost and periglacial processes occurred  
56 immediately to the south of the Scandinavian ice sheet, while the massive discharge of glacial  
57 clays and sands provided material to be redeposited by the wind as belts of loess across  
58 northern France, Benelux, Germany and central Europe (Lehmkuhl et al. 2021). Under these  
59 cooler and drier climatic conditions, forests are thought to have retreated to the relative  
60 shelter of Southern Europe and the Mediterranean, while relatively unproductive steppe and  
61 tundra dominated the region north of the Alps (Grichuk 1992).

62

63 This traditional view of the LGM has been established for many years, but many details  
64 concerning the climate and vegetation of the LGM remain debated. Much of this debate  
65 concerns information derived from the pollen record, which represents one of the most  
66 widely available and spatially-resolved sources of information concerning LGM vegetation  
67 and climate, and the primary terrestrial proxy used to evaluate climate models in the  
68 Palaeoclimate Modelling Intercomparison Project (PMIP) (Bartlein et al., 2011; Harrison et  
69 al., 2014).

70

71 For example, climate model simulations continue to indicate a climate that is less cold and  
72 more humid than pollen-based reconstructions (Jost et al., 2005). These results are similar to  
73 reconstructions based on glaciological modelling (Allen et al., 2008b). On the other hand, the  
74 pollen-based reconstructions that show the greatest disagreement with climate models have  
75 themselves been criticized for not considering the possible effect of low atmospheric CO<sub>2</sub> on  
76 the physiological relationship between plants and climate (Ramstein et al., 2007). Methods  
77 that use modern pollen samples are based on the assumption that the relationship between  
78 vegetation and climate remains the same through time, and that this is independent of change  
79 in CO<sub>2</sub> concentration. Studies have shown however that plant growth processes and plant  
80 resilience are sensitive to CO<sub>2</sub> concentration, and particularly water-use efficiency which  
81 would make plants more drought sensitive in low CO<sub>2</sub> environments (Cowling & Sykes  
82 1999). Atmospheric CO<sub>2</sub> during the LGM was around 190 ppm, some 100 ppm lower than  
83 the pre-industrial period, and 200 ppm lower than the levels experienced in the last 50 years.  
84 Concerns about the effects of lower CO<sub>2</sub> during the LGM has directly led to the development  
85 of pollen-climate reconstruction methods that can take account of CO<sub>2</sub> effects, either through  
86 use of a process-based vegetation model run in inverse mode (Guiot et al. 2000, Guiot et al.  
87 2009), or through the use of a correction algorithm (Prentice et al. 2017). Pollen-climate  
88 reconstructions based on inverse modelling that account for these low CO<sub>2</sub> effects show less  
89 cooling and drying and consequently greater agreement with climate models (Ramstein et al.,  
90 2007; Wu et al., 2007).

91

92 Further data-model discrepancies have also been highlighted concerning LGM vegetation  
93 cover. Earlier pollen synthesis studies, especially those that applied the biomisation method

94 (Elenga et al., 2000) give the impression that non-glaciated areas of LGM Europe were  
95 dominated by treeless steppe, while vegetation models driven by climate model simulations  
96 indicate large areas of forest and woodlands (Binney et al., 2017; Kaplan et al., 2016;  
97 Velasquez et al., 2021). The apparent data-model discrepancy associated with steppe has led  
98 to the suggestion that early humans, which are not included in vegetation models, could have  
99 reduced the forest cover with only a relatively moderate use of fire because of the cold  
100 climate and slow speed of vegetation recovery (Kaplan et al., 2016). This debate is important  
101 because of studies that have shown the sensitivity of the climate system to vegetation  
102 boundary conditions during the LGM (Ludwig et al., 2017; Velasquez et al., 2021). This  
103 suggests that accurate knowledge of the vegetation cover during the LGM is a necessary  
104 prerequisite to understanding the role of other influences on the climate system at this time.  
105

106 More recent pollen and macrofossil studies from eastern Central Europe have shown that at  
107 least in this region there existed areas of open boreal forest and woodland with some  
108 temperate broadleaf species (Kuneš et al., 2008; Willis and Van Andel, 2004). The evidence  
109 of forest, and particularly elements of temperate broadleaf forest, north of the Alps has come  
110 to represent a challenge to the traditional view that forest species only survived the LGM in  
111 sheltered refugia far to the south of the Fenoscandian ice sheet and close to the moderating  
112 influence of the Mediterranean Sea. The presence of micro-refugia north of the Alps is  
113 important because it would represent a very different baseline for understanding the later rate  
114 and route of plant migrations under the rapid warming that occurred during the Late Glacial  
115 to Holocene transition (Douda et al., 2014; Giesecke, 2016; Krebs et al., 2019; Nolan et al.,  
116 2018), as well as understanding patterns of present-day genetic diversity (Normand et al.,  
117 2011; Svenning et al., 2008). Modelling studies have shown difficulty in supporting the very  
118 high rates of postglacial expansion that would be necessary for southern refugia (Feurdean et  
119 al., 2013, Nogués-Bravo et al. 2018).  
120

121 Much of this debate has been informed by an increasing number of LGM pollen studies from  
122 an ever-broader geographical area, and especially from an increasing number of studies from  
123 north of the Alps. Nevertheless, the synthesis of these studies into a single narrative is made  
124 difficult by several factors, for instance: different taxonomic definitions, pollen percentages  
125 calculated from non-standardized pollen sums, and quantitative analyses such as climate  
126 reconstructions that are based on different training sets and methodologies. This has led to  
127 some modelling studies ignoring the pollen record completely, on the basis that data from the  
128 LGM is too scarce (Janská et al., 2017). Where standardized methods have been applied to  
129 multiple LGM pollen records, poor dating control has resulted in the inclusion of many  
130 records that may not actually be from the selected LGM time window. This is particularly  
131 important because the  $21 \pm 2.0$  ka time slice commonly used to represent the LGM period in  
132 PMIP data-model comparisons and other synthesis studies (MARGO members, 2009;  
133 Bartlein et al., 2011) occurs immediately after the glacial maxima in the Alps around 26-23  
134 ka (Heiri et al., 2014; Spötl et al., 2021) and Heinrich stadial HS-2 (24.3-26.5), whilst also  
135 being closely followed by Heinrich stadial HS-1(15.6-18.0 ka) (Sanchez-Goñi & Harrison,  
136 2010). These closely associated time periods can therefore be expected to represent both a  
137 different vegetation and climate than the LGM itself.  
138

139 For example, of the 18 European pollen records used in the PMIP benchmarking dataset  
140 (Bartlein et al., 2011), 10 fall into the worst class ('poor') in the COHMAP chronological  
141 quality classification scheme if relative dating such as pollen correlation is excluded. More  
142 recent synthesis studies have also relied heavily on records from the European Pollen  
143 Database (EPD) which currently has 116 records with samples of LGM age (as of June

144 2022). Many of these records however are based on chronologies that are considered reliable  
145 for the Holocene (Giesecke et al., 2014), but have large uncertainties for the LGM as a result  
146 of 1) excessive extrapolation back in time from Holocene age dates, 2) the use of pollen  
147 correlation or other relative dating despite poorly defined regional biostratigraphy, or 3) the  
148 inappropriate use of radiocarbon dates contaminated with old carbon. We found that 104 of  
149 these 116 EPD records (Neotoma, 2021) fall into the worst class ('poor') in the COHMAP  
150 chronological quality classification.

151

152 Here we address these problems using a new synthesis of LGM pollen records from  
153 throughout Europe, the Mediterranean and the Middle East (EurMedMidEst) based on  
154 rigorous quality control criteria. Records were compiled from an extensive review of public  
155 databases and archives, and the scientific literature. Pollen records were selected according to  
156 the robustness of their chronological control around the PMIP LGM time-window ( $21 \pm 2$   
157 ka), and combined into a single dataset based on a harmonized taxonomy and standardized  
158 pollen sum. The dataset was then analysed so that standardised maps could be produced to  
159 show the distribution of the major pollen taxa, biomes and total arboreal pollen at the LGM.  
160 In addition, quantitative reconstructions of forest cover as well as winter, summer and annual  
161 temperatures and precipitation were undertaken using the Modern Analogue Technique  
162 (MAT), utilizing the latest Eurasian Modern Pollen Database v2 dataset. These climate  
163 reconstructions are compared and evaluated against previous LGM pollen-climate  
164 reconstructions, as well as reconstructions based on other proxies. The dataset and results are  
165 fully documented and the complete data files are provided in the supplementary information.

166

## 167 **2 Methods**

168

### 169 **2.1 Pollen Data**

170

171 LGM fossil pollen data from Europe and bordering regions including North Africa and the  
172 Middle East were selected and collated into a single standardized project database. This data  
173 was sourced from the EPD/Neotoma database (Williams et al., 2021), the Pangaea data  
174 archive, publications in scientific journals, and from the original authors. We selected LGM  
175 pollen sites/data according to strict quality control criteria. Where possible, primary raw  
176 pollen counts were used where this was available. Where the original electronic data was not  
177 available, the data was digitized from the published diagram. Overall we have included 63  
178 records in our study, of which 35 were digitized and 28 consisted of the original pollen  
179 counts (Table 1).

180

181 The distribution of the 63 sites reflects the distribution of suitable archives, with fewer  
182 records available from climatically or environmentally challenging regions (Fig. 1). High  
183 rates of erosion and a drier and colder climate during the LGM reduced the number of  
184 suitable anoxic sediment sinks for pollen preservation, especially in Central Europe between  
185 the Scandinavian and Alpine ice sheets. Nevertheless, our dataset includes sites from this  
186 region, as well as North Africa and eastern Central Europe through to Iran, although most  
187 sites are located in an arc across eastern Spain, the Alps, and Italy. Lakes sites are the most  
188 numerous archive and tend to be located in the more sheltered and topographically favourable  
189 regions of Southern Europe and the Mediterranean. Peat is the next most important archive,  
190 followed by alluvial and colluvial sediments, as well as cave sites, the later also often being  
191 known for their archaeological significance. Sites located at the ice margins that appear to be  
192 under the ice reflect uncertainties in the location of the ice margin both in time and space  
193 during the LGM, as well as the fact that the selected time window for this study ( $21 \pm 2$  ka) is

194 later than the maximum ice advance in some regions (Hughes and Gibbard, 2015). For  
195 completeness, we also include 7 marine records which have the advantage of more  
196 continuous deposition and often better dating over the LGM period, but which are prone to  
197 taphonomic biases compared to terrestrial records. These biases are discussed later in this  
198 section.

199

200 LGM pollen records were selected according to a number of quality control criteria, but  
201 primary amongst these was the existence of sufficient independent chronological control  
202 points to accurately identify samples that would fall within the  $21 \pm 2$  ka BP time-slice of  
203 interest. We have used all of the samples within this time frame where the samples have been  
204 available in electronic form, else we have used the sample closest to the target time (21 ka  
205 BP). For records taken from the EPD we have used the latest Bayesian age-depth models  
206 where these were available (Giesecke et al., 2014), otherwise we have used the dates and  
207 chronology proposed by the original authors. We classified chronologies according to the  
208 COHMAP chronological quality scheme for the LGM period (Anderson et al., 1988; Yu and  
209 Harrison, 1995), which classifies record quality from 1-6 depending on whether a date falls  
210 within 2000 14C years (or less) of the time being assessed, or whether bracketing dates fall  
211 within 6000 and 8000 14C years (or less) about the time being assessed (Table A1).

212 Chronologies based on dates that fall outside of these limits fall into COHMAP class 7, and  
213 are regarded as ‘poorly dated’ with respect to the LGM. Importantly, we have only included  
214 radiometric and other absolute dates (such as varves) in this assessment, and have excluded  
215 dates based on correlation with regional pollen records. These pollen-based stratigraphic  
216 dates have been widely used in previous LGM studies, but do not include estimates of  
217 uncertainty and are generally regarded as unreliable at this time given the sparsity of well  
218 dated pollen sites and samples on which to base any correlation (Giesecke et al., 2014).

219

220 All records that were classified as poorly dated (COHMAP class 7) were subsequently  
221 excluded from our analysis. This has meant that many of the pollen records used in previous  
222 studies were excluded, including 16 of the 26 LGM records used by PMIP and associated  
223 studies in Europe (Bartlein et al., 2011; Elenga et al., 2000; Tarasov et al. 2000, Jost et al.,  
224 2005; Peyron et al., 1998; Wu et al., 2007; Cleator et al., 2020). We also excluded 104 of the  
225 116 records in the EPD with samples that fall within our LGM time window. Many of these  
226 EPD pollen records have been used in more recent studies, although the exact record (EPD  
227 Entity number) is often not stated. We estimate that we have excluded 16 of the 17 European  
228 sites used by Binney et al. (2017) (this study only included sites above latitude 40N), 5 of the  
229 6 European sites used by Allen et al. (2010), 28 of the 33 sites used by Cao et al. (2019) and  
230 27 of the 71 sites used by Kaplan et al. (2016).

231

232 Other quality control criteria were also used in the selection of LGM pollen records.  
233 Published pollen diagrams that only included a small part of the terrestrial pollen assemblage,  
234 or only presented summary taxa, were excluded. Records were also excluded where the  
235 dating information was incomplete, for instance where radiocarbon dating uncertainties were  
236 not published or where it was not possible to determine if the date shown was in calibrated or  
237 uncalibrated radiocarbon years.

238

239 The modern pollen data for the climate and tree cover reconstructions were sourced from the  
240 latest version 2 of the Eurasian Modern Pollen Database (Davis et al., 2020), which is  
241 managed as part of the EPD. The EMPD2 includes 8133 modern pollen samples from across  
242 the Palearctic biogeographic region from Europe to the far East of Asia. The taxa from both  
243 the fossil and modern pollen data were consolidated into 120 of the most commonly-

244 occurring terrestrial taxa types. This taxa list was designed to be compatible with the  
245 biomisation scheme used in our study (Peyron et al., 1998; Tarasov et al., 2000) and that used  
246 in the Holocene mapping study of Brewer et al. (2017). The count of *Larix* was amplified by  
247 a factor of 10 due to its low pollen representation (Edwards et al. 2000, Bigelow et al. 2003,  
248 Tarasov et al. 1998, 2000, 2013, Binney et al., 2017).

249

## 250 **2.2 Biomisation**

251

252 We converted pollen assemblages to biomes based on the European biomisation scheme of  
253 Peyron et al (1998), which in turn is based on Prentice et al. (1996). The method is described  
254 in detail in Collins et al. (2012). We expanded the number of taxa included in the biomisation  
255 procedure proposed by Peyron et al (1998) to include taxa from the Northern Eurasian  
256 biomisation procedure of Tarasov et al. (1998). The inclusion of additional Northern Eurasian  
257 taxa reflects recent evidence that modern analogues of LGM vegetation occur in parts of  
258 Siberia (Magyari et al., 2014a). The biomisation procedure (Prentice et al. 1996) assigns each  
259 taxa to a plant functional type (PFT) and calculates a score for each of these PFT's based on  
260 the sum of the square root of the percentage of each of the taxa included in that PFT. To  
261 reduce the influence of long-distance transport, taxa below 0.5% are removed at the start of  
262 the procedure. Each biome is then assigned one or more PFT's and a score for each biome is  
263 calculated as the sum of the associated PFT scores. The biome with the highest score is then  
264 viewed as the dominant biome. Where the highest score is the same for more than one biome,  
265 the dominant biome is decided based on a hierarchy of unique PFT's. Peyron et al. (1998)  
266 also included a procedure for distinguishing warm and cold steppe biomes based on re-  
267 assigning certain steppe PFT's according to the presence or otherwise of PFT's indicative of  
268 cold or warm conditions. Following the Biome6000 project (Elenga et al., 2000) and Allen et  
269 al. (2010), we did not apply this additional procedure and present only the merged steppe  
270 biome. In summary, the biomisation procedure categorised 39 arboreal pollen taxa and 39  
271 non-arboreal taxa into 22 plant functional types (PFT's), which were then combined into 12  
272 biomes.

273

## 274 **2.3 Quantitative climate reconstruction**

275

276 We reconstructed climate from pollen data based on a standard Modern Analogue Technique  
277 (MAT) that used PFT scores to match fossil samples with modern pollen samples (as used by  
278 Davis et al., 2003). "Other methods using PFT scores and artificial neural network techniques  
279 have been developed to reconstruct the climate of Europe during the LGM from pollen data  
280 (Peyron et al. (1998) and Jost et al (2005). PFT scores have been used in previous large-scale  
281 European pollen-based climate reconstructions for the Holocene (Davis et al., 2003; Mauri et  
282 al., 2014, 2015), where performance was found to be better than the conventional approach  
283 based on individual taxa (eg Marsicek et al., 2018). A particular advantage of the PFT  
284 approach for the LGM is that it can help overcome problems associated with vegetation  
285 (pollen) assemblages that may have no modern analogue (Davis et al. 2003). This can be a  
286 problem during the LGM when the climate and environment could be expected to be very  
287 different from today, and when many taxa formed unusual vegetation assemblages as a result  
288 of their forced retreat to sheltered refugia locations. The problem of modern analogues is also  
289 addressed in our reconstruction by using the latest EMPD2 modern pollen dataset. The  
290 EMPD2 provides a large number of potential modern analogues for many different LGM  
291 vegetation types and climates found today across the Palearctic region. PFT scores were  
292 calculated according to the methods outlined already in the Biomisation section, then

293 normalized so that each sample was proportional to every other sample (Juggins and Birks,  
294 2012).

295

296 The MAT method was applied using the Rioja program for R (Juggins, 2020). The modern  
297 pollen data was taken from the latest version 2 of the EMPD (as detailed earlier). The  
298 EMPD2 includes 8133 samples, which is considerably larger than the modern datasets used  
299 in previous LGM pollen-based reconstructions. For instance, Peyron et al. (1998) used a  
300 modern pollen dataset of 683 samples, which was updated by Jost et al (2005) to include an  
301 additional 185 samples. These datasets were also mainly taken from the steppes of Kazakstan  
302 and Mongolia, while the EMPD2 covers a much wider area, spanning most of the Eurasian  
303 Palearctic region (Davis et al., 2020). The size and distribution of the modern training set in  
304 climate and vegetation space is important because in order for the method to work  
305 effectively, it is necessary to have samples representative of the likely vegetation and climate  
306 space that could be occupied by the fossil assemblage (Turner et al. 2021, Chevalier et al.,  
307 2020; Salonen et al. 2012, Juggins, 2013).

308

309 A known problem with MAT is the role of spatial auto-correlation in providing  
310 unrealistically low estimates of uncertainty (Chevalier et al., 2020; Telford and Birks, 2009).  
311 This results from the fact that closely analogous modern pollen samples can also be located  
312 closely in physical space, and therefore in climate space. To reduce this problem it is possible  
313 to exclude closely located samples from the analogue matching process using a filter based  
314 on a set distance (h-block filter) (Telford and Birks, 2009). While this approach can help,  
315 there are also three main problems associated with it. The first is error substitution, since  
316 removing samples also reduces the number of potential analogues, creating a different source  
317 of error that is not easy to categorise. Secondly, multiple samples taken from the same  
318 location are actually a strength of pollen training sets, since they are more likely to capture  
319 the full range of the assemblage diversity associated with a given climate. Thirdly, current  
320 methods that limit spatial range such as the h-block filter only do so on the horizontal axis,  
321 and do not consider the fact that samples can also be found at different elevations. In hilly or  
322 mountainous regions samples can therefore be excluded because they are closely located in  
323 horizontal space, but in fact they actually occupy very different climates and vegetation  
324 associations, contradicting the logical premise of the h-block filter. It was therefore decided  
325 not to apply this filter.

326

327 Uncertainties for the pollen-climate reconstructions were calculated using a standard method  
328 for MAT (Juggins 2020) based on the spread of the climates associated with the best modern  
329 pollen analogues used for each fossil sample. The closer the climates of the best modern  
330 pollen analogues (6 in the case of this study) then the smaller are the calculated uncertainties  
331 assigned to the reconstructed climate of the fossil pollen sample.

332

333 Climate reconstructions are presented as anomalies. These have been calculated with respect  
334 to modern climate (1970-2000 average) at each core site location using WorldClim 2 (Fick  
335 and Hijmans, 2017) (Table A2), which was also used to assign the modern climate for the  
336 modern pollen samples in the transfer function (Davis et al., 2020).

337

## 338 **2.4 Quantitative tree cover reconstruction**

339

340 It has long been recognized that the proportional representation of individual pollen taxa in a  
341 pollen assemblage does not necessarily reflect the proportion of land area covered by that  
342 taxa in the pollen source area surrounding the sample site (Davis 1963, Gaillard et al. 2010,

343 Zanon et al. 2018). These differences can be caused by variations in pollen productivity,  
344 differential transport, deposition and preservation of pollen grains, and even the ease or  
345 otherwise of the identification of pollen grains themselves. This can make the interpretation  
346 of pollen taxa percentages difficult, even for relatively simple questions such as the  
347 proportion of forest to non-forest in the landscape.

348

349 There have been two main methods developed to account for this quantification problem, one  
350 using a physical modelling technique (PMT) based on estimates of pollen production for  
351 individual taxa (Gaillard et al., 2010), and the other using a MAT very similar to that used in  
352 pollen-climate reconstructions (Williams and Jackson, 2003). Both approaches have been  
353 widely applied during the Holocene in Europe (Zanon et al., 2018), but we know of no  
354 previous study that has applied either of these approaches to the LGM. The LGM presents a  
355 number of challenges, not least the problem of potential missing vegetation analogues, as  
356 well as low atmospheric CO<sub>2</sub>, which has been shown to influence pollen productivity (Leroy  
357 and Arpe, 2007).

358

359 Here we use the MAT to provide quantitative estimates of forest cover, following the  
360 approach of Zanon et al. (2018) who applied this method to the Holocene pollen record of  
361 Europe. We apply MAT in exactly the same way as for the climate reconstructions described  
362 earlier, including the use of PFT scores to match fossil and modern pollen samples. Instead of  
363 modern climate values, we assigned an estimate of modern forest cover to each of our  
364 modern pollen sites. To do this we use a high resolution (~100m) remote sensing dataset  
365 derived from satellite observations (Hansen et al., 2013). Zanon et al. (2018) have shown that  
366 the MAT calibrated in this way gives comparable results to the PMT approach in Europe, at  
367 least for the Holocene. One of the main differences however is that the PMT is designed to  
368 provide estimates of the proportions of different taxa, whereas the MAT (as applied here) is  
369 designed to provide estimates of the proportion of forest cover. Where the PMT can only  
370 reconstruct the proportion of forest forming trees, irrespective of their size, the MAT  
371 (following Zanon et al. 2018) is calibrated specifically to reconstruct forest composed of trees  
372 over 5m tall. This follows the FAO definition of forest as “land spanning more than 0.5  
373 hectares with trees higher than 5 meters and a canopy cover of more than 10 percent, or trees  
374 able to reach these thresholds in situ” (FAO Terms and definitions 2020  
375 <http://www.fao.org/3/I8661EN/i8661en.pdf>).

376

## 377 **2.5 Maps**

378

379 We present our results in the form of maps that include the main physiographic features of  
380 the LGM in the study area. The maps are based on the WGS84 projection. Coastlines reflect  
381 LGM sea level at 120m below present, while ice sheets are based on Ehlers et al. (2011).  
382 Modern national country boundaries are also included for reference.

383

## 384 **2.6 Marine pollen records**

385

386 We have included marine pollen records in our analysis for reasons explained below, but it is  
387 important that these records should be viewed with caution, particularly when used for biome  
388 and quantitative MAT reconstructions, and when compared with terrestrial records from  
389 different archives. Biomisation methods have been applied to individual marine pollen  
390 records (Combourieu Nebout et al., 2009), as well as multi-site synthesis studies such as the  
391 ACER project (ACER project members et al., 2017). However, marine records were  
392 specifically excluded from the Biome6000 project (Elena et al., 2000). Similarly,



393 quantitative climate methods have been applied to individual marine pollen records  
394 (Combourieu Nebout et al., 2009; Fletcher et al., 2010), as well as multi-site synthesis studies  
395 (Sánchez Goñi et al., 2005; Brewer et al., 2008; Salonen et al., 2021). However, marine  
396 records have also been specifically excluded from other major pollen-climate studies  
397 (Cheddadi et al., 1996; Davis et al., 2003; Marsicek et al., 2018), as well as quantitative forest  
398 cover reconstructions (Zanon et al. 2018).

399

400 Discussion on the advantages and problems associated with marine records can be found  
401 elsewhere (Chevalier et al., 2020; Daniau et al., 2019), but are reviewed briefly here where  
402 relevant to the methodologies applied in this study. Marine sedimentary records provide  
403 continuous and well dated pollen records for the LGM that are often lacking from many  
404 terrestrial regions, especially in arid areas with few alternative anaerobic sediment sinks.  
405 Conversely however, pollen source areas for marine sites may be many hundreds of  
406 kilometers from the coring site and may be liable to change through time in response to  
407 changes in distance to the coastline, rates of river discharge and ocean and atmospheric  
408 dynamics. This can theoretically give rise to changes in the vegetation shown in the pollen  
409 assemblage recorded at the marine site without any actual change in climate or other  
410 environmental pressure. The large and indeterminable source area of marine records also  
411 mean that it is difficult to apply quantitative MAT reconstruction methods, not least because  
412 the mean climate or forest cover of the source area is almost impossible to determine. In  
413 addition, the fossil pollen record and the modern pollen dataset to which it is being compared  
414 are composed largely of terrestrial lakes and bog sites with much smaller and more  
415 homogeneous source areas. This creates a series of problems, the more obvious of which is  
416 the calculation of anomalies, since we cannot assume that the modern climate at the (marine)  
417 coring site location is representative of the (terrestrial) source area. In this study we have  
418 taken the closest point on land as the modern climate for the calculation of anomalies, but  
419 provide the absolute values for all sites so that these can be recalculated if necessary (Table  
420 A2). The next problem is that the large source area may capture a combination of different  
421 vegetation types that is not going to be represented in a modern pollen dataset based on  
422 samples from terrestrial sites with much smaller source areas, for instance a mixture of  
423 coastal and mountain vegetation, or even vegetation from different continents (Magri and  
424 Parra, 2002). However, in our analysis we did not find any sample from a marine record (or  
425 terrestrial record) that did not have a reasonable modern analogue in our training set (chord  
426 distance <0.3)(Huntley, 1990), even though we did not adjust the pollen assemblage for the  
427 over-representation of *Pinus* (and other Pinaceae) in the marine pollen samples.

428

429 Typically, the Pinaceae component is excluded from the terrestrial pollen sum when  
430 calculating percentages for marine pollen samples, and in some cases as been excluded  
431 entirely from the samples used in marine pollen-climate reconstructions (Combourieu Nebout  
432 et al., 2009). The problem with excluding *Pinus* is two-fold, the first is that *Pinus* often  
433 represents the main forest forming tree in the Koeppen Csb climate zone on the Atlantic coast  
434 where many marine sites are located (García-Amorena et al., 2007), as well as representing  
435 the most abundant tree taxa in Europe during the LGM (Figure A3c).

436

437 The effect of excluding Pinaceae on the biomisation algorithm and MAT climate  
438 reconstruction process has not been widely investigated. We therefore decided to evaluate  
439 this problem for 1) biomisation, and 2) pollen-climate reconstruction. In table S3 we show  
440 the biomisation results for 8213 modern pollen samples taken from the EMPD2 modern  
441 pollen database. Using this as the control, we then artificially varied the amount of Pinaceae  
442 (*Pinus*, *Abies* and *Picea*) in the assemblage of each pollen sample and compiled the results

443 (Table S3). This shows quite clearly that removing all of the Pinaceae has a much more  
444 profound effect on the biomisation process than artificially inflating the amount of Pinaceae  
445 (as might be expected in a marine sample where Pinaceae can be over-represented). Even  
446 when Pinaceae was artificially inflated by as much as 400% of the original value, the biomes  
447 were changed in only 2348 samples, compared to 5860 samples if all the Pinaceae was  
448 removed entirely. In terms of the effects on individual biomes, removing the Pinaceae  
449 considerably increased the amount of CLDE, STEP and TUND, whilst greatly reducing the  
450 amount of XERO, almost eliminating the amount of TAIG, and completely eliminating the  
451 COCO biome. In contrast, the effect of inflating the amount of Pinaceae tended to be more  
452 evenly distributed between the biomes, with the biggest increase seen in TUND and biggest  
453 decrease in STEP. This suggests that even if the over-representation of Pinaceae was quite  
454 extreme in marine pollen samples, the effect on biome classification (and by definition, the  
455 underlying PFT scores) is less than removing Pinaceae completely from the pollen  
456 assemblage.

457

458 In a second test, we compared the reconstruction of LGM climate from marine pollen  
459 samples when Pinaceae was included, and excluded. The results are shown in table S4 and  
460 indicate reconstructed temperatures are generally 1-2C cooler, and precipitation slightly  
461 higher when Pinaceae is excluded. The differences between the two methods however are  
462 small, and generally less than half of the uncertainties, suggesting that differences are  
463 statistically indistinguishable when considered in the context of the overall uncertainties.

464

465 In summary we find that including Pinaceae in the biomisation process is less likely to lead to  
466 miss-assignment of the biome than excluding Pinaceae, except in extreme cases of over-  
467 representation. Percentages of Pinaceae in the LGM marine samples range on average  
468 between 23-88%, suggesting that while Pinaceae was high at some sites, it does not appear to  
469 completely overwhelm the assemblage as might be expected if over-representation was to be  
470 a significant problem. We also find that including Pinaceae in the pollen assemblage of the  
471 LGM marine pollen samples gives pollen-climate reconstructions that are statistically  
472 indistinguishable from those obtained by excluding Pinaceae from the assemblage. Including  
473 Pinaceae in marine samples also provides compatibility with terrestrial samples, particularly  
474 when calculating and plotting pollen taxa percentages. For these reasons we have included  
475 Pinaceae in the analysis of all marine pollen samples in this study, although it is important to  
476 recognize that Pinaceae in such samples can be subject to over-representation and that the  
477 results presented here from marine sites should consequently be viewed with caution.

478

479

### 480 **3. Results**

481

#### 482 **3.1 Vegetation & Biomes**

483

484 Results of the biomisation analysis shows that steppe (STEP) was the most common biome at  
485 the LGM across the study area, occurring at 36 out of 63 sites, indicating that the landscape  
486 was largely dominated by cool temperate grasslands across much of western Central Europe,  
487 central and eastern Mediterranean, as well as North Africa and the Middle East (Fig. 2).  
488 However, at the same time we also find that there were a significant number of sites where  
489 we find that woody and forest biomes occur, more particularly in southern and eastern Iberia,  
490 northern Italy and central eastern Europe. The most dominant of these forest and woody  
491 biomes are taiga (TAIG) in the north, and cool-mixed forest (COMX) and xerophytic  
492 woodlands (XERO) in the south.

493  
494 As would be expected, the dominance of STEP biomes is generally reflected in low arboreal  
495 pollen percentages across the same areas/sites (Fig. 3 & 4). Exceptions to this rule can be  
496 found at marine sites such as [MD99-2331 site #3] and [MD01-2430 site #58] where STEP is  
497 reconstructed despite arboreal pollen percentages of 71 and 80 percent respectively. This  
498 apparent contradiction illustrates some of the idiosyncrasies of the biomisation method,  
499 especially when applying the method to marine pollen samples. In this case it is important to  
500 remember that the AP% is calculated from the sum of the percentages of each relevant taxa,  
501 but the score for each biome is the sum of the square root of the percentages of each of its  
502 constituent taxa. This results in biomes with taxa with large percentage values scoring  
503 proportionally smaller, and biomes with taxa with small percentage values scoring  
504 proportionally larger. For example, a single taxa at 50% has a square root of 7.07, but the  
505 sum of the square roots of 10 taxa each at 5% is 22.36 even though the sum of the  
506 percentages is the same 50%. This effect can be particularly pronounced in marine pollen  
507 samples because they are usually dominated by a single taxa (*Pinus*) that forms a high  
508 percentage of the total assemblage. Since there are often more non-arboreal taxa than  
509 arboreal taxa in a pollen assemblage, the non-arboreal taxa can dominate in the biomisation  
510 process even if collectively their percentage of the assemblage is a lot less than the arboreal  
511 taxa, resulting in a non-arboreal biome such as STEP having the highest biome score.

512  
513 Of the main arboreal biomes, Taiga (TAIG) is the dominant biome at 3 sites at the eastern  
514 end of the Alpine ice sheet, as well as at a site just to the north in northern Germany and a  
515 site in Slovakia, while Cool Conifer Forest (COCO) is found at 1 site close to the  
516 Scandinavian ice sheet in Lithuania. Cool Mixed Forest (COMX) is found much more widely  
517 at 8 sites south of the Alps from south-west Iberia to Romania, with Xerophytic Scrub  
518 (XERO) occurring at 8 sites with a similar distribution but not as far east or west. Cold  
519 Mixed Forest (CLMX) occurs at just two sites in Georgia and the Alboran Sea at the far east  
520 and west of the study area, while Warm Mixed Forest (WAMX) is the dominant biome at just  
521 1 site in Southern Spain. We do not record Temperate Deciduous Forest (TEDE), Tundra  
522 (TUND) or Desert (DESE) as the dominant biome at any site at the LGM, although they do  
523 occur as sub-dominant biomes.

524  
525 An alternative picture of LGM tree-cover is provided by the MAT reconstructions (Fig. 4).  
526 MAT performance statistics for tree cover are shown in table 2, based on an evaluation using  
527 the modern training set. This shows a relatively large root mean square error (RMSE) of  
528 21.03. and an R2 of 0.52 that is not as good as for the MAT climate analysis, but overall the  
529 results are comparable with previous MAT tree cover studies (Zanon et al., 2018). In general,  
530 the MAT values (site average 34%) show forest-cover around 16% less than that suggested  
531 from AP% (site average 50%) (Fig. A1), although sites with very low AP% also show higher  
532 values based on MAT. These differences are consistent with comparisons between MAT and  
533 AP% in Zanon et al (2018), although it should be noted that uncertainties related to the MAT  
534 reconstructions are large ( $\pm 23\%$ ). Zanon et al (2018) found that the differences between  
535 MAT and AP% were greatest over Northern Europe and in Arctic and sub-Arctic climate  
536 regions that are likely to be comparable to many areas of Europe during the LGM. These  
537 regions today are associated with tree-forming taxa such as Birch that fail to grow to a height  
538 of 5m or more, developing only as shrubs or krummholz forms.

539  
540 Pollen taxa percentages are shown in supplementary figure A2, and distribution maps of the  
541 33 most common taxa are shown in the supplementary figures A3a-f. Of the 21 arboreal taxa,  
542 *Pinus* generally has the highest values and is the most widespread, being present at all 63

543 sites. Other acicular arboreal taxa include *Juniperus*, which also has a wide distribution  
544 across EurMedMidEst although at lower values. The rest of the acicular arboreal taxa have  
545 more regional distributions. *Picea* is found mainly to the north of the study region, away from  
546 the Mediterranean, whilst *Abies* is generally found more to the south. *Larix* occurs only in the  
547 central European area including the northern edge of the Po plain just south of the Alps,  
548 whilst *Cedrus* is found mainly across south and west Europe in locations much further north  
549 than its Holocene and modern distribution which is confined mainly to Morocco and Lebanon  
550 (Collins et al., 2012). Temperate broadleaf arboreal taxa which also include cold-tolerant  
551 species such as *Betula* and *Salix* are relatively widely spread across the EurMedMidEst  
552 during the LGM, while less drought tolerant taxa such as *Alnus*, *Carpinus* and *Corylus* are  
553 found more to the south-west through to the north-east. Other temperate broadleaf arboreal  
554 taxa such as *Quercus* (deciduous) and *Ulmus* have a much more southern distribution, with  
555 *Fraxinus*, *Olea*, and *Quercus* (evergreen) being more prevalent in the south-west. In contrast,  
556 *Fagus* occurs more to centre and the east, while *Tilia* is found even in more northern  
557 locations of central Europe. The remaining arboreal taxa are more shrubby and drought  
558 adapted, with *Ephedra* and particularly *Ephedra fragilis* having a southern distribution,  
559 whilst the more cold adapted *Hippophae* being found even in the north of central Europe  
560 (similar to *Tilia*).

561  
562 The main non-arboreal taxa generally indicate cool, dry and environmentally disturbed  
563 conditions across much of the EurMedMidEst. The most widely distributed taxon is Poaceae,  
564 which like Pinus, is found in all records. Other non-arboreal taxa with a widespread  
565 distribution include Rubiaceae, Apiaceae and Asteraceae (Asteroideae), while *Plantago*,  
566 Cayophyllaceae, Brassicaceae and Asteraceae (Cichorioideae) have a more southern and  
567 western distribution. *Thalictrum* can be found mostly at sites in the centre of the  
568 EurMedMidEst, along with *Helianthemum* which also extends to sites in the south-west.  
569 Other taxa such as *Chenopodiaceae* and *Artemisia* have a more southern distribution,  
570 reflecting their preference for drier and less cold climates.

571

### 572 **3.2 Climate reconstruction evaluation**

573

574 Evaluation of transfer function performance based on the modern training set is presented in  
575 table 2. This shows that root mean square error predicted (RMSEP) values were smallest for  
576 summer temperatures (2.21C), and largest for winter temperature (3.35C), with mean annual  
577 temperatures in between (2.28C). The weaker performance for winter temperatures largely  
578 reflects the much greater range of winter temperatures in the training set. In turn, this  
579 contributes to a better R2 performance for winter temperatures (0.91) than annual  
580 temperatures (0.9) and summer temperatures (0.81). Overall R2 performance for precipitation  
581 is weaker than for temperature, which is typical because of the higher spatial variability of  
582 precipitation compared to temperature. Summer precipitation has the strongest R2  
583 performance (0.75) compared to winter and annual precipitation (both 0.69), as well as  
584 smaller RMSE values (52mm) than winter (78mm).

585

586 Given the widespread occurrence of steppe during the LGM, we also undertook a separate  
587 evaluation of transfer function performance in this type of environment. For this we used a  
588 subset of 1588 pollen samples from the EMPD2 that are classified with the steppe pollen-  
589 biome (Davis et al. 2020). The results indicate (Table A5) little difference in performance  
590 compared to the full dataset, with a small decrease in performance in annual and summer  
591 seasons in both precipitation and temperature, and a slight increase in performance in winter.

592

593 The results overall indicate good transfer function performance especially for temperature,  
594 and are comparable with those found in other continental scale pollen-climate studies  
595 (Bartlein et al., 2011). It is important to remember though that comparisons between studies  
596 can only be made with caution because results are often heavily dependent on the nature of  
597 the modern pollen dataset used as the training set, which is not the same in all studies  
598 (Juggins, 2013).

599  
600

### 601 **3.3 Climate reconstruction**

602

603 Reconstructed LGM temperatures indicate an overall mean annual cooling of  $-7.2 \pm 3.3\text{C}$ ,  
604 with a greater cooling of around  $-9.3 \pm 4.5\text{C}$  in winter and  $-5.0 \pm 3.2\text{C}$  in summer (Fig. 5). All  
605 sites apart from Lake Van [site #62] in eastern Turkey show cooler temperatures at the LGM  
606 compared to modern (Fig. 6), and even at this site cooler conditions fall within the  
607 uncertainties. With greater cooling in winter compared to summer, the difference in  
608 temperature between winter and summer also increased (shown by positive anomalies) at  
609 most (but not all) sites (Fig. 6). This increase in continentality was around  $+4.2\text{C}$  on average  
610 across all sites (Fig. 5).

611

612 We reconstruct an overall decline in mean annual precipitation of around  $-91 \pm 270\text{mm}$  ( $-$   
613  $13\%$ ) at the LGM. Most of this decline is in winter ( $-38 \pm 90\text{mm}$ ) ( $-21\%$ ), while in summer a  
614 small increase is shown ( $10 \pm 57\text{mm}$ ) ( $6\%$ ), although uncertainties are large (Fig. 7).

615 Compared to temperature there is significant seasonal and spatial variability in positive and  
616 negative precipitation anomalies (Fig. 8). Positive anomalies appear more predominant in  
617 eastern and southern Spain and in central eastern Europe in both summer and winter, while  
618 positive anomalies are found more generally in summer across sites in Southern Europe and  
619 the Mediterranean. These more positive summer anomalies also reflect a relative shift from  
620 winter to summer in the seasonality of precipitation in this region.

621

### 622 **4.0 Discussion**

623

624 Before we consider the results of our analysis it is important to provide some context in terms  
625 of European LGM geography and environment, which was very different from today (Fig. 1).  
626 Major ice sheets covered Scandinavia and much of the UK, the Alps, and the Pyrenees. Sea  
627 level was 120m lower, resulting in much of the North Sea and English Channel becoming dry  
628 land, and the European coastline extending over 100 km out into the Atlantic and  
629 Mediterranean, especially around the Bay of Biscay and Adriatic. The Black Sea was no  
630 longer connected to the Mediterranean, and was smaller with a water level around 100m  
631 lower than today (Genov, 2016). These changes in sea or water level had two main  
632 consequences, the first being that the marine sites were closer to land, and therefore closer to  
633 (low lying) terrestrial vegetation and (pollen carrying) river discharge points than they are  
634 today. The second consequence of lower seas levels is that terrestrial pollen sites were  
635 located further from the moderating effect of the ocean than they are today, resulting in a  
636 localised modification of the climate experienced by the site irrespective of regional or global  
637 changes (Geiger, 1960).

638

639 The maps used in our analysis shows the maximum ice sheet at  $21\text{k} \pm 2\text{k}$  (Ehlers et al., 2011).  
640 The precise geographical location of the ice sheet is difficult to resolve at a fine spatial scale,  
641 however, which explains why some sites close to the ice margin appear to be actually located  
642 under the ice (for example sites Kersdorf-Briesen site #46 & Mickunai site #54). The

643 resolution of the map also shows the occurrence of permanent ice not only to the north and  
644 over the Alps, but also on many subsidiary areas of high ground across central and southern  
645 Europe, including areas such as the Pyrenees, Massif Central, Vosges and Carpathian  
646 Mountains. While global ice volume may have peaked ~21 ka individual ice sheets in Europe  
647 and other areas are known to have reached their maximum extent at different times (Hughes  
648 et al., 2016). The larger ice sheets are likely to have had a significant influence on regional  
649 climate and environmental conditions across Europe, but the smaller ice sheets had similar if  
650 more localized impacts as well. Surrounding each ice sheet would have been an unglaciated  
651 area of active peri-glacial processes and newly created and unstable ground. This would  
652 include outwash plains, impounded lakes and recently drained lake beds, seasonally and  
653 sporadically flooded areas, moraines, kettle holes and other glaciological and peri-glacial  
654 features. Soils in these areas would be non-existent or skeletal, and vegetation would find it  
655 difficult to obtain nutrients and water for survival, irrespective of the prevailing climatic  
656 conditions. Outside of these areas, permafrost is also likely to have been present, particularly  
657 north of the Alps (Vandenberghe et al., 2014), which would also act as an impediment to  
658 vegetation growth.

659  
660 In terms of regional climate, the major ice sheets would have provided significant barriers to  
661 westerly atmospheric circulation, or even north-south circulation in the case of the Alps and  
662 Pyrenees. As well as representing a physical obstruction, the thermodynamic response of the  
663 atmosphere to these high, cold obstructions would have been to encourage the formation of  
664 areas of semi-permanent high pressure, similar to those found today for instance over the  
665 Greenland ice sheet. In addition, the Laurentide ice sheet located over North America would  
666 have generated downstream effects over Europe (COHMAP, 1988). These physical and  
667 thermodynamic effects would have affected the direction of storm tracks, as well as more  
668 local climatic effects commonly associated with ice sheets such as strong katabatic winds  
669 (Kageyama, et al. 2021, Velasquez et al. 2021, Luetscher et al. 2015, Lefort et al. 2019)

670

#### 671 **4.1 Vegetation Cover**

672

673 The nature and extent of forest cover during the LGM remains a matter of considerable  
674 debate. Vegetation models driven by LGM climate model simulations generally indicate  
675 extensive areas of boreal forest north of the Alps, and a mix of temperate and warm-  
676 temperate woodland to the south across southern Europe and much of the Mediterranean.  
677 Treeless areas such as steppe are mainly confined to those areas where it is also found today,  
678 namely inland Iberia, Ukraine, southern Russia and Turkey, while Tundra is found to the  
679 north close to the Scandinavian Ice Sheet (Allen et al., 2010; Cao et al., 2019; Prentice et al.,  
680 2011; Velasquez et al., 2021).

681

682 Evaluation of these vegetation-model simulations against data has been largely based on  
683 comparison with compilations of pollen-biome reconstructions (Prentice et al., 2011; Allen et  
684 al., 2010; Cao et al., 2019; Velasquez et al., 2021). Early studies were based on only a limited  
685 number of sites from southern Europe, and showed steppe at all sites in contradiction with  
686 model simulations (Elenga et al. 2000). More recent pollen compilations have included more  
687 sites especially to the north that have revealed a more mixed picture of vegetation cover, with  
688 forest biomes at some sites both south and north of the Alps that appear more consistent with  
689 model simulations (Binney et al., 2017; Cao et al., 2019). However, many of these pollen  
690 sites used in these studies were assigned an LGM age based on poor or incorrect dating  
691 control, and likely date to MIS3, the Late-Glacial or even the Holocene. Nevertheless, based  
692 on our compilation of more securely dated LGM pollen sites, we also show a wider

693 distribution of forest biomes particularly in Iberia, northern Italy and Central Europe,  
694 although with greater areas of steppe than suggested by the models over the remaining  
695 regions.

696

697 However, the interpretation of biome reconstructions requires care since the forest cover and  
698 vegetation composition may not be as clear as the dominant biome suggests. For instance, we  
699 find that steppe is still reconstructed as the dominant biome at some sites despite arboreal  
700 pollen forming 70-80% of the pollen assemblage. In addition, it is important to remember  
701 that pollen-biomes are based only on the proportion of taxa that can form forest and  
702 woodland, while these taxa may in fact exist only as shrubs or stunted krummholz forms in  
703 the challenging climate and environment of the LGM. Alternatively, similar conditions may  
704 favour low-lying non-arboreal taxa forms with poor pollen dispersion or even insect  
705 pollinated taxa forms that may be poorly represented in the pollen assemblage, giving greater  
706 prominence to arboreal taxa whose pollen may be the result of long-distance transport  
707 particularly *Pinus*. However there also appear to be plenty of samples with low or even very  
708 low (<20%) arboreal percentages, so not all sites in open areas may be affected by long-  
709 distance transport of *Pinus* in the same way.

710

711 Quantitative MAT based reconstructions of forest cover can overcome some of these  
712 problems, where they can be detected, based on the composition of the pollen assemblage  
713 when compared with the modern land-cover. Chord-distance measurements of the match  
714 between fossil and modern pollen assemblages indicate good LGM analogues exist in our  
715 large Eurasian modern pollen dataset. The results of the MAT forest cover reconstruction  
716 indicates that forest cover was low but not entirely devoid of woodland in most areas, similar  
717 to the modern boreal forests of Siberia and consistent with a steppe-tundra-woodland mosaic  
718 proposed by many authors (e.g. Birks and Willis, 2008; Willis and Van Andel, 2004). This is  
719 confirmed in an analysis of the most commonly found modern analogue ecoregions for LGM  
720 pollen samples at each site (Table A6). Uncertainties are large, but for comparison the MAT  
721 site-average of 33% forest cover is slightly less than the average today over the Boreal region  
722 of Europe (43%) and slightly more than the average today over Mediterranean region (27%)  
723 (Zanon et al. 2018).

724

725 By calculating the percentage of each of the taxa in each LGM pollen sample using a  
726 standardized pollen sum, we are able to make direct comparisons between different LGM  
727 pollen records and their taxa percentages (Figure A2, A3). The results show a preponderance  
728 of boreal forest taxa to the north of the Alps, consistent with biome results mentioned earlier.  
729 *Pinus* is the most common forest forming taxa in this boreal zone, together with *Picea*, and  
730 including *Larix* to the east and *Abies* to the west. The occurrence of *Betula* and *Juniperus*  
731 also suggests shrubby elements consistent with arctic shrub-tundra, although high Poaceae  
732 and other herbaceous taxa such as *Artemisia* and *Chenopodiaceae* indicate more steppe than  
733 tundra. Other deciduous taxa found north of the Alps include cold tolerant generalists such as  
734 *Corylus* and *Alnus*, as well as low percentages of relatively thermophilous taxa in the east,  
735 such as *Carpinus* and *Tilia*.

736

737 These results are consistent with charcoal (Magyari et al., 2014a; Willis and Van Andel,  
738 2004), malacological (Juříčková et al., 2014), biomarkers (Zech et al., 2010) and genetic  
739 evidence (Stivrins et al., 2016; Willis and Van Andel, 2004) that the main forest region north  
740 of the Alps was in the eastern region of Central Europe around the Carpathian basin. This  
741 was also an area where cold and moisture sensitive deciduous taxa were also able to survive  
742 (Magyari et al., 2014), although evidence of temperate taxa found in the pollen record has yet

743 to be supported by charcoal and macrofossil records (Feurdean et al., 2014). Our pollen  
744 evidence indicates an open taiga or cool mixed forest that extended in central and eastern  
745 Europe to areas close to the Scandinavian and Alpine ice caps, as proposed by Willis and Van  
746 Andel (2004) and Huntley and Allen (2003), although whether this represents isolated  
747 pockets of forest or an extended open steppe-forest is difficult to determine (Kuneš et al.,  
748 2008). Even steppe or tundra areas in western Europe show a low but significant presence of  
749 the pollen of tree taxa at sites close to the ice sheets that are unlikely to be solely the result of  
750 long distance transport or reworking (Kelly et al., 2010). The presence of woodland in these  
751 areas is also supported by mammalian remains, for instance at Kents Cavern in SW England  
752 (Stewart and Lister, 2001).

753  
754 Overall however, our results clearly show a much greater predominance of thermophilous  
755 and moisture sensitive deciduous taxa south of the Alps, particularly in Iberia and Northern  
756 Italy, where temperate broadleaf forests survived in sheltered refugia (Kaltenrieder et al.,  
757 2009). Most of these appear to be in hilly areas with the ability to generate orographic rainfall  
758 (Monegato et al., 2015), on south facing slopes to make the most of the sun's radiant energy  
759 and located above the valley floor to escape frost and flooding. We might also expect these  
760 areas to be sheltered from cold northerly winds, and benefit from relatively mild and moisture  
761 laden winds coming from the Mediterranean Sea. For instance, the presence of woodland and  
762 low glacier altitudes along the southern slopes of the Alps around the Po Valley and Trentino  
763 region is consistent with strong orographic rains generated by southerly and easterly winds  
764 that today can be generated by low pressure located south of the Alps in the Gulf of Genoa,  
765 and consistent with a southerly storm track around the Alps (Kehrwald et al., 2010; Luetscher  
766 et al., 2015). Generally, as might be expected, areas of forest reconstruct similar or increased  
767 precipitation compared to today, and areas of steppe indicate decreased precipitation (see next  
768 section).

769  
770 Independent evidence of LGM vegetation is provided by archaeozoological data. This data  
771 supports the palynological evidence for the existence of forest and woodland refugia across  
772 the ice-free areas of Europe at latitudes north of the Alps. For instance, large vertebrates in  
773 these areas show patterns of extirpation and extinction in response to shifts in climate and  
774 vegetation cover that is different for different species, indicating a variety of environments  
775 and niches (Lister and Stuart, 2008; Stewart and Lister, 2001). As with the pollen record, the  
776 presence of temperate adapted large vertebrate taxa within the glacial landscape of Western  
777 Europe also suggests the existence of temperate "micro-refugia" (Stewart and Lister, 2001) ,  
778 consistent with suggestions that temperate arboreal taxa were not entirely extirpated from the  
779 region during the LGM (Magri, 2010). Further east, mammal assemblages indicate  
780 generalized loss of forest components in the East European Plain (Demay et al. 2021,  
781 Puzachenko et al., 2021) which is consistent with our data indicating low forest cover in this  
782 region. In other areas, evidence of the prevailing land cover at the LGM comes from studies  
783 of small vertebrate communities, which have a closer affinity to the prevailing environment  
784 than large vertebrates (López-García and Blain, 2020) that have the propensity to migrate  
785 large distances, often on a seasonal basis. These studies of small vertebrate assemblages also  
786 support the existence of temperate "micro-refugia" in France (Royer et al., 2016) and the  
787 existence of woodland components in many regions across Southern Europe including parts  
788 of Iberia (Bañuls-Cardona et al., 2014) Italy (Berto et al., 2019) and the Balkan Peninsula  
789 (Mauch Lenardić et al., 2018).

790  
791 Other paleobotanical evidence also supports our land cover reconstruction. Schafer et al.  
792 (2016) suggest leaf wax patterns from palaeosols in Spain may indicate the presence of



793 drought intolerant deciduous trees and more humid conditions during the LGM. Significantly,  
794 none of the pollen sites indicate that temperate broadleaf forests were dominant, and  
795 broadleaf temperate taxa always appear part of a mixed woodland together with cold or  
796 aridity adapted evergreen and needleleaf taxa, including typical Mediterranean taxa. This type  
797 of mixed vegetation probably extended to the Balkans where the hilly terrain and proximity  
798 to the Mediterranean would appear to have provided favourable climatic conditions, although  
799 we still lack LGM sites from this region. At sites in central and southern Italy and east  
800 through Greece and Turkey to the Middle East (and including North Africa), the vegetation  
801 appears drier with a greater prevalence of steppe. Only a site in Georgia at the edge of the  
802 Caucasian mountains indicates the presence of significant amounts of forest (mainly *Pinus*), a  
803 result that was also found by Tarasov et al. (2000), and probably linked to favourable  
804 orographic precipitation and proximity to the Black Sea.

805  
806 Comparison with LGM land cover from vegetation modelling studies driven by climate  
807 model simulations indicate a much wider presence of forest than that shown by the pollen  
808 data (Kaplan et al., 2016). Data-model agreement appears to be closest over eastern-central  
809 Europe where pollen indicates the presence of open Boreal forest, and over south-west  
810 Europe with the presence of cool mixed temperate forest, including broadleaf deciduous and  
811 thermophilous elements (Prentice et al., 2011; Allen et al., 2010; Cao et al., 2019; Velasquez  
812 et al., 2021). Nevertheless, agreement still appears to be weak over western-central Europe  
813 and Southern and Eastern Europe through to the Middle East, where pollen data continues to  
814 indicate widespread steppe. One proposed explanation for this data-model discrepancy has  
815 been the role of fire (including man-made fire) in maintaining forest openness, a factor  
816 influencing forest cover that is not included in most vegetation models (Kaplan et al., 2016).  
817 In the Carpathian basin Magyari et al. (2014a) noted that charcoal increased as forest cover  
818 declined, suggesting that wildfires played a role in decreasing forest cover during the LGM.  
819 Other studies have noted low levels of charcoal and therefore fires during the LGM, although  
820 these tend to be from steppe areas with low biomass and fuel availability (Connor et al.,  
821 2013; Kaltenrieder et al., 2009). Recent LGM vegetation simulations that include fire indicate  
822 much lower values of forest cover than those without fire over western central Europe, while  
823 forest remains in central eastern Europe (see figure 6 in Velasquez et al., 2021). This appears  
824 closer to the data, but the values are perhaps too low compared with our MAT  
825 reconstructions here (Figure 4).

826

## 827 **4.2 Climate**

828

### 829 **4.2.1 Comparison with previous pollen-based reconstructions**

830

831 The climate of the LGM is generally considered to have been cooler and drier than today, but  
832 data-model comparisons continue to highlight important discrepancies, not only in the degree  
833 of cooling and drying but also in their seasonal and spatial distribution. Data-model  
834 comparisons over Europe have mainly used pollen-based climate reconstructions, especially  
835 the Paleoclimate Modelling Intercomparison Project (PMIP/CMIP) (Kageyama et al., 2021,  
836 Bartlein et al., 2011; Harrison et al., 2015; Kageyama et al., 2006). The most commonly used  
837 reconstructions have been based on two main methods, a neural-network methodology  
838 (ANN) of Peyron et al. (1998) and Jost et al. (2005), and an Inverse Modelling approach  
839 (INV) applied by Wu et al. (2007). The ANN method uses modern pollen samples and does  
840 not include any correction for CO<sub>2</sub> effects, being similar in these respects with the MAT  
841 method used in this study. In contrast the INV method does not use modern pollen samples,  
842 but instead uses a process-based vegetation model run in inverse mode. Ordinarily, a

843 vegetation model will use climate as an input to generate a vegetation as an output, but in  
844 inverse mode the model is reconfigured to generate climate as an output given a particular  
845 vegetation (pollen) assemblage as an input. One of the advantages of the INV method is that  
846 CO<sub>2</sub> can also be varied as an input, and therefore the effect of changes in CO<sub>2</sub> on the  
847 vegetation, and therefore reconstructed climate, can be investigated. Comparison of these  
848 ANN and INV reconstructions have shown important differences, with the INV  
849 reconstruction generally not as cold and somewhat drier than ANN (Wu et al. 2007). These  
850 differences between pollen-climate methods have often been attributed to CO<sub>2</sub> effects (Wu et  
851 al. 2007) but this is not clear since there may be other factors, such as the size and location of  
852 the training set used in the ANN reconstruction.

853

854 We make a comparison with these earlier reconstructions based on 10 sites/records in our  
855 dataset which we identified as also being included in these earlier studies (Fig. 9). While we  
856 were able to identify the site and data source, as well as the time window, we were unable to  
857 establish if the the data represented a single sample or the mean of multiple samples within a  
858 time-window or the exact depth of those samples, or the actual sediment core in the case of  
859 multiple cores from the same site. While these aspects are unknown, it seems likely that the  
860 pollen data we used in our analysis was very similar if not identical in most cases, and  
861 reconstructed biomes for these sites from our pollen dataset are identical to the biomes  
862 reconstructed using the earlier pollen dataset (Elenka et al., 2000).

863

864 We compare our MAT with the ANN and INV reconstructions in figure 9. On average across  
865 all 10 records, the MAT and INV methods give almost identical results for both anomalies of  
866 mean annual temperature (MAT -6.6C, INV -7.2C) and precipitation (MAT 158mm, INV  
867 165mm). Uncertainties are also similar for both methods. In contrast, the ANN method gives  
868 much cooler mean annual temperature anomalies (ANN -13.9C) and drier precipitation  
869 anomalies (ANN -474mm). On a site by site basis the MAT and INV methods show closer  
870 agreement for temperatures than precipitation, although precipitation has proportionally  
871 larger uncertainties. The reconstructions based on these two methods are close enough that  
872 the uncertainties overlap at all sites for both temperature and precipitation, except the  
873 precipitation reconstruction at Lac de Bouchet (site #25). The reason for this is not clear, but  
874 there could easily be minor differences with the pollen data analysed by Wu et al. (2007) in  
875 their INV reconstruction since the pollen record (Reille and de Beaulieu, 1988) includes  
876 multiple cores each with many different samples covering the LGM period.

877

878 This comparison shows that our MAT reconstructions are very similar to the INV method,  
879 but not as cold or dry as the ANN method. This has two main implications. The first is that  
880 our reconstructions indicate greater agreement with the results of climate model simulations  
881 since climate models indicate temperatures closer to the INV reconstructions (Latombe et al.,  
882 2018) than the ANN reconstructions (Jost et al., 2005; Kageyama et al., 2006). The difference  
883 between our MAT and earlier ANN reconstructions is likely the result of the modern pollen  
884 datasets used, since the ANN reconstruction was based on a considerably smaller number of  
885 samples taken mainly from the cold dry steppes of Kazakhstan and Mongolia.

886

887 The second implication is that the MAT method may not be significantly impacted by the  
888 effects of lower CO<sub>2</sub> (Cowling and Sykes, 1999; Prentice and Harrison, 2009; Williams et  
889 al., 2000) or indeed insolation changes during the LGM, since the MAT results are similar to  
890 those based on the INV method which specifically takes account of these non-climatic factors  
891 (Wu et al., 2007). This would suggest that MAT could also work well for pollen-based  
892 climate reconstructions on longer glacial-interglacial timescales where insolation and CO<sub>2</sub>

893 vary significantly from their modern values. This is consistent with the findings of Pini et al.  
894 (2021) who applied a correction algorithm developed by Prentice et al. (2017) and Cleator et  
895 al. (2020) to a MAT reconstruction of mean annual precipitation at Lake Fimon in Northern  
896 Italy. This shows a very small correction of 0mm to 30mm for samples across the LGM time-  
897 window, which indicates that CO<sub>2</sub> is not a very significant factor in influencing this type of  
898 reconstruction, at least compared to the overall uncertainties (+/- 200mm) of the  
899 reconstruction itself. The uncertainties associated with the correction algorithm are not  
900 discussed, but given that inputs include estimates of both LGM temperature and cloud cover,  
901 it seems likely that these could be significant. Importantly, both Pini et al (2021) and Cleator  
902 et al (2020) specifically exclude the necessity of applying a correction algorithm to  
903 temperature reconstructions, since they consider only hydrological variables to be affected by  
904 changes in atmospheric CO<sub>2</sub>.

905  
906

## 907 **4.2.2 Comparison with climate reconstructions based on other proxies**

908

### 909 **4.2.2.1 Temperature**

910

911 Proxies that are not based on plants should remain unaffected by the CO<sub>2</sub> problem during the  
912 LGM, and provide an alternative basis for evaluating pollen-based reconstructions. Samartin  
913 et al. (2016) reconstructed LGM summer temperatures based on chironomid remains from  
914 Lago della Costa (site #34) in Northern Italy. They also undertook pollen analysis on the  
915 same samples down the core, allowing us to make a sample-by-sample comparison between  
916 the chironomid temperature record and our MAT reconstruction (Fig. 10). Our pollen-climate  
917 reconstruction is for JJA mean temperature, while the chironomid reconstruction is for July  
918 mean temperature, with the anomalies based on the modern equivalent JJA and July mean  
919 temperatures respectively. The average anomaly values for all 8 samples reconstructed by the  
920 pollen-climate MAT are  $-10.2 \pm 3.5^{\circ}\text{C}$ , and for the chironomids  $-9.5 \pm 3.0^{\circ}\text{C}$ . This indicates  
921 that pollen and chironomid average summer temperature reconstructions are very similar on  
922 average, taking into account the overlapping uncertainties, while also showing a strong  
923 similarity on a sample-by-sample basis throughout the time-series.

924

925 Other reconstructions based on other proxies provide a basis for more general regional  
926 comparisons (Figure A4, A5). We reconstruct both summer and winter temperatures and  
927 show that cooling in winter was greater than in summer at most sites, associated with an  
928 increase in continentality (increased temperature difference between summer and winter). A  
929 similar seasonal pattern of temperature change has also been shown in other studies that  
930 reconstruct both summer and winter LGM temperatures, including Prud'homme et al. (2016)  
931 using d<sub>18</sub>O analysis of earthworm calcite granules at Nussloch near the French-German  
932 border, Bañuls-Cardona et al. (2014) using faunal remains of small mammals at 4 locations in  
933 western Spain, and Ferguson et al. (2011) who examined seasonal temperature change using  
934 d<sub>18</sub>O and Mg/Ca analysis of limpet shells at Gibraltar in southern Spain. The increase in  
935 continentality at Nussloch (Prud'homme et al., 2016) was reconstructed at between 11.6 to  
936 15.6 °C, comparable at the lower end with nearby pollen sites [La Grotte Walou site #28]  
937  $10.4 \pm 5.8^{\circ}\text{C}$  and [Bergsee site #29]  $7.9 \pm 5.7^{\circ}\text{C}$ . The faunal sites in western Spain studied  
938 by Bañuls-Cardona et al. (2014) gave much reduced increases in continentality, but  
939 nevertheless similar to nearby pollen sites. For instance at Valdavara  $5.1^{\circ}\text{C}$  [MD99-2331 site  
940 #3]  $5.2 \pm 3.1^{\circ}\text{C}$ , El Miron  $1.2^{\circ}\text{C}$  [Tourbiere de l'Estarrès site #19]  $5.1 \pm 6.2^{\circ}\text{C}$ , El Portalon  
941  $0.9^{\circ}\text{C}$  [Torrecilla de Valmadrid site #16]  $2.8 \pm 1.8^{\circ}\text{C}$  and Cueva de Maltrivieso  $6.1^{\circ}\text{C}$  [SU81-18  
942 site #2]  $4.8 \pm 3.4^{\circ}\text{C}$ . Further south at Gibraltar the limpet-based study of Ferguson et al.

943 (2011) also shows a relatively small increase of 2 °C. The nearest pollen site [Gorham Cave  
944 site #5] however shows a larger increase of  $4.7 \pm 2.3$  °C, although differences could be  
945 expected given the different temporal resolution of annual laminae on mollusk shells  
946 compared to pollen assemblages that reflecting much slower changes in trees and other long-  
947 lived flora.

948

949 Summer temperatures were warm enough during the LGM over the Alpine areas that Swiss  
950 lakes were largely ice free in summer, while glacier ELA's around the time of the LGM  
951 suggest summers were -6.5 to -7.7 °C cooler compared to the LIA (Heiri et al., 2014). This  
952 cooling was similar to that found at Nussloch some 200km north of the Swiss border by  
953 Prud'homme et al. (2016), who reconstructed anomalies of -6 to  $-8 \pm 4$  °C from  $\delta^{18}O$   
954 analysis of earthworm calcite granules (representing warm season May-September  
955 temperatures). Slightly less cooling was found close by at the nearby site of Achenheim  
956 where analysis of Mollusc assemblages gave summer (August) cooling estimates of -3.5 to -  
957 6.5 °C based on MAT (Rousseau, 1991), and -5.5 to -9.5 °C based on the Mutual Climatic  
958 Range method (Moine et al., 2002). These reconstructions appear somewhat cooler than  
959 nearby pollen sites [La Grotte Walou site #28]  $-1.4 \pm 3.6$  °C and [Bergsee site #29]  $-2.7 \pm 5.1$   
960 °C, although comparable with the pollen site [Pilsensee site #32]  $-7.3 \pm 5.0$  °C 200 km further  
961 east. Similar differences also occur at the site of Les Echets on the western edge of the Alps  
962 where a diatom based reconstruction of summer (July) temperatures (Ampel et al., 2010)  
963 indicated a greater cooling (-10.5 to -11.5 °C) than our pollen reconstruction [Les Echets G  
964 site #27] ( $-4 \pm 2.7$  °C). However, the authors caution that the results were based on poor  
965 analogues and rare taxa, as well as a small training set of only 90 lakes in Switzerland.

966

967 South of the Alps, other proxies show the opposite relationship with the pollen  
968 reconstructions. For instance, at Lago della Costa in the Po valley, a summer (July)  
969 temperature chironomid reconstruction by Samartin et al. (2016) is around 1-2 °C less cool  
970 than the pollen reconstruction (JJA) for the same site [Lago della Costa site #34]  $-11.4 \pm$   
971  $2.7$  °C, although both reconstructions fall within their respective uncertainty ranges (Figure 8).  
972 In the Pindus Mountains in Greece, Hughes et al. (2006) estimated LGM summer  
973 temperature anomalies of -7 °C based on glacier modelling, which is comparable with that  
974 reconstructed at the nearest pollen site [Ioannina site #51]  $-7.7 \pm 2.8$  °C. In Spain the analysis  
975 of small mammal remains by Bañuls-Cardona et al. (2014) shows similarly less cooling in  
976 summer or even warmer than present positive anomalies compared to the nearest pollen sites,  
977 such as Valdavara 1.4 °C [MD99-2331 site #3]  $-2.3 \pm 2.8$  °C, El Miron -2.3 °C [Tourbiere de  
978 l'Estarres site #19]  $-5.7 \pm 5.4$  °C, El Portalon 0.8 °C [Torrecilla de Valmadrid site #16]  $-2.6 \pm$   
979  $1.1$  °C and Cueva de Maltrivieso -1.1 °C [SU81-18 site #2]  $-10.4 \pm 2.8$  °C. Further south at  
980 Gibraltar, the limpet-based study of Ferguson et al. (2012) suggests an anomaly of around -7  
981 °C, which is a greater cooling than the pollen reconstruction from this location [Gorham Cave  
982 site #5]  $-1.3 \pm 2.2$  °C, although comparable with other pollen sites slightly further east.

983

984 Winter temperature reconstructions from non-pollen proxies show a similar pattern in relation  
985 to pollen reconstructions as for summer temperatures. North of the Alps at Achenheim,  
986 Prud'homme et al. (2016) use  $\delta^{18}O$  on earthworm remains to reconstruct particularly cold  
987 winter anomalies of -17.6 to -23.6 °C compared to nearby pollen sites [La Grotte Walou site  
988 #28]  $-11.8 \pm 8.0$  °C and [Bergsee site #29]  $-10.6 \pm 6.3$  °C. South of the Alps in Spain, the  
989 analysis by Bañuls-Cardona et al (2014) based on the remains of small mammals shows less  
990 cooling in winter compared to the nearest pollen sites, in particular Valdavara -3.7 °C  
991 [MD99-2331 site #3]  $-7.5 \pm 3.4$  °C, El Miron -3.5 °C [Tourbiere de l'Estarres site #19]  $-10.8$   
992  $\pm 7.0$  °C, El Portalon -0.1 °C [Torrecilla de Valmadrid #16]  $-5.4 \pm 2.5$  °C and Cueva de

993 Maltrvieso  $-7.2\text{C}$  [SU81-18 site #2]  $-15.2 \pm 4.0$  °C. And again, in southern Spain at Gibraltar,  
994 analysis of limpet shells by Ferguson et al (2011) suggests winter cooling of around  $-9$  °C  
995 while the pollen reconstruction suggests [Gorham Cave site #5]  $-6.0 \pm 2.5$  °C, although sites  
996 further east indicate cooler conditions.

997  
998 A number of additional proxies have also been used to reconstruct LGM mean annual  
999 temperature. Heyman et al. (2013) applied glacier mass balance modelling at sites located in  
1000 the smaller mountain regions north of the Alps. These are generally slightly cooler than our  
1001 pollen-based reconstructions at sites close to the Vosge Mountains  $-12.7 \pm 2.0$  °C and Black  
1002 Forest  $-11.4 \pm 2.3$  °C [Bergsee site #29]  $-8.2 \pm 3.3$  °C, Bavarian Forest  $-10.7 \pm 2.2$  [Pilsensee  
1003 site #32]  $-9.2 \pm 1.2$  °C and Giant Mountains  $-8.5 \pm 1.8$  [Kersdorf-Briesen site #46]  $-7.3 \pm 0.3$   
1004 °C. These values obtained by Heyman et al. (2013) are warmer than Pud'homme et al. (2016)  
1005 who estimated annual mean temperature anomalies of  $-15.1$  to  $-19.1$  °C based on  $\delta 18\text{O}$  of  
1006 earthworm calcite at the Nussloch site just north of the Vosge and Black Forest. The annual  
1007 temperatures reconstructed by Heyman et al. (2013) are also around 2C warmer than Allen et  
1008 al. (2008) who applied a similar, although simpler method to over 29 different mountainous  
1009 regions across Europe that had been glaciated during the LGM. Since glacier mass balance is  
1010 a function of both snowfall and temperature, these estimated temperatures vary according to  
1011 estimated changes in precipitation. For instance, mean annual temperature estimates by Allen  
1012 et al. (2008a) are much cooler than reconstructed by pollen, with an average anomaly of  $-13.2$   
1013 °C for the 29 sites assuming a 40% reduction in precipitation, but this is reduced to  $-11.8$  °C  
1014 assuming the same precipitation as modern. This compares with  $-7.2$  °C for our 63 pollen  
1015 sites. The glacier mass balance modelling by Allen et al. (2008a) assumes a seasonal  
1016 distribution of precipitation that is similar to the present day, and does not consider increases  
1017 in winter precipitation or mean annual precipitation above present day levels. Both of these  
1018 are suggested by the pollen data in some regions, and both could explain glacier extent found  
1019 during the LGM based on less extreme temperature anomalies more comparable with the  
1020 pollen data.

1021  
1022 To the east of the Alps in the Panonian basin, mean annual temperature anomaly estimates  
1023 have been made from noble gas measurements on groundwater ranging from  $-2$  to  $-4$  °C  
1024 (Stute and Deak, 1990) up to  $-9$  °C (Varsányi et al., 2011). These are similar to estimates  
1025 ranging from  $-2$  to  $-9$  °C from oxygen isotope ratios from mammoth tooth enamel (Kovács et  
1026 al., 2012) and are comparable with nearby pollen sites [Feher Lake site #50]  $-8.2 \pm 3.3$  °C and  
1027 [Kokad site #52]  $-4.5 \pm 2.3$  °C. On a broader scale, Sanchi et al (2014) estimated LGM  
1028 cooling in the Danube and Dneiper basins based on Lipid biomarkers in a core from the  
1029 Black Sea and came up with similar mean annual temperature anomalies between  $-6$  to  $-10$   
1030 °C, which again are comparable with pollen sites from the region that range from  
1031 [Nagymohos site #48]  $-10.5 \pm 4.1$  °C to [Straldzha site #57]  $-4.3 \pm 5.8$  °C.

1032  
1033 Further south and west, García-Amorena et al. (2007) reported mean annual temperature  
1034 anomalies of  $-2.0$  to  $-11.3$  °C at LGM sites along the Portuguese coast, based on an indicator  
1035 species method using plant macrofossils. This is similar to the closest marine pollen sites off  
1036 the coast, which recorded values of [MD95-2039 site #1]  $-10.5 \pm 4.6$  °C and [MD99-2331 site  
1037 #3]  $-5.3 \pm 2.9$  °C. Meanwhile, in the far east of the study area, Zaarur et al. (2016) estimated a  
1038 mean annual temperature anomaly of around  $-3$  °C based on clumped isotope analysis of  
1039 *Melanopsis* shells from LGM sediments in the Sea of Galilee. This limited cooling appears  
1040 similar to the nearest pollen site [Lake Zeribar site #63] where we reconstruct a cooling of  $-$   
1041  $2.2 \pm 4.6$  °C.

1042

1043 Reconstructions of LGM sea surface temperatures (SST's) provide yet another source of  
1044 comparison with our terrestrial pollen-based reconstructions, although many of the physical  
1045 processes controlling surface sea temperatures such as upwelling, surface mixing, surface  
1046 currents, stratification and thermal inertia through the seasonal cycle, represent quite different  
1047 processes to those controlling surface temperatures over land, particularly at the sub-regional  
1048 scale. Nevertheless, the Atlantic coastal waters of Iberia and the waters throughout the  
1049 Mediterranean Sea include many SST sites that lie in relative proximity to our terrestrial  
1050 pollen-sites, allowing us to make a comparison at the largest scale. Within this area the  
1051 MARGO database (MARGO Members, 2009) includes 13 Alkenone, 2 Mg/Ca and 41  
1052 Foraminifera based SST records of mean annual temperature, with the Foraminifera records  
1053 also providing an additional 41 winter (JFM) and summer (JAS) SST estimates. We compare  
1054 the SST records with the 36 closest terrestrial pollen records which fall within a box of -11 to  
1055 35 degrees longitude and 32 to 43 degrees latitude containing all of the SST records. A  
1056 simple site average indicates a mean annual SST anomaly of  $-5.5 \pm 1.0$  °C which is relatively  
1057 close to the value of  $-7.2 \pm 3.4$  °C obtained from the terrestrial pollen sites [sites #1-4, 5, 7-  
1058 24, 25, 26, 30, 35-38, 41, 47, 51, 53, 56-59]. Interestingly the inter-site variance (standard  
1059 deviation of the reconstructed temperatures across all sites) is almost identical for the two  
1060 datasets,  $2.57$  °C for the SST sites and  $2.63$  °C for the pollen sites, despite representing very  
1061 different environments, proxies and uncertainties. However, when we look at the seasonal  
1062 temperature anomalies, we find very different results. Site averaged winter SST anomalies  
1063 are  $-3.7 \pm 1.1$  °C compared to  $-9.3 \pm 4.2$  °C for winter temperatures from terrestrial pollen  
1064 sites, while in summer the values are reversed,  $-7.0 \pm 0.8$  °C compared to  $-5.38 \pm 3.3$  °C  
1065 respectively. This suggests that SST's experienced greater cooling in summer compared to  
1066 winter, which is the opposite to that generally found in terrestrial seasonal temperature  
1067 reconstructions throughout the region, although this is consistent with model simulations  
1068 (Mikolajewicz, 2011).

1069

#### 1070 **4.2.2.2 Precipitation**

1071

1072 Few proxies apart from pollen provide quantitative reconstructions of precipitation during the  
1073 LGM. Glacier mass balance modelling includes assumptions about precipitation in order to  
1074 derive temperatures (Allen et al., 2008a), but neither is independent of the other. Hughes et  
1075 al. (2006) estimate from glacier modelling that mean annual precipitation during the LGM at  
1076 sites in the Pindus mountains in Greece was around  $2300 \pm 200$ mm, which they consider to  
1077 be similar to the present day ( $>2000$ mm). A small change in precipitation compared to  
1078 modern values is also indicated by the nearest pollen site, which is around 47 km to the south  
1079 [Ioannina #51], and indicates a mean annual precipitation anomaly of  $-152 \pm 294$ mm,  
1080 representing just 15% of the modern value. A larger reduction in mean annual precipitation of  
1081 -45% (maximum) is reconstructed by García-Amorena et al. (2007) based on plant  
1082 macrofossil remains from sites on the Portuguese coast. In comparison, the closest pollen  
1083 sites record values which are a little lower, ranging from [MD95-2039 site #1] -22% to  
1084 [MD99-2331 site #3] -34%. Further north in south-west Germany, Prud'homme et al. (2018)  
1085 reconstructed mean annual precipitation from the delta  $^{13}C$  of earthworm calcite granules at  
1086 Fussloch. They estimate a field site average of 333 (159-574) mm/yr at the LGM, which  
1087 represents an anomaly of -503 mm/yr (-60%) relative to the modern precipitation of 836  
1088 mm/yr. This is comparable with the closest pollen site [Bergsee #29] with an anomaly of -  
1089 540 mm/yr.

1090

1091 As with glaciers, lake levels reflect changes in moisture balance that includes the effects of  
1092 both temperature (via evapotranspiration) and precipitation, rather than just precipitation.

1093 They also represent semi-quantitative data at best, with changes often described relative to  
1094 the modern or other baseline. There are few lake level records available north of the Alps, but  
1095 to the south, many records indicate high lake levels in areas such as Spain (Lacey et al., 2016;  
1096 Moreno et al., 2012; Vegas et al., 2010), Italy (Belis et al., 1999; Giraudi, 2017), Greece and  
1097 Turkey (Harrison et al., 1996; Reimer et al., 2009) and the Middle East (Kolodny et al., 2005;  
1098 Lev et al., 2019). These lake records are also supported by evidence of higher river levels in  
1099 Morocco (El Amrani et al., 2008). The cause of the higher lake levels has been the subject of  
1100 some debate, since many pollen records (and especially early biome reconstructions) show  
1101 steppe vegetation that would suggest aridity that appears incompatible with higher lake  
1102 levels. Prentice et al. (1992) proposed that the co-existence of steppe vegetation and high lake  
1103 levels could be possible if precipitation increased outside of the summer growing season,  
1104 while summers themselves were drier and cooler with decreased evaporation. However, the  
1105 results of our analysis tend to indicate the opposite in regions with higher lake levels, with  
1106 increased summer rainfall and decreased winter rainfall. In addition, the increase in summer  
1107 precipitation was enough to compensate for the decrease in winter rainfall, leading to an  
1108 overall increase in mean annual precipitation at many pollen sites in Spain and Greece for  
1109 instance. This together with depressed temperatures and consequently decreased evaporation  
1110 could explain the higher lake levels, whilst also limiting the growth of trees as a result of  
1111 cooler temperatures and prolonged aridity outside of the summer season. Davis & Stevenson  
1112 (2007) also note a differential hydrological response between summer and winter rainfall in  
1113 the Mediterranean during the Holocene that may also provide an explanation. In this case  
1114 sporadic summer storms may result in high rates of runoff that may fill run-off fed lakes, but  
1115 low rates of soil moisture recharge that fails to benefit vegetation in the same way winter  
1116 rainfall does.

1117  
1118 Overall, we reconstruct only a small reduction in precipitation during the LGM of around  
1119 91mm (13%) averaged over all sites, which is less than the ~200mm reduction based on the  
1120 sites in the pollen-climate compilation used by PMIP (Bartlein et al., 2011). Since our  
1121 precipitation reconstruction on average matches that of the INV reconstruction by Wu et al  
1122 (2007), we can attribute much of the difference to the greater aridity shown in the ANN  
1123 reconstruction by Peyron et al and Jost et al (2005) (see figure 9). As with temperature, this is  
1124 probably a reflection of the modern training set used in the ANN reconstruction which is  
1125 much smaller than our training set and is largely taken from the arid steppes of Kazakhstan  
1126 and Mongolia. However, it is also important to recognize the significant spatial variability in  
1127 precipitation, which means that a simple average of different sets of sites from different  
1128 regions may not accurately reflect the change in LGM precipitation at the European scale.  
1129 Nevertheless, one of the most consistent signals in our dataset is for an increase in summer  
1130 precipitation over many areas of Southern Europe and the Mediterranean. This is also found  
1131 in climate models, where it has been attributed to an increase in convection-driven  
1132 precipitation, although the amount of precipitation generated by this mechanism varies  
1133 significantly between models (Beghin et al., 2016). It may seem counter-intuitive to see an  
1134 increase in reconstructed precipitation in the same regions where we also find a  
1135 preponderance of steppe or xerophytic biomes and taxa, including *Artemisia* and  
1136 *Chenopodiaceae*. This is attributable to the fact that climate can change quite markedly with  
1137 necessarily invoking a major change in vegetation, and especially the pollen biome. For  
1138 instance, a semi-arid climate ranges from 250-500mm rainfall a year, so we could expect a  
1139 semi-arid vegetation to be dominant even if the rainfall increases 250mm (100%).

1140  
1141 A more consistent response in models is for an increase in winter precipitation across  
1142 Southern Europe and the Mediterranean related to a stronger and more southerly displaced jet

1143 stream, with winter precipitation also accounting for much of the change in mean annual  
1144 precipitation (Beghin et al., 2016). Our reconstruction of winter precipitation however shows  
1145 less support for this scenario with a more general decrease in winter precipitation apart from  
1146 southern and eastern Iberia, and with summer precipitation generally more important in those  
1147 sites that show an overall increase in mean annual precipitation. This may not necessarily  
1148 contradict the models in terms of the strength and position of the winter jet stream, but may  
1149 instead indicate that models over-estimate the amount of moisture being carried westward  
1150 from the cold North Atlantic along the storm track, especially across the far northern  
1151 Mediterranean. The increase in winter precipitation across southern and eastern Iberia is  
1152 however entirely consistent with a strengthened and more southerly jet stream, which also  
1153 brings increased winter precipitation to the region today as a result of blocking over northern  
1154 Europe/Atlantic and a negative NAO (Vicente-Serrano et al., 2011).

1155

1156 Other areas that show an increase in winter precipitation include pollen sites around the  
1157 eastern end of the Alps. This is consistent with a recent study by Spötl et al (2021) who  
1158 argued, on the basis of cryogenic carbonates preserved in a cave in Austria, that heavy winter  
1159 (and autumn) precipitation was a significant factor in driving LGM glaciation in the region.  
1160 The seasonally specific nature of this precipitation is also supported by the same pollen sites,  
1161 which do not show any increase in summer precipitation at this time.

1162

## 1163 **5.0 Conclusions**

1164

1165 We have reconstructed the climate and vegetation cover across Europe, North Africa and the  
1166 Middle East at the time of the LGM based on 63 pollen records. These records were selected  
1167 using strict quality control criteria, with particular attention paid to dating control, which led  
1168 to the exclusion of many records that have been used in previous studies. This fully  
1169 documented dataset represents the most chronologically precise and spatially resolved view  
1170 of LGM climate and vegetation during the PMIP benchmarking time window at  $21 \pm 2$  ka.  
1171 Nevertheless, it is important to recognize that there are still significant spatial gaps in pollen  
1172 sites especially north of the Alps, the Balkans, Turkey and the Middle East, and we continue  
1173 to have only a partial understanding of the LGM over these areas.

1174

1175 One of the key questions concerning the vegetation landscape of the LGM in Europe has  
1176 been the extent to which forest rather than steppe covered the continent, and to what extent  
1177 temperate elements could be found north of the classical refugia areas of Southern Europe  
1178 and the Mediterranean. Our results show that although steppe and tundra was extensive at the  
1179 time of the LGM, areas of open forest also occurred in many regions, particularly (but not  
1180 exclusively) in Iberia, northern Italy and Central Europe. These forest or woodland stands are  
1181 likely to have been located in environmentally favourable areas, with good soils, elevated  
1182 rainfall and shelter from cold, desiccating winds. In those areas where woodland existed,  
1183 Boreal taxa generally dominated north and east of the Alps, while temperate and  
1184 thermophilous (mainly drought adapted) taxa were generally confined to areas south of the  
1185 Alps and around the Mediterranean. The temperate deciduous forests that compose the  
1186 climax community in many areas of Europe today were displaced to the south and reduced to  
1187 a partnership role with Boreal elements. Overall our new reconstruction indicates greater  
1188 agreement with model land cover simulations, but models still appear to over-estimate the  
1189 amount of forest and woodland over areas such as France and the Benelux, Greece, Turkey  
1190 and the Far East.

1191



1192 Another key question about the LGM concerns the ability of climate models to simulate the  
1193 climate of this period and whether pollen-based climate reconstructions which show  
1194 disagreement with models have been biased by the effects of low CO<sub>2</sub> on plant physiology.  
1195 We find that our new pollen-climate reconstruction shows much closer agreement with  
1196 climate models than previous reconstructions that did not take account of low CO<sub>2</sub> effects.  
1197 We also find close agreement with previous reconstructions that did take account of CO<sub>2</sub>  
1198 effects. Since our MAT method itself does not specifically take account of low CO<sub>2</sub> effects,  
1199 this would suggest that this problem is not a significant hindrance to MAT performance at the  
1200 time of the LGM, at least not compared to other uncertainties. Instead, we suggest that the  
1201 main factor in the performance of pollen-climate transfer functions that use modern analogue  
1202 methods is the provision of a large enough modern pollen dataset with suitable LGM  
1203 analogues.

1204  
1205 This conclusion is supported by comparison with climate reconstructions based on other  
1206 proxies. We found little difference between our MAT reconstruction and a Chironomid-based  
1207 summer temperature record based on a downcore sample by sample comparison, as well as  
1208 comparisons with records from a variety of other proxies at a regional scale. However, it is  
1209 notable that some studies using glacier mass balance modelling methods indicate LGM  
1210 temperatures that are much cooler than our pollen-based reconstruction. The reasons behind  
1211 this are not clear, but our pollen-based results indicate higher than present precipitation in  
1212 some areas that could potentially explain low elevation glacier ELA's without the need for  
1213 such cold temperatures.

1214  
1215 We also find that although our pollen-based reconstruction and those of SST's generally  
1216 agree in terms of mean annual temperatures, SST's indicate greater cooling in summer  
1217 compared to winter, while terrestrial records indicate greater cooling in winter compared to  
1218 summer. These seasonal differences are also reproduced in climate models, and probably  
1219 reflect the different processes driving seasonal temperature change in the terrestrial and  
1220 marine domain.

1221  
1222 Our reconstructions of precipitation show large spatial and seasonal variability, but generally  
1223 indicate less overall aridity than previously suggested from smaller scale studies which  
1224 sampled less of the spatial domain. We find that in some regions of Southern Europe  
1225 precipitation may actually have been greater than present, especially in summer, but also in  
1226 winter in southern and eastern Iberia and around the southern slopes of the Alps. This may  
1227 have important implications in understanding the development of LGM glaciation, which  
1228 may be less a function of temperature than previously supposed. This could also help better  
1229 explain the observed asynchronous nature of glaciation even within relatively small regions  
1230 such as Europe, as a result of more localized controls on ice sheet development such as  
1231 precipitation.

1232  
1233 We hope that this new continental-scale dataset of climate and vegetation reconstructions will  
1234 provide an improved baseline for data-model comparisons and other studies that will allow us  
1235 to better understand the complex LGM environment.

1236  
1237

1238 **Code/Data availability**

1239

1240 All of the data shown in the figures together with the fossil and modern pollen datasets will  
1241 be made available on pangaea.de once the review process has been completed and these  
1242 datasets are therefore no longer subject to change.  
1243

#### 1244 **Author contribution**

1245  
1246 BASD designed the study, undertook the analysis and wrote the manuscript. MF and ER  
1247 designed and prepared the maps. JOK and AB reviewed the manuscript and provided  
1248 additional input.  
1249

#### 1250 **Competing interests**

1251  
1252 The authors declare that they have no conflict of interest.  
1253

#### 1254 **Acknowledgements**

1255  
1256 This work was supported by a grant from the Fonds de Recherche du Québec Société et  
1257 Culture (2019-SE3-254686) to AB. Data were obtained from the European Pollen Database  
1258 (EPD), based within the Neotoma Paleoecology Database (<http://www.neotomadb.org>). The  
1259 work of data contributors, data stewards, and the Neotoma and EPD community is gratefully  
1260 acknowledged. We dedicate this paper in memory of Eric Grimm, whose tireless work for the  
1261 EPD and Neotoma helped make this study possible.  
1262

1263  
1264  
1265  
1266  
1267  
1268  
1269  
1270  
1271  
1272  
1273  
1274  
1275  
1276  
1277  
1278  
1279  
1280  
1281  
1282  
1283  
1284  
1285  
1286  
1287  
1288  
1289  
1290  
1291  
1292  
1293  
1294  
1295  
1296  
1297  
1298  
1299  
1300  
1301  
1302  
1303  
1304  
1305  
1306  
1307  
1308  
1309  
1310  
1311

## References

- ACER project members, Goñi, M. F. S., Desprat, S., Daniau, A. L., Bassinot, F. C., Polanco-Martínez, J. M., Harrison, S. P., Allen, J. R. M., Scott Anderson, R., Behling, H., Bonnefille, R., Burjachs, F., Carrión, J. S., Cheddadi, R., Clark, J. S., Combourieu-Nebout, N., Mustaphi, C. J. C., Debusk, G. H., Dupont, L. M., Finch, J. M., Fletcher, W. J., Giardini, M., González, C., Gosling, W. D., Grigg, L. D., Grimm, E. C., Hayashi, R., Helmens, K., Heusser, L. E., Hill, T., Hope, G., Huntley, B., Igarashi, Y., Irino, T., Jacobs, B., Jiménez-Moreno, G., Kawai, S., Peter Kershaw, A., Kumon, F., Lawson, I. T., Ledru, M. P., Lézine, A. M., Mei Liew, P., Magri, D., Marchant, R., Margari, V., Mayle, F. E., Merna Mckenzie, G., Moss, P., Müller, S., Müller, U. C., Naughton, F., Newnham, R. M., Oba, T., Pérez-Obiol, R., Pini, R., Ravazzi, C., Roucoux, K. H., Rucina, S. M., Scott, L., Takahara, H., Tzedakis, P. C., Urrego, D. H., Van Geel, B., Guido Valencia, B., Vandergoes, M. J., Vincens, A., Whitlock, C. L., Willard, D. A. and Yamamoto, M.: The ACER pollen and charcoal database: A global resource to document vegetation and fire response to abrupt climate changes during the last glacial period, *Earth Syst. Sci. Data*, 9(2), 679–695, doi:10.5194/essd-9-679-2017, 2017.
- Allen, J. R. M., Hickler, T., Singarayer, J. S., Sykes, M. T., Valdes, P. J. and Huntley, B.: Last glacial vegetation of northern Eurasia, *Quat. Sci. Rev.*, 29(19–20), 2604–2618, doi:10.1016/j.quascirev.2010.05.031, 2010.
- Allen, R., Siegert, M. J. and Payne, A. J.: Reconstructing glacier-based climates of LGM Europe and Russia – Part 2 : A dataset of LGM precipitation / temperature relations derived from degree-day modelling of palaeo glaciers, , 249–263, 2008a.
- Allen, R., Siegert, M. J. and Payne, A. J.: Reconstructing glacier-based climates of LGM Europe and Russia – Part 3 : Comparison with previous climate reconstructions, , (1999), 265–280, 2008b.
- Ampel, L., Bigler, C., Wohlfarth, B., Risberg, J., Lotter, A. F. and Veres, D.: Modest summer temperature variability during DO cycles in western Europe, *Quat. Sci. Rev.*, 29(11–12), 1322–1327, doi:10.1016/j.quascirev.2010.03.002, 2010.
- El Amrani, M., Macaire, J. J., Zarki, H., Bréhéret, J. G. and Fontugne, M.: Contrasted morphosedimentary activity of the lower Kert River (northeastern Morocco) during the Late Pleistocene and the Holocene. Possible impact of bioclimatic variations and human action, *Comptes Rendus - Geosci.*, 340(8), 533–542, doi:10.1016/j.crte.2008.05.004, 2008.
- Anderson, P. M., Barnosky, C. W., Bartlein, P. J., Behling, P. J., Brubaker, L., Cushing, E. J., Dodson, J., Dworetsky, B., Guetter, P. J., Harrison, S. P., Huntley, B., Kutzbach, J. E., Markgraf, V., Marvel, R., McGlone, M. S., Mix, A., Moar, N. T., Morley, J., Perrott, R. A., Peterson, G. M., Prell, W. L., Prentice, I. C., Ritchie, J. C., Roberts, N., Ruddiman, W. F., Salinger, M. J., Spaulding, W. G., Street-Perrott, F. A., Thompson, R. S., Wang, P. K., Webb, T., Winkler, M. G. and Wright, H. E.: Climatic changes of the last 18,000 years: Observations and model simulations, *Science* (80-. ), 241(4869), 1043–1052, doi:10.1126/science.241.4869.1043, 1988.

1312 Arpe, K., Leroy, S. A. G. and Mikolajewicz, U.: A comparison of climate simulations for the  
1313 last glacial maximum with three different versions of the ECHAM model and implications  
1314 for summer-green tree refugia, *Clim. Past*, 91–114, doi:10.5194/cp-7-91-2011, 2011.  
1315

1316 Arslanov, K. A., Dolukhanov, P. M. and Gei, N. A.: Climate, Black Sea levels and human  
1317 settlements in Caucasus Littoral 50,000-9000 BP, *Quat. Int.*, 167–168, 121–127,  
1318 doi:10.1016/j.quaint.2007.02.013, 2007.  
1319

1320 Bañuls-Cardona, S., López-García, J. M., Blain, H. A., Lozano-Fernández, I. and Cuenca-  
1321 Bescós, G.: The end of the Last Glacial Maximum in the Iberian Peninsula characterized by  
1322 the small-mammal assemblages, *J. Iber. Geol.*, 40(1), 19–27,  
1323 doi:10.5209/rev\_JIGE.2014.v40.n1.44085, 2014.  
1324

1325 Bartlein, P. J., Harrison, S. P., Brewer, S., Connor, S., Davis, B. A. S., Gajewski, K., Guiot,  
1326 J., Harrison-Prentice, T. I., Henderson, A., Peyron, O., Prentice, I. C., Scholze, M., Seppä, H.,  
1327 Shuman, B., Sugita, S., Thompson, R. S., Viau, A. E., Williams, J. and Wu, H.: Pollen-based  
1328 continental climate reconstructions at 6 and 21 ka: A global synthesis, *Clim. Dyn.*, 37(3),  
1329 775–802, doi:10.1007/s00382-010-0904-1, 2011.  
1330

1331 de Beaulieu, J.-L. and Reille, M.: Pollen analysis of a long upper Pleistocene continental  
1332 sequence in a Velay maar (Massif Central, France), *Palaeogeogr. Palaeoclimatol. Palaeoecol.*,  
1333 80(1), 35–48, 1990.

1334 Beghin, P., Charbit, S., Kageyama, M., Combourieu-Nebout, N., Hatté, C., Dumas, C. and  
1335 Peterschmitt, J. Y.: What drives LGM precipitation over the western Mediterranean? A study  
1336 focused on the Iberian Peninsula and northern Morocco, *Clim. Dyn.*, 46(7–8), 2611–2631,  
1337 doi:10.1007/s00382-015-2720-0, 2016.  
1338

1339 Belis, C. A., Lami, A., Guilizzoni, P., Ariztegui, D. and Geiger, W.: The late Pleistocene  
1340 ostracod record of the crater lake sediments from Lago di Albano (Central Italy): Changes in  
1341 trophic status, water level and climate, *J. Paleolimnol.*, 21(2), 151–169,  
1342 doi:10.1023/A:1008095805748, 1999.  
1343

1344 Berto, C., López-García, J. M. and Luzi, E.: Changes in the Late Pleistocene small-mammal  
1345 distribution in the Italian Peninsula, *Quat. Sci. Rev.*, 225,  
1346 doi:10.1016/j.quascirev.2019.106019, 2019.  
1347

1348 Bigelow, N.H., Brubaker, L.B., Edwards, M.E., Harrison, S.P., Prentice, I.C., Anderson,  
1349 P.M., Andreev, A.A., Bartlein, P.J., Christiansen, T.R., Cramer, W., Kaplan, J.O., Lozhkin,  
1350 A.V., Matveyeva, N.V., Murray, D.F., McGuire, A.D., Razzhivin, V.Y., Ritchie, J.C., Smith,  
1351 B., Walker, D.A., Gajewski, K., Wolf, V., Holmqvist, B.H., Igarashi, Y., Kremenetskii, K.,  
1352 Paus, A., Pisaric, M.F.J., Volkova, V.S.: Climate change and arctic ecosystems: 1. Vegetation  
1353 changes north of 55 N between the last glacial maximum, mid-Holocene, and present. *J.*  
1354 *Geophys. Res.* 108 (D19), 8170. [doi.org/10.1029/2002JD002558](https://doi.org/10.1029/2002JD002558), 2013.  
1355

1356 Binney, H., Edwards, M., Macias-Fauria, M., Lozhkin, A., Anderson, P., Kaplan, J. O.,  
1357 Andreev, A., Bezrukova, E., Blyakharchuk, T., Jankovska, V., Khazina, I., Krivonogov, S.,  
1358 Kremenetski, K., Nield, J., Novenko, E., Ryabogina, N., Solovieva, N., Willis, K. and  
1359 Zernitskaya, V.: Vegetation of Eurasia from the last glacial maximum to present: Key  
1360 biogeographic patterns, *Quat. Sci. Rev.*, 157, 80–97, doi:10.1016/j.quascirev.2016.11.022,  
1361 2017.

1362  
1363 Birks, H. J. B. and Willis, K. J.: Alpines, trees, and refugia in Europe, *Plant Ecol. Divers.*,  
1364 1(2), 147–160, doi:10.1080/17550870802349146, 2008.  
1365  
1366 Bonatti, E.: Pollen sequence in the lake sediments. In: *Ianula: an account of the history and*  
1367 *development of the Lago di Monterosi, Latium, Italy*, in *Trans. Am. phil. Soc.*, vol. 60, edited  
1368 by G. E. Hutchinson, pp. 26–31., 1970.  
1369  
1370 Brewer, S., Guiot, J., Sánchez-Goñi, M. F. and Klotz, S.: The climate in Europe during the  
1371 Eemian: a multi-method approach using pollen data, *Quat. Sci. Rev.*, 27(25–26), 2303–2315,  
1372 doi:10.1016/j.quascirev.2008.08.029, 2008.  
1373  
1374 Brewer, S., Giesecke, T., Davis, B. A. S., Finsinger, W., Wolters, S., Binney, H., de  
1375 Beaulieu, J. L., Fyfe, R., Gil-Romera, G., Köhl, N., Kuneš, P., Leydet, M. and Bradshaw, R.  
1376 H.: Mapping Lateglacial and Holocene European pollen data: The maps, *J. Maps*, 13(2), 921–  
1377 928, doi:10.1080/17445647.2016.1197613, 2017.  
1378  
1379 Camuera, J., Jiménez-Moreno, G., Ramos-Román, M. J., García-Alix, A., Toney, J. L.,  
1380 Anderson, R. S., Jiménez-Espejo, F., Bright, J., Webster, C., Yanes, Y. and Carrión, J. S.:  
1381 Vegetation and climate changes during the last two glacial-interglacial cycles in the western  
1382 Mediterranean: A new long pollen record from Padul (southern Iberian Peninsula), *Quat. Sci.*  
1383 *Rev.*, 205, 86–105, doi:10.1016/j.quascirev.2018.12.013, 2019.  
1384  
1385 Cao, X., Tian, F., Dallmeyer, A. and Herzschuh, U.: Northern Hemisphere biome changes  
1386 (>30°N) since 40 cal ka BP and their driving factors inferred from model-data comparisons,  
1387 *Quat. Sci. Rev.*, 220, 291–309, doi:10.1016/j.quascirev.2019.07.034, 2019.  
1388  
1389 Carrión, J. S.: Late quaternary pollen sequence from Carihuela Cave, southern Spain, *Rev.*  
1390 *Palaeobot. Palynol.*, 71(1–4), doi:10.1016/0034-6667(92)90157-C, 1992.  
1391  
1392 Carrión, J. S.: Patterns and processes of Late Quaternary environmental change in a montane  
1393 region of southwestern Europe, *Quat. Sci. Rev.*, 21, 2047–2066, 2002.  
1394  
1395 Carrión, J. S., Finlayson, C., Fernández, S., Finlayson, G., Allué, E., López-Sáez, J. A.,  
1396 López-García, P., Gil-Romera, G., Bailey, G. and González-Sampériz, P.: A coastal reservoir  
1397 of biodiversity for Upper Pleistocene human populations: palaeoecological investigations in  
1398 Gorham’s Cave (Gibraltar) in the context of the Iberian Peninsula, *Quat. Sci. Rev.*, 27(23–  
1399 24), 2118–2135, doi:10.1016/j.quascirev.2008.08.016, 2008.  
1400  
1401 Cheddadi, R., Yu, G., Guiot, J., Harrison, S. P. and Colin Prentice, I.: The climate of Europe  
1402 6000 years ago, *Clim. Dyn.*, 13(1), 1–9, 1996.  
1403  
1404 Chevalier, M., Davis, B. A. S., Heiri, O., Seppä, H., Chase, B. M., Gajewski, K., Lacourse,  
1405 T., Telford, R. J., Finsinger, W., Guiot, J., Köhl, N., Maezumi, S. Y., Tipton, J. R., Carter, V.  
1406 A., Brussel, T., Phelps, L. N., Dawson, A., Zanon, M., Vallé, F., Nolan, C., Mauri, A., de  
1407 Vernal, A., Izumi, K., Holmström, L., Marsicek, J., Goring, S., Sommer, P. S., Chaput, M.  
1408 and Kupriyanov, D.: Pollen-based climate reconstruction techniques for late Quaternary  
1409 studies, *Earth-Science Rev.*, 210, doi:10.1016/j.earscirev.2020.103384, 2020.  
1410

1411 Cleator, S. F., Harrison, S. P., Nichols, N. K., Colin Prentice, I. and Roulstone, I.: A new  
1412 multivariable benchmark for Last Glacial Maximum climate simulations, *Clim. Past*, 16(2),  
1413 699–712, doi:10.5194/cp-16-699-2020, 2020.

1414  
1415 COHMAP,: Climatic changes of the last 18,000 years: observations and model  
1416 simulations. *Science*, 241, 1043-1052, 1988.

1417  
1418 Collins, P. M., Davis, B. A. S. and Kaplan, J. O.: The mid-Holocene vegetation of the  
1419 Mediterranean region and southern Europe, and comparison with the present day, *J.*  
1420 *Biogeogr.*, 39(10), doi:10.1111/j.1365-2699.2012.02738.x, 2012.

1421  
1422 Combourieu Nebout, N., Peyron, O., Dormoy, I., Desprat, S., Beaudouin, C., Kotthoff, U.  
1423 and Marret, F.: Rapid climatic variability in the west Mediterranean during the last 25 000  
1424 years from high resolution pollen data, *Clim. Past*, 5(3), 503–521, doi:10.5194/cp-5-503-  
1425 2009, 2009.

1426  
1427 Connor, S. E., Ross, S. A., Sobotkova, A., Herries, A. I. R., Mooney, S. D., Longford, C. and  
1428 Iliev, I.: Environmental conditions in the SE Balkans since the Last Glacial Maximum and  
1429 their influence on the spread of agriculture into Europe, *Quat. Sci. Rev.*, 68, 200–215,  
1430 doi:10.1016/j.quascirev.2013.02.011, 2013.

1431  
1432 Cowling, S. A. and Sykes, M. T.: Physiological significance of low atmospheric CO<sub>2</sub> for  
1433 plant-climate interactions, *Quat. Res.*, 52(2), 237–242, doi:10.1006/qres.1999.2065, 1999.

1434  
1435 Damblon, F.: L'enregistrement palynologique de la sequence pléistocène et holocène de la  
1436 grotte Walou, in *La grotte Walou à Trooz (Belgique)*, edited by C. Draily, S. Pirson, and M.  
1437 Toussaint, pp. 84–129, Service public de Wallonie (Etudes et Documents, Archéologie, 21),  
1438 2011.

1439  
1440 Daniau, A.-L., Desprat, S., Aleman, J. C., Bremond, L., Davis, B., Fletcher, W., Marlon, J.  
1441 R., Marquer, L., Montade, V., Morales-Molino, C., Naughton, F., Rius, D. and Urrego, D. H.:  
1442 Terrestrial plant microfossils in palaeoenvironmental studies, pollen, microcharcoal and  
1443 phytolith. Towards a comprehensive understanding of vegetation, fire and climate changes  
1444 over the past one million years, *Rev. Micropaleontol.*, 63, doi:10.1016/j.revmic.2019.02.001,  
1445 2019.

1446  
1447 Davis, B. A. S. and Stevenson, A. C.: The 8.2 ka event and Early-Mid Holocene forests, fires  
1448 and flooding in the Central Ebro Desert, NE Spain, *Quat. Sci. Rev.*, 26(13–14),  
1449 doi:10.1016/j.quascirev.2007.04.007, 2007.

1450  
1451 Davis, B. A. S., Brewer, S., Stevenson, A. C., Guiot, J., Allen, J., Almqvist-Jacobson, H.,  
1452 Ammann, B., Andreev, A. A., Argant, J., Atanassova, J., Balwierz, Z., Barnosky, C. D.,  
1453 Bartley, D. D., De Beaulieu, J. L., Beckett, S. C., Behre, K. E., Bennett, K. D., Berglund, B.  
1454 E. B., Beug, H.-J., Bezusko, L., Binka, K., Birks, H. H., Birks, H. J. B., Björck, S.,  
1455 Bliakheartchouk, T., Bogdel, I., Bonatti, E., Bottema, S., Bozilova, E. D. B., Bradshaw, R.,  
1456 Brown, A. P., Brugiapaglia, E., Carrion, J., Chernavskaya, M., Clerc, J., Clet, M., Coûteaux,  
1457 M., Craig, A. J., Cserny, T., Cwynar, L. C., Dambach, K., De Valk, E. J., Digerfeldt, G.,  
1458 Diot, M. F., Eastwood, W., Elina, G., Filimonova, L., Filipovitch, L., Gaillard-Lemdhal, M.  
1459 J., Gauthier, A., Göransson, H., Guenet, P., Gunova, V., Hall, V. A. H., Harmata, K., Hicks,  
1460 S., Huckerby, E., Huntley, B., Huttunen, A., Hyvärinen, H., Ilves, E., Jacobson, G. L., Jahns,

1461 S., Jankovská, V., Jóhansen, J., Kabailiene, M., Kelly, M. G., Khomutova, V. I., Königsson,  
 1462 L. K., Kremenetski, C., Kremenetskii, K. V., Krisai, I., Krisai, R., Kvavadze, E., Lamb, H.,  
 1463 Lazarova, M. A., Litt, T., Lotter, A. F., Lowe, J. J., Magyari, E., Makohonienko, M.,  
 1464 Mamakowa, K., Mangerud, J., Mariscal, B., Markgraf, V., McKeever, Mitchell, F. J. G.,  
 1465 Munuera, M., Nicol-Pichard, S., Noryskiewicz, B., Odgaard, B. V., Panova, N. K.,  
 1466 Pantaleon-Cano, J., Paus, A. A., Pavel, T., Peglar, S. M., Penalba, M. C., Pennington, W.,  
 1467 Perez-Obiol, R., et al.: The temperature of Europe during the Holocene reconstructed from  
 1468 pollen data, *Quat. Sci. Rev.*, 22(15–17), doi:10.1016/S0277-3791(03)00173-2, 2003.  
 1469  
 1470 Davis, B. A. S., Chevalier, M., Sommer, P., Carter, V. A., Finsinger, W., Mauri, A., Phelps,  
 1471 L. N., Zanon, M., Abegglen, R., Åkesson, C. M., Alba-Sánchez, F., Scott Anderson, R.,  
 1472 Antipina, T. G., Atanassova, J. R., Beer, R., Belyanina, N. I., Blyakharchuk, T. A., Borisova,  
 1473 O. K., Bozilova, E., Bukreeva, G., Jane Bunting, M., Clò, E., Colombaroli, D., Combourieu-  
 1474 Nebout, N., Desprat, S., Di Rita, F., Djamali, M., Edwards, K. J., Fall, P. L., Feurdean, A.,  
 1475 Fletcher, W., Florenzano, A., Furlanetto, G., Gaceur, E., Galimov, A. T., Gałka, M., García-  
 1476 Moreiras, I., Giesecke, T., Grindean, R., Guido, M. A., Gvozdeva, I. G., Herzs Schuh, U.,  
 1477 Hjelle, K. L., Ivanov, S., Jahns, S., Jankovska, V., Jiménez-Moreno, G., Karpińska-Kołodziej,  
 1478 M., Kitaba, I., Kołodziej, P., Lapteva, E. G., Latałowa, M., Lebreton, V., Leroy, S., Leydet,  
 1479 M., Lopatina, D. A., López-Sáez, J. A., Lotter, A. F., Magri, D., Marinova, E., Matthias, I.,  
 1480 Mavridou, A., Mercuri, A. M., Mesa-Fernández, J. M., Mikishin, Y. A., Milecka, K.,  
 1481 Montanari, C., Morales-Molino, C., Mrotzek, A., Sobrino, C. M., Naidina, O. D., Nakagawa,  
 1482 T., Nielsen, A. B., Novenko, E. Y., Panajiotidis, S., Panova, N. K., Papadopoulou, M.,  
 1483 Pardoe, H. S., Pędziszewska, A., Petrenko, T. I., Ramos-Román, M. J., Ravazzi, C., Rösch,  
 1484 M., Ryabogina, N., Ruiz, S. S., Sakari Salonen, J., Sapelko, T. V., Schofield, J. E., Seppä, H.,  
 1485 Shumilovskikh, L., Stivrins, N., Stojakowits, P., Svitavska, H. S., Święta-Musznicka, J.,  
 1486 Tantau, I., Tinner, W., Tobolski, K., Tonkov, S., Tsakiridou, M., et al.: The Eurasian Modern  
 1487 Pollen Database (EMPD), version 2, *Earth Syst. Sci. Data*, 12(4), 2423–2445,  
 1488 doi:10.5194/essd-12-2423-2020, 2020.  
 1489  
 1490 Davis M.B.: On the theory of pollen analysis. *American Journal of Sciences*, 26, 897–912,  
 1491 1963.  
 1492  
 1493 Demay, L., Julien, M.A., Anghelinu, M., Shydlovskiy, P.S., Koulakovska, L.V., P’ean, S.,  
 1494 Stupak, D.V., Vasyliiev, P.M., Obřada, T., Wojtal, P., Belyaeva, V.I.: Study of human  
 1495 behaviors during the Late Pleniglacial in the East European Plain through their relation to the  
 1496 animal world. *Quat. Int.* <https://doi.org/10.1016/j.quaint.2020.10.047>, 2021.  
 1497  
 1498 Douda, J., Doudová, J., Drařnarová, A., Kuneř, P., Hadincová, V., Krak, K., Zákřavský, P.  
 1499 and Mandák, B.: Migration patterns of subgenus *Alnus* in Europe since the last glacial  
 1500 maximum: A systematic review, *PLoS One*, 9(2), doi:10.1371/journal.pone.0088709, 2014.  
 1501  
 1502 Duprat-Oualid, F., Rius, D., Bégeot, C., Magny, M., Millet, L., Wulf, S. and Appelt, O.:  
 1503 Vegetation response to abrupt climate changes in Western Europe from 45 to 14.7k cal a BP:  
 1504 the Bergsee lacustrine record (Black Forest, Germany), *J. Quat. Sci.*, 32(7), 1008–1021,  
 1505 doi:10.1002/jqs.2972, 2017.  
 1506  
 1507 Dupre Ollivier, M.: *Palinología y paleoambiente- nuevos datos españoles referencias*,  
 1508 Universidad de Valencia., 1988.  
 1509

1510 Edwards, M. E., Anderson, P. M., Brubaker, L. B., Ager, T., Andreev, A. A., Bigelow, N. H.,  
1511 Cwynar, L. C., Eisner, W. R., Harrison, S. P., Hu, F.-S., Jolly, D., Lozhkin, A. V.,  
1512 MacDonald, G. M., Mock, C. J., Ritchie, J. C., Sher, A. V., Spear, R. W., Williams, J. & Yu,  
1513 G.: Pollen-based biomes for Beringia 18,000, 6000 and 0 14C yr bp. *Journal of*  
1514 *Biogeography*, **27**, 521– 554, doi: [10.1046/j.1365-2699.2000.00426.x](https://doi.org/10.1046/j.1365-2699.2000.00426.x), 2000.  
1515  
1516 Ehlers, J., Gibbard, P. L. and Hughes, P. D.: Quaternary Glaciations - Extent and Chronology  
1517 A Closer Look, edited by J. Ehlers, P. L. Gibbard, and P. D. Hughes, Elsevier., 2011.  
1518  
1519 Elenga, H., Peyron, O., Bonnefille, R., Jolly, D., Cheddadi, R., Guiot, J., Andrieu, V.,  
1520 Bottema, S., Buchet, G., De Beaulieu, J. L., Hamilton, A. C., Maley, J., Marchant, R., Perez-  
1521 Obiol, R., Reille, M., Riollet, G., Scott, L., Straka, H., Taylor, D., Van Campo, E., Vincens,  
1522 A., Laarif, F. and Jonson, H.: Pollen-based biome reconstruction for southern Europe and  
1523 Africa 18,000 yr BP, *J. Biogeogr.*, **27**(3), 621–634, doi:10.1046/j.1365-2699.2000.00430.x,  
1524 2000.  
1525  
1526 Ferguson, J. E., Henderson, G. M., Fa, D. A., Finlayson, J. C. and Charnley, N. R.: Increased  
1527 seasonality in the Western Mediterranean during the last glacial from limpet shell  
1528 geochemistry, *Earth Planet. Sci. Lett.*, **308**(3–4), 325–333, doi:10.1016/j.epsl.2011.05.054,  
1529 2011.  
1530  
1531 Feurdean A, Bhagwat SA, Willis KJ, Birks HJB, Lischke H, Hickler T.: Tree migration-rates:  
1532 narrowing the gap between inferred post-glacial rates and projected rates. *PLoS ONE* **8**:  
1533 e71797, 2013.  
1534  
1535 Feurdean, A., Perşoiu, A., Tanţău, I., Stevens, T., Magyari, E. K., Onac, B. P., Marković, S.,  
1536 Andrič, M., Connor, S., Fărcaş, S., Gałka, M., Gaudeny, T., Hoek, W., Kolaczek, P., Kuneš,  
1537 P., Lamentowicz, M., Marinova, E., Michezyńska, D. J., Perşoiu, I., Płóciennik, M.,  
1538 Słowiński, M., Stancikaite, M., Sumegi, P., Svensson, A., Tămaş, T., Timar, A., Tonkov, S.,  
1539 Toth, M., Veski, S., Willis, K. J. and Zernitskaya, V.: Climate variability and associated  
1540 vegetation response throughout Central and Eastern Europe (CEE) between 60 and 8ka, *Quat.*  
1541 *Sci. Rev.*, **106**, 206–224, doi:10.1016/j.quascirev.2014.06.003, 2014.  
1542  
1543 Fick, S. E. and Hijmans, R. J.: WorldClim 2: new 1-km spatial resolution climate surfaces for  
1544 global land areas, *Int. J. Climatol.*, **37**(12), 4302–4315, doi:10.1002/joc.5086, 2017.  
1545  
1546 Fletcher, W. J., Goni, M. F. S., Peyron, O. and Dormoy, I.: Abrupt climate changes of the last  
1547 deglaciation detected in a Western Mediterranean forest record, *Clim. Past*, **6**(2), 245–264,  
1548 doi:10.5194/cp-6-245-2010, 2010.  
1549  
1550 Gaillard, M. J., Sugita, S., Mazier, F., Trondman, A. K., Broström, A., Hickler, T., Kaplan, J.  
1551 O., Kjellström, E., Kokfelt, U., Kuneš, P., Lemmen, C., Miller, P., Olofsson, J., Poska, A.,  
1552 Rundgren, M., Smith, B., Strandberg, G., Fyfe, R., Nielsen, A. B., Alenius, T., Balakauskas,  
1553 L., Barnekow, L., Birks, H. J. B., Bjune, A., Björkman, L., Giesecke, T., Hjelle, K., Kalnina,  
1554 L., Kangur, M., Van Der Knaap, W. O., Koff, T., Lageras, P., Latałowa, M., Leydet, M.,  
1555 Lechterbeck, J., Lindbladh, M., Odgaard, B., Peglar, S., Segerström, U., Von Stedingk, H.  
1556 and Seppä, H.: Holocene land-cover reconstructions for studies on land cover-climate  
1557 feedbacks, *Clim. Past*, **6**(4), 483–499, doi:10.5194/cp-6-483-2010, 2010.  
1558



1559 García-Amorena, I., Gómez Manzaneque, F., Rubiales, J. M., Granja, H. M., Soares de  
1560 Carvalho, G. and Morla, C.: The Late Quaternary coastal forests of western Iberia: A study of  
1561 their macroremains, *Palaeogeogr. Palaeoclimatol. Palaeoecol.*, 254(3–4), 448–461,  
1562 doi:10.1016/j.palaeo.2007.07.003, 2007.

1563  
1564 Genov, I.: The Black Sea level from the Last Glacial Maximum to the present time, *Geol.*  
1565 *Balc.*, 45(1–3), 3–19, 2016.

1566  
1567 Giesecke, T.: Did thermophilous trees spread into central Europe during the Late Glacial?,  
1568 *New Phytol.*, 212(1), 15–18, doi:10.1111/nph.14149, 2016.

1569  
1570 Giesecke, T., Davis, B., Brewer, S., Finsinger, W., Wolters, S., Blaauw, M., de Beaulieu, J.-  
1571 L., Binney, H., Fyfe, R. M., Gaillard, M.-J., Gil-Romera, G., van der Knaap, W. O., Kuneš,  
1572 P., Köhl, N., van Leeuwen, J. F. N., Leydet, M., Lotter, A. F., Ortu, E., Semmler, M. and  
1573 Bradshaw, R. H. W.: Towards mapping the late Quaternary vegetation change of Europe,  
1574 *Veg. Hist. Archaeobot.*, 23(1), doi:10.1007/s00334-012-0390-y, 2014.

1575  
1576 Geiger, R.: *The climate near the ground*. Cambridge: Blue Hill Met. Observ. Harvard  
1577 University 1960

1578  
1579 Giraudi, C.: Lake levels and climate for the last 30,000 years in the fucino area (Abruzzo-  
1580 Central Italy) - A review, *Palaeogeogr. Palaeoclimatol. Palaeoecol.*, 70(1–3), 249–260,  
1581 doi:10.1016/0031-0182(89)90094-1, 1989.

1582  
1583 Giraudi, C.: Climate evolution and forcing during the last 40 ka from the oscillations in  
1584 Apennine glaciers and high mountain lakes, Italy, *J. Quat. Sci.*, 32(8), 1085–1098,  
1585 doi:10.1002/jqs.2985, 2017.

1586  
1587 Guido, M. A., Molinari, C., Moneta, V., Branch, N., Black, S., Simmonds, M., Stastney, P.  
1588 and Montanari, C.: Climate and vegetation dynamics of the Northern Apennines (Italy)  
1589 during the Late Pleistocene and Holocene, *Quat. Sci. Rev.*, 231,  
1590 doi:10.1016/j.quascirev.2020.106206, 2020.

1591 Hansen, M. C., Potapov, P. V., Moore, R., Hancher, M., Turubanova, S. A., Tyukavina, A.,  
1592 Thau, D., Stehman, S. V., Goetz, S. J., Loveland, T. R., Kommareddy, A., Egorov, A., Chini,  
1593 L., Justice, C. O. and Townshend, J. R. G.: High-resolution global maps of 21st-century  
1594 forest cover change, *Science (80-. )*, 342(6160), 850–853, doi:10.1126/science.1244693,  
1595 2013.

1596  
1597 Grichuk, V. P.: Main types of vegetation (ecosystems) for the maximum cooling of the last  
1598 glaciation. B. Frenzel, B. Pecs, A.A. Velichko (Eds.), *Atlas of Palaeoclimates and*  
1599 *Palaeoenvironments of the Northern Hemisphere*, NQUA/Hungarian Academy of  
1600 Sciences, Budapest, pp. 123-124, doi: [10.2307/1551555](https://doi.org/10.2307/1551555), 1992.

1601  
1602 Guiot, J., Torre, F., Jolly, D., Peyron, O., Boreux, J.J., Cheddadi, R.: Inverse vegetation  
1603 modeling by Monte Carlo sampling to reconstruct palaeoclimates under changed precipitation

1604 seasonality and CO<sub>2</sub> conditions: application to glacial climate in Mediterranean region. *Ecol.*  
1605 *Model.* 127, 119–140. doi: 10.1016/  
1606 S0304-3800(99)00219-7, 2000.

1607

1608 Harrison, S. P., Yu, G. E. and Tarasov, P. E.: Late Quaternary Lake-Level Record from  
1609 Northern Eurasia, *Quat. Res.*, 45(2), 138–159, doi:10.1006/qres.1996.0016, 1996.

1610

1611 Harrison, S. P., Bartlein, P. J., Brewer, S., Prentice, I. C., Boyd, M., Hessler, I., Holmgren,  
1612 K., Izumi, K. and Willis, K.: Climate model benchmarking with glacial and mid-Holocene  
1613 climates, *Clim. Dyn.*, 43(3–4), 671–688, doi:10.1007/s00382-013-1922-6, 2014.

1614

1615 Harrison, S. P., Bartlein, P. J., Izumi, K., Li, G., Annan, J., Hargreaves, J., Braconnot, P. and  
1616 Kageyama, M.: Evaluation of CMIP5 palaeo-simulations to improve climate projections, *Nat.*  
1617 *Clim. Chang.*, 5(8), 735–743, doi:10.1038/nclimate2649, 2015.

1618

1619 Heiri, O., Koinig, K. A., Spötl, C., Barrett, S., Brauer, A., Drescher-Schneider, R., Gaar, D.,  
1620 Ivy-Ochs, S., Kerschner, H., Luetscher, M., Moran, A., Nicolussi, K., Preusser, F., Schmidt,  
1621 R., Schoeneich, P., Schwörer, C., Sprafke, T., Terhorst, B. and Tinner, W.: Palaeoclimate  
1622 records 60–8 ka in the Austrian and Swiss Alps and their forelands, *Quat. Sci. Rev.*, 106,  
1623 186–205, doi:10.1016/j.quascirev.2014.05.021, 2014.

1624

1625 Heyman, B. M., Heyman, J., Fickert, T., Harbor, J. M. and Forest, B.: Paleo-climate of the  
1626 central European uplands during the last glacial maximum based on glacier mass-balance  
1627 modeling Bavarian Forest Republic, *Quat. Res.*, 79(1), 49–54,  
1628 doi:10.1016/j.yqres.2012.09.005, 2013.

1629

1630 Hughes, A. L. C., Gyllencreutz, R., Lohne, Ø. S., Mangerud, J. and Svendsen, J. I.: The last  
1631 Eurasian ice sheets - a chronological database and time-slice reconstruction, *DATED-1,*  
1632 *Boreas*, 45(1), 1–45, doi:10.1111/bor.12142, 2016.

1633

1634 Hughes, P. D. and Gibbard, P. L.: A stratigraphical basis for the Last Glacial Maximum  
1635 (LGM), *Quat. Int.*, 383(June 2014), 174–185, doi:10.1016/j.quaint.2014.06.006, 2015.

1636

1637 Hughes, P. D., Woodward, J. C. and Gibbard, P. L.: Late Pleistocene glaciers and climate in  
1638 the Mediterranean, *Glob. Planet. Change*, 50(1–2), 83–98,  
1639 doi:10.1016/j.gloplacha.2005.07.005, 2006.

1640 Huntley, B.: Dissimilarity mapping between fossil and contemporary pollen spectra in  
1641 Europe for the past 13,000 years, *Quat. Res.*, 33(3), 360–376, doi:10.1016/0033-  
1642 5894(90)90062-P, 1990.

1643

1644 Huntley B.: Dissimilarity mapping between fossil and contemporary pollen spectra in Europe  
1645 for the past 13,000 years. *Quaternary Research* 33:360–376, 1990.

1646

1647 Huntley, B. and Allen, J. R. M.: Glacial environments III. Palaeovegetation patterns in late  
1648 glacial Europe, in Neanderthals and modern humans in the European landscape during the  
1649 last glaciation, edited by T. H. Van Andel and H. C. Davies, pp. 79–102, McDonald Institute  
1650 for Archaeological Research, Cambridge., 2003.

1651

- 1652 Huntley, B. and Birks, H. J. B.: An Atlas of Past and Present Pollen Maps for Europe: 0–  
1653 13,000 B.P. years ago, Cambridge University Press, Cambridge., 1983.  
1654
- 1655 Jalut, G., Andrieu, V., Delibrias, G., Fontaugne, M. and Pages, P.: Palaeoenvironment of the  
1656 valley of Ossau (Western French Pyrenees) during the last 27 000 year, *Pollen et Spores*,  
1657 30(3–4), 357–393, 1988.  
1658
- 1659 Jalut, G., Marti, J. M., Fontugne, M., Delibrias, G., Vilaplana, J. M. and Julia, R.: Glacial to  
1660 interglacial vegetation changes in the northern and southern Pyrénées: Deglaciation,  
1661 vegetation cover and chronology, *Quat. Sci. Rev.*, 11(4), 449–480, doi:10.1016/0277-  
1662 3791(92)90027-6, 1992.  
1663
- 1664 Jankovska, V.: Vegetation cover in West Carpathians during the Last Glacial period -  
1665 analogy of present day siberian forest-tundra nad taiga, *Palynol. Stratigr. geoecology*,  
1666 (SEPTEMBER 2008), 282–289, 2008.  
1667
- 1668 Janská, V., Jiménez-Alfaro, B., Chytrý, M., Divíšek, J., Anenkhonov, O., Korolyuk, A.,  
1669 Lashchinskyi, N. and Culek, M.: Palaeodistribution modelling of European vegetation types  
1670 at the Last Glacial Maximum using modern analogues from Siberia: Prospects and  
1671 limitations, *Quat. Sci. Rev.*, 159, 103–115, doi:10.1016/j.quascirev.2017.01.011, 2017.  
1672
- 1673 Jost, A., Lunt, D., Abe-Ouchi, A., Abe-Ouchi, A., Peyron, O., Valdes, P. J. and Ramstein, G.:  
1674 High-resolution simulations of the last glacial maximum climate over Europe: A solution to  
1675 discrepancies with continental palaeoclimatic reconstructions?, *Clim. Dyn.*, 24(6), 577–590,  
1676 doi:10.1007/s00382-005-0009-4, 2005.  
1677
- 1678 Juggins, S.: Quantitative reconstructions in palaeolimnology : new paradigm or sick  
1679 science ?, *Quat. Sci. Rev.*, 64, 20–32, doi:10.1016/j.quascirev.2012.12.014, 2013.  
1680
- 1681 Juggins, S.: Rioja: Analysis of Quaternary Science Data, [online] Available from:  
1682 <https://cran.r-project.org/package=rioja>, 2020.  
1683
- 1684 Juggins, S. and Birks, H. J. B.: Quantitative Environmental Reconstructions from Biological  
1685 Data, in *Developments in Palaeoenvironmental Research 5*, edited by H. J. B. Birks, pp. 431–  
1686 494, Springer ScienceCBusiness Media B.V., 2012.  
1687
- 1688 Juříčková, L., Horáčková, J. and Ložek, V.: Direct evidence of central European forest  
1689 refugia during the last glacial period based on mollusc fossils, *Quat. Res. (United States)*,  
1690 82(1), 222–228, doi:10.1016/j.yqres.2014.01.015, 2014.  
1691
- 1692 Kageyama, M., Laine, A., Abe-Ouchi, A., Braconnot, P., Cortijo, E., Crucifix, M., de Vernal,  
1693 A., Guiot, J., Hewitt, C. D., Kitoh, A., Kucera, M., Marti, O., Ohgaito, R., Otto-Bliesner, B.,  
1694 Peltier, W. R., Rosell-Melé, A., Vettoretti, G., Weber, S. L. and Yu, Y.: Last Glacial  
1695 Maximum temperatures over the North Atlantic, Europe and western Siberia: a comparison  
1696 between PMIP models, MARGO sea-surface temperatures and pollen-based reconstructions,  
1697 *Quat. Sci. Rev.*, 25(17–18), 2082–2102, doi:10.1016/j.quascirev.2006.02.010, 2006.  
1698
- 1699 Kageyama, M., Harrison, S. P., Kapsch, M. L., Lofverstrom, M., Lora, J. M., Mikolajewicz,  
1700 U., ... & Zhu, J. The PMIP4 Last Glacial Maximum experiments: preliminary results and  
1701 comparison with the PMIP3 simulations. *Climate of the Past*, 17(3), 1065-1089, 2021.

1702  
1703 Kaltenrieder, P., Belis, C. A., Hofstetter, S., Ammann, B., Ravazzi, C. and Tinner, W.:  
1704 Environmental and climatic conditions at a potential Glacial refugial site of tree species near  
1705 the Southern Alpine glaciers. New insights from multiproxy sedimentary studies at Lago  
1706 della Costa (Euganean Hills, Northeastern Italy), *Quat. Sci. Rev.*, 28(25–26), 2647–2662,  
1707 doi:10.1016/j.quascirev.2009.05.025, 2009.  
1708  
1709 Kaplan, J. O., Pfeiffer, M., Kolen, J. C. A. and Davis, B. A. S.: Large scale anthropogenic  
1710 reduction of forest cover in last glacial maximum Europe, *PLoS One*, 11(11),  
1711 doi:10.1371/journal.pone.0166726, 2016.  
1712  
1713 Kehrwald, N. M., McCoy, W. D., Thibeault, J., Burns, S. J. and Oches, E. A.: Paleoclimatic  
1714 implications of the spatial patterns of modern and LGM European land-snail shell  $\delta^{18}\text{O}$ ,  
1715 *Quat. Res.*, 74(1), 166–176, doi:10.1016/j.yqres.2010.03.001, 2010.  
1716  
1717 Kelly, A., Charman, D. J. and Newnham, R. M.: A last glacial maximum pollen record from  
1718 bodmin moor showing a possible cryptic Northern refugium in Southwest England, *J. Quat.*  
1719 *Sci.*, 25(3), 296–308, doi:10.1002/jqs.1309, 2010.  
1720  
1721 Kolodny, Y., Stein, M. and Machlus, M.: Sea-rain-lake relation in the Last Glacial East  
1722 Mediterranean revealed by  $\delta^{18}\text{O}$ - $\delta^{13}\text{C}$  in Lake Lisan aragonites, *Geochim. Cosmochim.*  
1723 *Acta*, 69(16), 4045–4060, doi:10.1016/j.gca.2004.11.022, 2005.  
1724  
1725 Kovács, J., Moravcová, M., Újvári, G. and Pintér, A. G.: Reconstructing the  
1726 paleoenvironment of East Central Europe in the Late Pleistocene using the oxygen and  
1727 carbon isotopic signal of tooth in large mammal remains, *Quat. Int.*, 276–277, 145–154,  
1728 doi:10.1016/j.quaint.2012.04.009, 2012.  
1729  
1730 Krebs, P., Pezzatti, G. B., Beffa, G., Tinner, W. and Conedera, M.: Revising the sweet  
1731 chestnut (*Castanea sativa* Mill.) refugia history of the last glacial period with extended pollen  
1732 and macrofossil evidence, *Quat. Sci. Rev.*, 206, 111–128,  
1733 doi:10.1016/j.quascirev.2019.01.002, 2019.  
1734  
1735 Kuneš, P., Pelánková, B., Chytrý, M., Jankovská, V., Pokorný, P. and Petr, L.: Interpretation  
1736 of the last-glacial vegetation of eastern-central Europe using modern analogues from southern  
1737 Siberia, *J. Biogeogr.*, 35(12), 2223–2236, doi:10.1111/j.1365-2699.2008.01974.x, 2008.  
1738  
1739 Küster, H.: Postglaziale Vegetationsgeschichte Südbayerns. Geobotanische Studien zur  
1740 Prähistorischen Landschaftskunde, Akademie Verlag, Berlin., 1995.  
1741  
1742 Lacey, J. H., Leng, M. J., Höbig, N., Reed, J. M., Valero-Garcés, B. and Reicherter, K.:  
1743 Western Mediterranean climate and environment since Marine Isotope Stage 3: a 50,000-year  
1744 record from Lake Banyoles, Spain, *J. Paleolimnol.*, 55(2), 113–128, doi:10.1007/s10933-015-  
1745 9868-9, 2016.  
1746  
1747 Latombe, G., Burke, A., Vrac, M., Levavasseur, G. and Dumas, C.: Comparison of spatial  
1748 downscaling methods of general circulation model results to study climate variability during  
1749 the Last Glacial Maximum, , 2563–2579, 2018.  
1750

- 1751 Lefort J.P., Monnier J.L., Danukalova G.: Transport of Late Pleistocene loess particles by  
1752 katabatic winds during the lowstands of the English Channel. *Journal of the Geological*  
1753 *Society* 176: 1169–1181, doi: [10.1144/jgs2019-07](https://doi.org/10.1144/jgs2019-07), 2019.
- 1754  
1755 Lehmkuhl, F., Nett, J.J., Pöfner, S., Schulte, P., Sprafke, T., Jary, Z., Antoine, P., Wacha, L.,  
1756 Wolf, D., Zerboni, A., Hošek, J., Marković, S.B., Obrecht, I., Sümeği, P., Veres, D.,  
1757 Zeeden, C., Boemke, B., Schaubert, V., Viehweger, J., Hambach, U.: Loess landscapes of  
1758 Europe re-mapping, geomorphology, and zonal differentiation. *Earth Sci. Rev.* 215, 103496.  
1759 <https://doi.org/10.1016/j.earscirev.2020.103496>, 2021.
- 1760  
1761 Leroy, S. A. G. and Arpe, K.: Glacial refugia for summer-green trees in Europe and south-  
1762 west Asia as proposed by ECHAM3 time-slice atmospheric model simulations, *J. Biogeogr.*,  
1763 34(12), 2115–2128, doi:10.1111/j.1365-2699.2007.01754.x, 2007.
- 1764  
1765 Lev, L., Stein, M., Ito, E., Fruchter, N., Ben-Avraham, Z. and Almogi-Labin, A.:  
1766 Sedimentary, geochemical and hydrological history of Lake Kinneret during the past 28,000  
1767 years, *Quat. Sci. Rev.*, 209, 114–128, doi:10.1016/j.quascirev.2019.02.015, 2019.
- 1768  
1769 Lister, A. M. and Stuart, A. J.: The impact of climate change on large mammal distribution  
1770 and extinction: Evidence from the last glacial/interglacial transition, *Comptes Rendus -*  
1771 *Geosci.*, 340(9–10), 615–620, doi:10.1016/j.crte.2008.04.001, 2008.
- 1772  
1773 López-García, J. M. and Blain, H. A.: Quaternary small vertebrates: State of the art and new  
1774 insights, *Quat. Sci. Rev.*, 233, doi:10.1016/j.quascirev.2020.106242, 2020.
- 1775  
1776 Ludwig, P., Pinto, J. G., Raible, C. C. and Shao, Y.: Impacts of surface boundary conditions  
1777 on regional climate model simulations of European climate during the Last Glacial  
1778 Maximum, *Geophys. Res. Lett.*, 44(10), 5086–5095, doi:10.1002/2017GL073622, 2017.
- 1779  
1780  
1781 Luetscher, M., Boch, R., Sodemann, H., Spötl, C., Cheng, H., Edwards, R. L., Frisia, S., Hof,  
1782 F. and Müller, W.: North Atlantic storm track changes during the Last Glacial Maximum  
1783 recorded by Alpine speleothems, *Nat. Commun.*, 6, 27–32, doi:10.1038/ncomms7344, 2015.
- 1784  
1785 Magri, D.: Persistence of tree taxa in Europe and Quaternary climate changes, *Quat. Int.*,  
1786 219(1–2), 145–151, doi:10.1016/j.quaint.2009.10.032, 2010.
- 1787  
1788 Magri, D. and Parra, I.: Late Quaternary western Mediterranean pollen records and African  
1789 winds, *Earth Planet. Sci. Lett.*, 200(3–4), 401–408, doi:10.1016/S0012-821X(02)00619-2,  
1790 2002.
- 1791  
1792 Magri, D. and Sadori, L.: Late Pleistocene and Holocene pollen stratigraphy at Lago di Vico,  
1793 central Italy, *Veg. Hist. Archaeobot.*, 8(4), 247–260, doi:10.1007/BF01291777, 1999.
- 1794  
1795 Magyari, E., Jakab, G., Rudner, E. and Sümeği, P.: Palynological and plant macrofossil data  
1796 on Late Pleistocene short-term climatic oscillations in NE-Hungary, *Acta Palaeobot. Suppl.*,  
1797 2(January), 491–502, 1999.
- 1798  
1799 Magyari, E. K., Kuneš, P., Jakab, G., Sümeği, P., Pelánková, B., Schäbitz, F., Braun, M. and  
1800 Chytrý, M.: Late Pleniglacial vegetation in eastern-central Europe: Are there modern

1801 analogues in Siberia?, *Quat. Sci. Rev.*, 95, 60–79, doi:10.1016/j.quascirev.2014.04.020,  
1802 2014a.

1803

1804 Magyari, E. K., Veres, D., Wennrich, V., Wagner, B., Braun, M., Jakab, G., Karátson, D.,  
1805 Pál, Z., Ferenczy, G., St-Onge, G., Rethemeyer, J., Francois, J. P., von Reumont, F. and  
1806 Schäbitz, F.: Vegetation and environmental responses to climate forcing during the Last  
1807 Glacial Maximum and deglaciation in the East Carpathians: Attenuated response to  
1808 maximum cooling and increased biomass burning, *Quat. Sci. Rev.*, 106, 278–298,  
1809 doi:10.1016/j.quascirev.2014.09.015, 2014b.

1810

1811 Magyari, E. K., Pál, I., Vincze, I., Veres, D., Jakab, G., Braun, M., Szalai, Z., Szabó, Z. and  
1812 Korponai, J.: Warm Younger Dryas summers and early late glacial spread of temperate  
1813 deciduous trees in the Pannonian Basin during the last glacial termination (20-9 kyr cal BP),  
1814 *Quat. Sci. Rev.*, 225, doi:10.1016/j.quascirev.2019.105980, 2019.

1815

1816 Margari, V., Gibbard, P. L., Bryant, C. L. and Tzedakis, P. C.: Character of vegetational and  
1817 environmental changes in southern Europe during the last glacial period; evidence from  
1818 Lesvos Island, Greece, *Quat. Sci. Rev.*, 28(13–14), 1317–1339,  
1819 doi:10.1016/j.quascirev.2009.01.008, 2009.

1820

1821 Marsicek, J., Shuman, B. N., Bartlein, P. J., Shafer, S. L. and Brewer, S.: Reconciling  
1822 divergent trends and millennial variations in Holocene temperatures, *Nature*, 554(7690), 92–  
1823 96, doi:10.1038/nature25464, 2018.

1824

1825 Mauch Lenardić, J., Oros Sršen, A. and Radović, S.: Quaternary fauna of the Eastern Adriatic  
1826 (Croatia) with the special review on the Late Pleistocene sites, *Quat. Int.*, 494, 130–151,  
1827 doi:10.1016/j.quaint.2017.11.028, 2018.

1828

1829 Mauri, A., Davis, B. A. S., Collins, P. M. and Kaplan, J. O.: The influence of atmospheric  
1830 circulation on the mid-Holocene climate of Europe: A data-model comparison, *Clim. Past*,  
1831 10(5), 1925–1938, doi:10.5194/cp-10-1925-2014, 2014.

1832

1833 Mauri, A., Davis, B. A. S., Collins, P. M. and Kaplan, J. O.: The climate of Europe during the  
1834 Holocene: A gridded pollen-based reconstruction and its multi-proxy evaluation, *Quat. Sci.*  
1835 *Rev.*, 112, doi:10.1016/j.quascirev.2015.01.013, 2015.

1836

1837 MARGE Project Members.: Constraints on the magnitude and patterns of ocean cooling at  
1838 the Last Glacial Maximum, , (January), 1–6, doi:10.1038/ngeo411, 2009.

1839

1840 Mikolajewicz, U.: Modeling mediterranean ocean climate of the last glacial maximum, *Clim.*  
1841 *Past*, 7(1), 161–180, doi:10.5194/cp-7-161-2011, 2011.

1842

1843 Miola, A., Bondesan, A., Corain, L., Favaretto, S., Mozzi, P., Piovan, S. and Sostizzo, I.:  
1844 Wetlands in the Venetian Po Plain (northeastern Italy) during the Last Glacial Maximum:  
1845 Interplay between vegetation, hydrology and sedimentary environment, *Rev. Palaeobot.*  
1846 *Palynol.*, 141(1–2), 53–81, doi:10.1016/j.revpalbo.2006.03.016, 2006.

1847

1848 Mix, A. C., Bard, E. and Schneider, R.: Environmental processes of the ice age: Land,  
1849 oceans, glaciers (EPILOG), *Quat. Sci. Rev.*, 20(4), 627–657, doi:10.1016/S0277-  
1850 3791(00)00145-1, 2001.

- 1851 Moine, O., Rousseau, D. D., Jolly, D. and Vianey-Liaud, M.: Paleoclimatic reconstruction  
 1852 using mutual climatic range on terrestrial mollusks, *Quat. Res.*, 57(1), 162–172,  
 1853 doi:10.1006/qres.2001.2286, 2002.
- 1854
- 1855 Monegato, G., Ravazzi, C., Donegana, M., Pini, R., Calderoni, G. and Wick, L.: Evidence of  
 1856 a two-fold glacial advance during the last glacial maximum in the Tagliamento end moraine  
 1857 system (eastern Alps), *Quat. Res.*, 68(2), 284–302, doi:10.1016/j.yqres.2007.07.002, 2007.
- 1858
- 1859 Monegato, G., Ravazzi, C., Culiberg, M., Pini, R., Bavec, M., Calderoni, G., Jež, J. and  
 1860 Perego, R.: Sedimentary evolution and persistence of open forests between the south-eastern  
 1861 Alpine fringe and the Northern Dinarides during the Last Glacial Maximum, *Palaeogeogr.*  
 1862 *Palaeoclimatol. Palaeoecol.*, 436, 23–40, doi:10.1016/j.palaeo.2015.06.025, 2015.
- 1863
- 1864 Moreno, A., González-Sampériz, P., Morellón, M., Valero-Garcés, B. L. and Fletcher, W. J.:  
 1865 Northern Iberian abrupt climate change dynamics during the last glacial cycle: A view from  
 1866 lacustrine sediments, *Quat. Sci. Rev.*, 36, 139–153, doi:10.1016/j.quascirev.2010.06.031,  
 1867 2012.
- 1868
- 1869 Nogues-Bravo D, Rodríguez-Sánchez F, Orsini L, de Boer E, Jansson R, Morlon, H.,  
 1870 Fordham, D.A., Jackson, S.T.: Cracking the code of biodiversity responses to past climate  
 1871 change. *Trends Ecol. Evol.* 33:765–76, 2018.
- 1872
- 1873
- 1874 Nolan, C., Overpeck, J. T., Allen, J. R. M., Anderson, P. M., Betancourt, J. L., Binney, H. A.,  
 1875 Brewer, S., Bush, M. B., Chase, B. M., Cheddadi, R., Djamali, M., Dodson, J., Edwards, M.  
 1876 E., Gosling, W. D., Haberle, S., Hotchkiss, S. C., Huntley, B., Ivory, S. J., Kershaw, A. P.,  
 1877 Kim, S. H., Latorre, C., Leydet, M., Lézine, A. M., Liu, K. B., Liu, Y., Lozhkin, A. V.,  
 1878 McGlone, M. S., Marchant, R. A., Momohara, A., Moreno, P. I., Müller, S., Otto-Bliesner, B.  
 1879 L., Shen, C., Stevenson, J., Takahara, H., Tarasov, P. E., Tipton, J., Vincens, A., Weng, C.,  
 1880 Xu, Q., Zheng, Z. and Jackson, S. T.: Past and future global transformation of terrestrial  
 1881 ecosystems under climate change, *Science* (80-. ), 361(6405), 920–923,  
 1882 doi:10.1126/science.aan5360, 2018.
- 1883
- 1884 Normand, S., Treier, U. A. and Odgaard, B. V.: Tree refugia and slow forest development in  
 1885 response to post - LGM warming in North - Eastern European Russia, , 2(4), 2–5, 2011.
- 1886
- 1887 Paganelli, A.: Evolution of vegetation and climate in the Veneto-Po Plain during the Late-  
 1888 Glacial and Early Holocene using pollen-stratigraphical data, *Alp. Mediterr. Quat.*, 9(2),  
 1889 581–589, 1996.
- 1890
- 1891 Peyron, O., Guiot, J., Cheddadi, R., Tarasov, P., Reille, M., De Beaulieu, J. L., Bottema, S.  
 1892 and Andrieu, V.: Climatic Reconstruction in Europe for 18,000 YR B.P. from Pollen Data,  
 1893 *Quat. Res.*, 49(2), 183–196, doi:10.1006/qres.1997.1961, 1998a.
- 1894
- 1895 Pons, A. and Reille, M.: The Holocene- and upper Pleistocene pollen record from Padul  
 1896 (Granada, Spain): A new study, *Palaeogeogr. Palaeoclimatol. Palaeoecol.*, 66(3–4),  
 1897 doi:10.1016/0031-0182(88)90202-7, 1988.
- 1898
- 1899 Potì, A., Kehl, M., Broich, M., Carrión Marco, Y., Hutterer, R., Jentke, T., Linstädter, J.,  
 1900 López-Sáez, J. A., Mikdad, A., Morales, J., Pérez-Díaz, S., Portillo, M., Schmid, C., Vidal-

1901 Matutano, P. and Weniger, G. C.: Human occupation and environmental change in the  
1902 western Maghreb during the Last Glacial Maximum (LGM) and the Late Glacial. New  
1903 evidence from the Iberomaurusian site Ifri El Baroud (northeast Morocco), *Quat. Sci. Rev.*,  
1904 220, 87–110, doi:10.1016/j.quascirev.2019.07.013, 2019.

1905  
1906 Prentice, I. C., Cleator, S. F., Huang, Y. H., Harrison, S. P., and Roulstone, I.: Reconstructing  
1907 ice-age palaeoclimates: Quantifying low-CO<sub>2</sub> effects on plants, *Global Planet. Change*, 149,  
1908 166–176, <https://doi.org/10.1016/j.gloplacha.2016.12.012>, 2017.

1909  
1910 Prentice, I. C. and Harrison, S. P.: Ecosystem effects of CO<sub>2</sub> concentration: Evidence from  
1911 past climates, *Clim. Past*, 5(3), 297–307, doi:10.5194/cp-5-297-2009, 2009.

1912  
1913 Prentice, I. C., Guiot, J. and Harrison, S. P.: Mediterranean vegetation, lake levels and  
1914 palaeoclimate at the Last Glacial Maximum, *Nature*, 360(6405), 658–660,  
1915 doi:10.1038/360658a0, 1992.

1916  
1917 Prentice, I. C., Guiot, J., Huntley, B., Jolly, D. and Cheddadi, R.: Reconstructing biomes  
1918 from palaeoecological data: A general method and its application to European pollen data at  
1919 0 and 6 ka, *Clim. Dyn.*, 12(3), 185–194, doi:10.1007/BF00211617, 1996.

1920  
1921 Prentice, I. C., Harrison, S. P. and Bartlein, P. J.: Global vegetation and terrestrial carbon  
1922 cycle changes after the last ice age, *New Phytol.*, 189(4), 988–998, doi:10.1111/j.1469-  
1923 8137.2010.03620.x, 2011.

1924  
1925 Prud'homme, C., Lécuyer, C., Antoine, P., Moine, O., Hatté, C., Fourel, F., Martineau, F. and  
1926 Rousseau, D. D.: Palaeotemperature reconstruction during the Last Glacial from  $\delta^{18}\text{O}$  of  
1927 earthworm calcite granules from Nussloch loess sequence, Germany, *Earth Planet. Sci. Lett.*,  
1928 442, 13–20, doi:10.1016/j.epsl.2016.02.045, 2016.

1929  
1930 Prud'homme, C., Lécuyer, C., Antoine, P., Hatté, C., Moine, O., Fourel, F., Amiot, R.,  
1931 Martineau, F. and Rousseau, D. D.:  $\delta^{13}\text{C}$  signal of earthworm calcite granules: A new proxy  
1932 for palaeoprecipitation reconstructions during the Last Glacial in western Europe, *Quat. Sci.*  
1933 *Rev.*, 179, 158–166, doi:10.1016/j.quascirev.2017.11.017, 2018.

1934  
1935 Puzachenko, A. Y., Markova, A. K. and Pawłowska, K.: Evolution of Central European  
1936 regional mammal assemblages between the late Middle Pleistocene and the Holocene (MIS7–  
1937 MIS1), *Quat. Int.*, (November), doi:10.1016/j.quaint.2021.11.009, 2021.

1938  
1939 Ramstein, G., Kageyama, M., Guiot, J. and Wu, H.: How cold was Europe at the Last Glacial  
1940 Maximum ? A synthesis of the progress achieved since the first PMIP model-data  
1941 comparison, , 331–339, 2007.

1942  
1943 Reille, M. and Andrieu, V.: The late Pleistocene and Holocene in the Lourdes Basin, Western  
1944 Pyrénées, France: new pollen analytical and chronological data, *Veg. Hist. Archaeobot.*, 4(1),  
1945 1–21, doi:10.1007/BF00198611, 1995.

1946  
1947 Reille, M. and de Beaulieu, J. L.: History of the Würm and Holocene vegetation in western  
1948 velay (Massif Central, France): A comparison of pollen analysis from three corings at Lac du  
1949 Bouchet, *Rev. Palaeobot. Palynol.*, 54(3–4), 233–248, doi:10.1016/0034-6667(88)90016-4,  
1950 1988.



1951

1952 Reimer, A., Landmann, G. and Kempe, S.: Lake Van, Eastern Anatolia, hydrochemistry and

1953 history, *Aquat. Geochemistry*, 15(1–2), 195–222, doi:10.1007/s10498-008-9049-9, 2009.

1954

1955 Rousseau, D. D.: Climatic transfer function from quaternary molluscs in European loess

1956 deposits, *Quat. Res.*, 36(2), 195–209, doi:10.1016/0033-5894(91)90025-Z, 1991.

1957

1958 Royer, A., Montuire, S., Legendre, S., Discamps, E., Jeannet, M. and Lécuyer, C.:

1959 Investigating the influence of climate changes on rodent communities at a regional-scale

1960 (MIS 1-3, Southwestern France), *PLoS One*, 11(1), 1–25, doi:10.1371/journal.pone.0145600,

1961 2016.

1962

1963 Ruiz-Zapata, M. B., Vegas, J., Garcia-Cortes, A., Gil Garcia, M. J., Torres, T., Ortiz, J. E.

1964 and Perez-Gonzalez, A.: Vegetation evolution during the Last Maximum Glacial Period in

1965 FU-1 sequence (Fuentillejo Lacustrin Maar, Campo de Calatrava, Ciudad Real), *Polen*, 18,

1966 37–49, 2008.

1967

1968 Salonen, J., Sanchez Goñi, M.F., Renssen, H. and Plikk, A.: Contrasting northern and

1969 southern European winter climate trends during the Last Interglacial. *Geology* 49.

1970 10.1130/G49007.1. 2021

1971

1972 Salonen, J.S., Ilvonen, L., Seppä, H., Holmström, L., Telford, R.J., Gaidamavicius, A.,

1973 Stancikaite, M., Subetto, D. Comparing different calibration methods (WA/WA-PLS

1974 regression and Bayesian modelling) and different-sized calibration sets in pollen-based

1975 quantitative climate reconstruction. *The Holocene* 22, 413–424, 2012.

1976

1977 Samartin, S., Heiri, O., Kaltenrieder, P., Köhl, N. and Tinner, W.: Reconstruction of full

1978 glacial environments and summer temperatures from Lago della Costa, a refugial site in

1979 Northern Italy, *Quat. Sci. Rev.*, 143, 107–119, doi:10.1016/j.quascirev.2016.04.005, 2016.

1980

1981 Sánchez Goñi, M.F., Loutre, M.F., Crucifix, M., Peyron, O., Santos, L., Duprat, J., Malaizé,

1982 B., Turon, J.-L., and Peypouquet, J.-P.: Increasing vegetation and climate gradient in western

1983 Europe over the Last Glacial inception (122–110 ka): Data–model comparison. *Earth and*

1984 *Planetary Science Letters*, 231, 111–130, doi: 10.1016/j.epsl.2004.12.010, 2005.

1985

1986 Sanchez Goñi, M.F., Harrison, S.P.: Millennial-scale climate variability and vegetation

1987 changes during the Last Glacial: concepts and terminology. *Quaternary Science*

1988 *Reviews* 29, 2823–2827, doi: [10.1016/j.quascirev.2009.11.014](https://doi.org/10.1016/j.quascirev.2009.11.014), 2010.

1989

1990 Sanchi, L., Ménot, G. and Bard, E.: Insights into continental temperatures in the northwestern

1991 Black Sea area during the Last Glacial period using branched tetraether lipids, *Quat. Sci.*

1992 *Rev.*, 84, 98–108, doi:10.1016/j.quascirev.2013.11.013, 2014.

1993

1994 Satkūnas, J. and Grigienė, A.: Eemian-Weichselian palaeoenvironmental record from the

1995 Mickūnai glacial depression (Eastern Lithuania), *Geologija*, 54(2), 35–51,

1996 doi:10.6001/geologija.v54i2.2482, 2012.

1997 Schäfer, I. K., Bliedtner, M., Wolf, D., Faust, D. and Zech, R.: Evidence for humid

1998 conditions during the last glacial from leaf wax patterns in the loess-paleosol sequence El

1999 Paraíso, Central Spain, *Quat. Int.*, 407, 64–73, doi:10.1016/j.quaint.2016.01.061, 2016.

2000

2001 Scourse, J. D.: Late Pleistocene stratigraphy and palaeobotany of the Isles of Scilly, *Philos.*  
2002 *Trans. - R. Soc. London, B*, 334(1271), 405–448, doi:10.1098/rstb.1991.0125, 1991.  
2003  
2004 Spötl, C., Koltai, G., Jarosch, A. H. and Cheng, H.: Increased autumn and winter  
2005 precipitation during the Last Glacial Maximum in the European Alps, *Nat. Commun.*, 12(1),  
2006 doi:10.1038/s41467-021-22090-7, 2021.  
2007  
2008 Stewart, J. R. and Lister, A. M.: Cryptic northern refugia and the origins of the modern biota,  
2009 *Trends Ecol. Evol.*, 16(11), 608–613, doi:10.1016/S0169-5347(01)02338-2, 2001.  
2010  
2011 Stivrins, N., Soininen, J., Amon, L., Fontana, S. L., Gryguc, G., Heikkilä, M., Heiri, O.,  
2012 Kisielienė, D., Reitalu, T., Stančikaitė, M., Veski, S. and Seppä, H.: Biotic turnover rates  
2013 during the Pleistocene-Holocene transition, *Quat. Sci. Rev.*, 151, 100–110,  
2014 doi:10.1016/j.quascirev.2016.09.008, 2016.  
2015  
2016 Strahl, J.: Zur Pollenstratigraphie des Weichselspätglazials von Berlin-Brandenburg [On the  
2017 palynostratigraphy of the Late Weichselian in Berlin-Brandenburg], *Brand.*  
2018 *Geowissenschaftliche Beiträge*, 12, 87–112, 2005.  
2019  
2020 Stute, M. and Deak, J.: Environmental isotope study (14C, 13C, 18O, D, noble gases) on  
2021 deep groundwater circulation systems in Hungary with reference to paleoclimate,  
2022 *Radiocarbon*, 31(3), 902–918, doi:10.1017/s0033822200012522, 1990.  
2023  
2024 Svenning, J., Normand, S. and Kageyama, M.: Glacial refugia of temperate trees in Europe :  
2025 insights from species distribution modelling, (Svenning 2003), 1117–1127,  
2026 doi:10.1111/j.1365-2745.2008.01422.x, 2008.  
2027  
2028 Tarasov, P. E., Webb, T., Andreev, A. A., Afanas'eva, N. B., Berezina, N. A., Bezusko, L.  
2029 G., Blyakharchuk, T. A., Bolikhovskaya, N. S., Cheddadi, R., Chernavskaya, M. M.,  
2030 Chernova, G. M., Dorofeyuk, N. I., Dirksen, V. G., Elina, G. A., Filimonova, L. V., Glebov,  
2031 F. Z., Guiot, J., Gunova, V. S., Harrison, S. P., Jolly, D., Khomutova, V. I., Kvavadze, E. V.,  
2032 Osipova, I. M., Panova, N. K., Prentice, I. C., Saarse, L., Sevastyanov, D. V., Volkova, V. S.  
2033 and Zernitskaya, V. P.: Present-day and mid-Holocene biomes reconstructed from pollen and  
2034 plant macrofossil data from the former Soviet Union and Mongolia, *J. Biogeogr.*, 25(6),  
2035 1029–1053, doi:10.1046/j.1365-2699.1998.00236.x, 1998.  
2036  
2037 Tarasov, P. E., Volkova, V. S., Webb, T., Guiot, J., Andreev, A. A., Bezusko, L. G.,  
2038 Bezusko, T. V., Bykova, G. V., Dorofeyuk, N. I., Kvavadze, E. V., Osipova, I. M., Panova,  
2039 N. K. and Sevastyanov, D. V.: Last glacial maximum biomes reconstructed from pollen and  
2040 plant macrofossil data from northern Eurasia, *J. Biogeogr.*, 27(3), 609–620,  
2041 doi:10.1046/j.1365-2699.2000.00429.x, 2000.  
2042  
2043 Tarasov, P.E., Andreev, A.A., Anderson, P.M., Lozhkin, A.V., Haltia-Hovi, E., Nowaczyk,  
2044 N.R., Wennrich, V., Brigham-Grette, J., Melles, M.: A pollen-based biome reconstruction  
2045 over the last 3.562 million years in the Far East Russian Arctic e new insights on climate-  
2046 vegetation relationships at the regional scale. *Clim. Past* 9, 2759-2775, doi: 10.5194/cp-9-  
2047 2759-2013, 2013.  
2048

- 2049 Telford, R. J. and Birks, H. J. B.: Evaluation of transfer functions in spatially structured  
 2050 environments, *Quat. Sci. Rev.*, 28(13–14), 1309–1316, doi:10.1016/j.quascirev.2008.12.020,  
 2051 2009.
- 2052
- 2053 Turner, M. G., Wei, D., Prentice, I. C., & Harrison, S. P. The impact of methodological  
 2054 decisions on climate reconstructions using WA-PLS. *Quaternary Research*, 99, 341-356,  
 2055 2021.
- 2056
- 2057 Valero-Garcés, B. L., González-Sampériz, P., Navas, A., Machin, J., Delgado-Huertas, A.,  
 2058 Pena-Monné, J. L., Sancho-Marcén, C., Stevenson, T. and Davis, B.: Paleohydrological  
 2059 fluctuations and steppe vegetation during the last glacial maximum in the central Ebro valley  
 2060 (NE Spain), *Quat. Int.*, 122(1 SPEC. ISS.), doi:10.1016/j.quaint.2004.01.030, 2004.
- 2061
- 2062 Valsecchi, V., Sanchez Goñi, M. F. and Londeix, L.: Vegetation dynamics in the  
 2063 Northeastern Mediterranean region during the past 23 000 yr: Insights from a new pollen  
 2064 record from the Sea of Marmara, *Clim. Past*, 8(5), 1941–1956, doi:10.5194/cp-8-1941-2012,  
 2065 2012.
- 2066
- 2067 Vandenberghe, J., French, H. M., Gorbunov, A., Marchenko, S., Velichko, A. A., Jin, H.,  
 2068 Cui, Z., Zhang, T. and Wan, X.: The Last Permafrost Maximum (LPM) map of the Northern  
 2069 Hemisphere: Permafrost extent and mean annual air temperatures, 25-17ka BP, *Boreas*,  
 2070 43(3), 652–666, doi:10.1111/bor.12070, 2014.
- 2071
- 2072 Varsányi, I., Palcsu, L. and Kovács, L. Ó.: Groundwater flow system as an archive of  
 2073 palaeotemperature: Noble gas, radiocarbon, stable isotope and geochemical study in the  
 2074 Pannonian Basin, Hungary, *Appl. Geochemistry*, 26(1), 91–104,  
 2075 doi:10.1016/j.apgeochem.2010.11.006, 2011.
- 2076
- 2077 Vegas-Vilarrúbia, T., González-Sampériz, P., Morellón, M., Gil-Romera, G., Pérez-Sanz, A.  
 2078 and Valero-Garcés, B.: Diatom and vegetation responses to late glacial and early holocene  
 2079 climate changes at lake estanya (southern pyrenees, NE spain), *Palaeogeogr. Palaeoclimatol.*  
 2080 *Palaeoecol.*, 392, 335–349, doi:10.1016/j.palaeo.2013.09.011, 2013.
- 2081
- 2082 Vegas, J., Ruiz-Zapata, B., Ortiz, J. E., Galán, L., Torres, T., García-Cortés, Á., Gil-García,  
 2083 M. J., Pérez-González, A. and Gallardo-Millán, J. L.: Identification of arid phases during the  
 2084 last 50 cal. ka BP from the Fuentillejo maar-lacustrine record (Campo de Calatrava Volcanic  
 2085 Field, Spain), *J. Quat. Sci.*, 25(7), 1051–1062, doi:10.1002/jqs.1262, 2010.
- 2086
- 2087 Velasquez, P., Kaplan, J. O., Messmer, M., Ludwig, P. and Raible, C. C.: The role of land  
 2088 cover in the climate of glacial Europe, *Clim. Past*, 17(3), 1161–1180, doi:10.5194/cp-17-  
 2089 1161-2021, 2021.
- 2090
- 2091 Vicente-Serrano, S. M., Trigo, R. M., López-Moreno, J. I., Liberato, M. L. R., Lorenzo-  
 2092 Lacruz, J., Beguería, S., Morán-Tejeda, E. and El Kenawy, A.: Extreme winter precipitation  
 2093 in the Iberian Peninsula in 2010: Anomalies, driving mechanisms and future projections,  
 2094 *Clim. Res.*, 46(1), 51–65, doi:10.3354/cr00977, 2011.
- 2095
- 2096 Williams, J.W., Grimm, E.G., Blois, J., Charles, D.F., Davis, E., Goring, S.J., Graham, R.,  
 2097 Smith, A.J., Anderson, M., Arroyo-Cabrales, J., Ashworth, A.C., Betancourt, J.L., Bills,  
 2098 B.W., Booth, R.K., Buckland, P., Curry, B., Giesecke, T., Hausmann, S., Jackson, S.T.,

2099 Latorre, C., Nichols, J., Purdum, T., Roth, R.E., Stryker, M., Takahara, H. :The Neotoma  
2100 Paleocology Database: A multi-proxy, international community-curated data resource. *Quat.*  
2101 *Res.* 89, 156-177, doi:10.1017/qua.2017.105, 2018.  
2102  
2103 Williams, J. W. and Jackson, S. T.: Palynological and AVHRR observations of modern  
2104 vegetational gradients in eastern North America, *J. Geophys. Res.*, 4, 485–497, 2003.  
2105  
2106 Williams, J. W., Webb, T., Shurman, B. N. and Bartlein, P. J.: Do Low CO<sub>2</sub> Concentrations  
2107 Affect Pollen-Based Reconstructions of LGM Climates? A Response to “Physiological  
2108 Significance of Low Atmospheric CO<sub>2</sub> for Plant–Climate Interactions” by Cowling and  
2109 Sykes, *Quat. Res.*, 53(3), 402–404, doi:10.1006/qres.2000.2131, 2000.  
2110  
2111 Willis, K. J. and Van Andel, T. H.: Trees or no trees? The environments of central and  
2112 eastern Europe during the Last Glaciation, *Quat. Sci. Rev.*, 23(23–24), 2369–2387,  
2113 doi:10.1016/j.quascirev.2004.06.002, 2004.  
2114  
2115 Wu, H., Guiot, J., Brewer, S. and Guo, Z.: Climatic changes in Eurasia and Africa at the last  
2116 glacial maximum and mid-Holocene: Reconstruction from pollen data using inverse  
2117 vegetation modelling, *Clim. Dyn.*, 29(2–3), 211–229, doi:10.1007/s00382-007-0231-3, 2007.  
2118  
2119 Yu, G. and Harrison, S. P.: Lake status records from Europe: data base documentation,  
2120 NOAA Paleoclimatology Publications Series, Boulder, Colorado., 1995.  
2121  
2122 Zaarur, S., Affek, H. P. and Stein, M.: Last glacial-Holocene temperatures and hydrology of  
2123 the Sea of Galilee and Hula Valley from clumped isotopes in *Melanopsis* shells, *Geochim.*  
2124 *Cosmochim. Acta*, 179, 142–155, doi:10.1016/j.gca.2015.12.034, 2016.  
2125  
2126 Zanon, M., Davis, B. A. S., Marquer, L., Brewer, S. and Kaplan, J. O.: European forest cover  
2127 during the past 12,000 years: A palynological reconstruction based on modern analogs and  
2128 remote sensing, *Front. Plant Sci.*, 9, doi:10.3389/fpls.2018.00253, 2018.  
2129  
2130 Zech, M., Buggle, B., Leiber, K., Marković, S., Glaser, B., Hambach, U., Huwe, B., Stevens,  
2131 T., Sümegei, P., Wiesenberg, G. and Zöller, L.: Reconstructing Quaternary vegetation history  
2132 in the Carpathian Basin, SE-Europe, using n-alkane biomarkers as molecular fossils:  
2133 Problems and possible solutions, potential and limitations, *Quat. Sci. J.*, 58(2), 148–155,  
2134 doi:10.3285/eg.58.2.03, 2010.  
2135  
2136

2137  
2138  
2139

Tables

Site	Site Name	Country/Ocean	Latitude	Longitude	Elevation	Site Type	Data Type	Samples	Source	Reference
1	MD95-2039 (M)	Atlantic	40.578333	-10.348333	-3381	Marine	Raw Count	21	EPD (E#1472)	Roucoux et al. 2005
2	SU81-18 (M)	Atlantic	37.77	-9.82	-3135	Marine	Raw Count	10	ACER	Turon et al. 2003
3	MD99-2331 (M)	Atlantic	41.15	-9.68	-2110	Marine	Raw Count	41	ACER	Naughton et al. 2006
4	Carn Morval	United Kingdom	49.926111	-6.313889	5	Lake	Digitised	1	Publication	Scourse 1991
5	Gorham Cave	Spain	36.132826	-5.347358	0	Cave	Digitised	1	Publication	Carrion et al. 2008
6	Dozmary Pool	United Kingdom	50.5347222	-4.5358333	265	Lake	Raw Count	32	Author	Kelly et al. 2010
7	Bajondillo	Spain	36.619722	-4.496389	20	Cave	Raw Count	1	EPD (E#1570)	Cortes-Sanchez et al. 2011
8	Laguna del maar de Fuentillejo	Spain	38.937996	-4.0539	637	Lake	Digitised	1	Publication	Ruiz-Zapata et al. 2009
9	Padul-1	Spain	37.016338	-3.608503	785	Peat Bog	Digitised	13	Publication	Pons & Reille 1988
10	Padul-2	Spain	37.010833	-3.603889	726	Peat Bog	Digitised	1	Publication	Camuera et al. 2019
11	Cova di Carihuela	Spain	37.4489	-3.4297	1020	Cave	Digitised	1	Publication	Carrion 1992
12	Ifri El Baroud	Morocco	34.75	-3.3	539	Cave	Digitised	1	Publication	Poti et al. 2019
13	MD95-2043 (M)	Mediterranean	36.14	-2.621	-1841	Marine	Raw Count	7	ACER	Fletcher et al. 2008
14	San Rafael	Spain	36.773611	-2.601389	0	Peat Bog	Raw Count	2	EPD (E#574)	Pantaléon-Cano 1997
15	Siles	Spain	38.24	-2.3	1320	Lake	Digitised	1	Publication	Carrion 2002
16	Torreçilla de Valmadrid	Spain	41.4469444	-0.895	570	Colluvium	Digitised	1	Publication	Valero-Garces et al. 2004
17	Navarrés-1	Spain	39.1	-0.683333	225	Peat Bog	Raw Count	1	EPD (E#469)	Carrion & Dupré-Olivier 1996
18	Navarrés-2	Spain	39.1	-0.683333	225	Peat Bog	Raw Count	1	EPD (E#470)	Carrion & Dupré-Olivier 1996
19	Tourbiere de l'Estarrès	France	43.0933	-0.3792	356	Lake	Digitised	1	Publication	Jalut et al. 1988
20	Cova de les Malladetes	Spain	39.058	-0.321	20	Cave	Digitised	1	Publication	Dupré-Olivier 1988
21	Lourdes	France	43.033333	-0.075	430	Lake	Digitised	15	Publication	Reille & Andrieu 1995
22	Lake Estanya	Spain	42.0333333	0.53333333	670	Lake	Digitised	1	Publication	Vegas-Villarubia et al. 2013
23	Freychinede	France	42.7833	1.4333	1350	Lake	Digitised	1	Publication	Jalut et al. 1992
24	Banyoles	Spain	42.133333	2.75	173	Lake	Raw Count	13	EPD (E#931)	Pérez-Obiol & Julia 1994
25	Lac du Bouchet B5	France	44.916667	3.783333	1200	Lake	Digitised	14	Publication	Reille & de Beaulieu 1988
26	MD99-2348 (103) (M)	Mediterranean	42.692778	3.841667	-296	Marine	Raw Count	41	EPD (E#1474)	Beaudouin et al. 2007
27	Les Echets G	France	45.9	4.93	267	Peat Bog	Digitised	136	ACER	de Beaulieu & Reille 1984
28	La Grotte Walou	Belgium	50.585278	5.536389	252	Cave	Digitised	1	Publication	Damblon 2011
29	Bergsee	Germany	47.5722222	7.93638889	382	Lake	Digitised	1	Publication	Duprat-Oualid et al. 2017
30	Garaat El-Ouez	Algeria	36.818333	8.33333	45	Peat Bog	Raw Count	6	EPD (E#1501)	Benslama et al. 2010
31	Pian del Lago	Italy	44.321561	9.485682	833	Lake	Digitised	1	Publication	Guido et al. 2020
32	Pilsensee	Germany	48.0267	11.1883	534	Lake	Digitised	1	Publication	Küster 1995
33	Orgiano	Italy	45.29	11.43	19	Peat Bog	Digitised	1	Publication	Paganelli 1996
34	Lago della Costa	Italy	45.2702778	11.7430556	7	Lake	Digitised	8	Publication	Kaltenrieder et al. 2009
35	Lagaccione	Italy	42.566667	11.85	355	Lake	Raw Count	7	ACER	Magri 1999
36	Lago Vico	Italy	42.3166667	12.166667	510	Lake	Digitised	15	Publication	Magri & Sadori 1999
37	Stracciaccia	Italy	42.13	12.32	220	Lake	Raw Count	2	ACER	Giardini 2007
38	Lago di Monterosi	Italy	42.2166667	12.4333333	237	Lake	Raw Count	1	Publication	Bonatti 1970
39	Venice	Italy	45.629523	12.654086	0	Peat Bog	Digitised	1	Publication	Miola et al. 2006
40	Azzano Decimo	Italy	45.8833	12.7165	10	Alluvial Fan	Raw Count	6	ACER	Pini et al. 2009
41	Valle di Castiglione	Italy	41.89	12.75	44	Lake	Raw Count	2	ACER	Follieri et al. 1989
42	Travesio	Italy	46.2	12.87	220	Lake	Digitised	1	Publication	Monegato et al. 2007
43	Orvenco	Italy	46.252088	13.169771	380	Alluvial Fan	Digitised	1	Publication	Monegato et al. 2007
44	Rio Doidis	Italy	46.12	13.19	152	Lake	Digitised	1	Publication	Monegato et al. 2007
45	Billerio	Italy	46.22	13.21	300	Lake	Digitised	1	Publication	Monegato et al. 2007
46	Kersdorf-Briesen	Germany	52.333704	14.269142	44	Lake	Digitised	1	Publication	Strahl 2005
47	Lago Grande di Monticchio	Italy	40.944444	15.6	1326	Lake	Raw Count	6	EPD (E#932)	Watts et al. 1996
48	Nagymohos	Hungary	48.326944	20.436389	297	Peat Bog	Raw Count	14	Publication	Magyari et al. 1999
49	Safarka	Slovakia	48.8819444	20.575	600	Peat Bog	Digitised	1	Publication	Jankovska 2008
50	Fehér Lake	Hungary	46.45	20.65	86	Lake	Raw Count	10	Publication	Magyari et al. 2014
51	Ioannina	Greece	39.75	20.85	470	Peat Bog	Raw Count	20	ACER	Tzedakis et al. 2004
52	Kokad	Hungary	47.4027778	21.9286111	112	Peat Bog	Raw Count	2	Publication	Magyari et al. 2019
53	Lake Xinias	Greece	39.05	22.27	500	Lake	Raw Count	5	EPD (E#976)	Bottema 1979
54	Mickunai	Lithuania	54.722114	25.532218	143	Lake	Digitised	1	Publication	Satkunas & Grigiene 2012
55	Lake Sfanta Anna	Romania	46.1263889	25.880556	946	Lake	Digitised	1	Publication	Magyari et al. 2014
56	Megali Limni	Greece	39.1	26.3	323	Lake	Digitised	1	Publication	Margari et al. 2009
57	Straldzha	Bulgaria	42.630278	26.77	138	Peat Bog	Raw Count	3	Publication	Connor et l. 2013
58	MD01-2430 (M)	Turkey	40.796833	27.725166	-580	Marine	Digitised	1	Publication	Valsecchi et al. 2012
59	Lake Iznik	Turkey	40.433889	29.533056	88	Lake	Raw Count	7	EPD (E#714)	Miebach et al. 2016
60	M72/5 628-1 (M)	Black Sea	42.1035	36.62383	-418	Marine	Raw Count	6	Pangaea (833387)	Shumilovskikh et al. 2014
61	Dziguta	Georgia	42.99	41.07	35	Peat Bog	Digitised	1	Publication	Arslanov et al. 2007
62	Lake Van LG	Turkey	38.667	42.669	1649	Lake	Raw Count	10	Pangaea (853779)	Pickarski et al. 2015
63	Lake Zeribar	Iran	35.533333	46.116667	1286	Lake	Raw Count	17	EPD (E#714)	van Zeist & Bottema 1977

Table 1. List of selected sites

2140  
2141  
2142  
2143  
2144  
2145

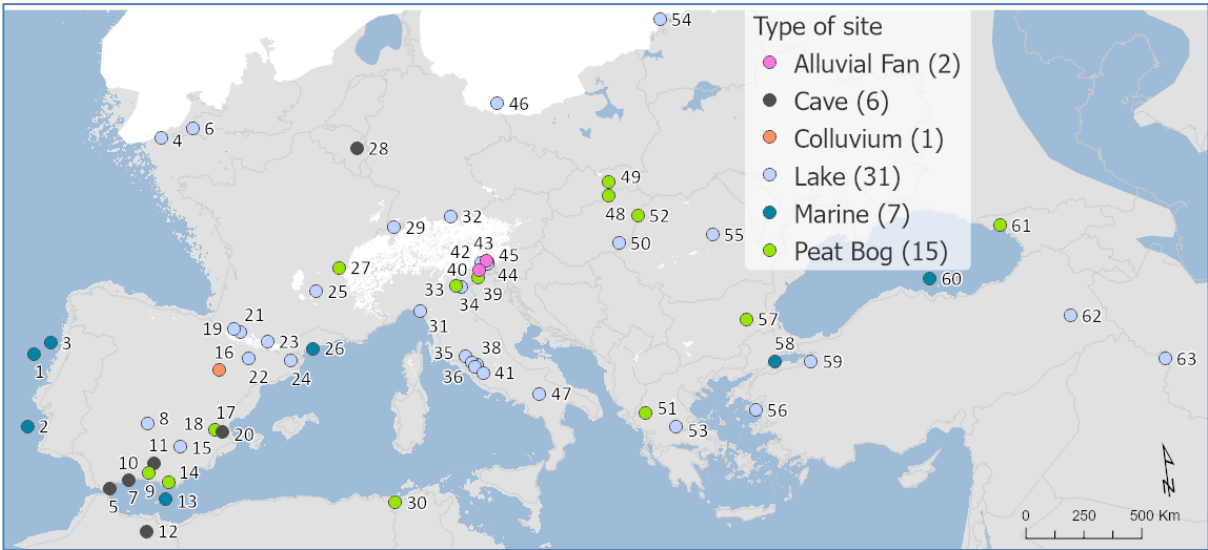
2146  
2147  
2148  
2149  
2150

	<b>RMSE</b>	<b>R2</b>
<b>TANN</b>	2.28	0.9
<b>TDJF</b>	3.35	0.91
<b>TJJA</b>	2.21	0.81
<b>PANN</b>	224.94	0.69
<b>PDJF</b>	78.51	0.69
<b>PJJA</b>	52.49	0.75
<b>Tree Cover</b>	21.03	0.52

2151  
2152  
2153  
2154  
2155  
2156  
2157  
2158  
2159  
2160

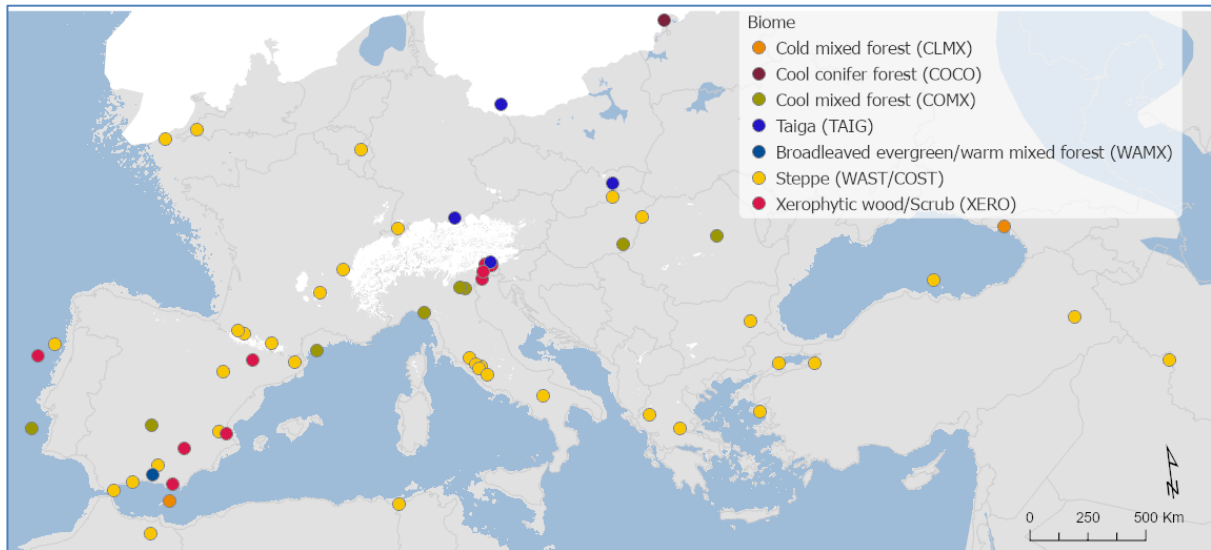
Table 2. MAT performance statistics based on the modern pollen sample training set. This includes Mean Annual Temperature and Precipitation (TANN and PANN), Mean Winter Temperature and Precipitation (TDJF and PDJF) and Mean Summer Temperature and Precipitation (TJJA and PJJA).

2161 **Figures**  
2162  
2163  
2164



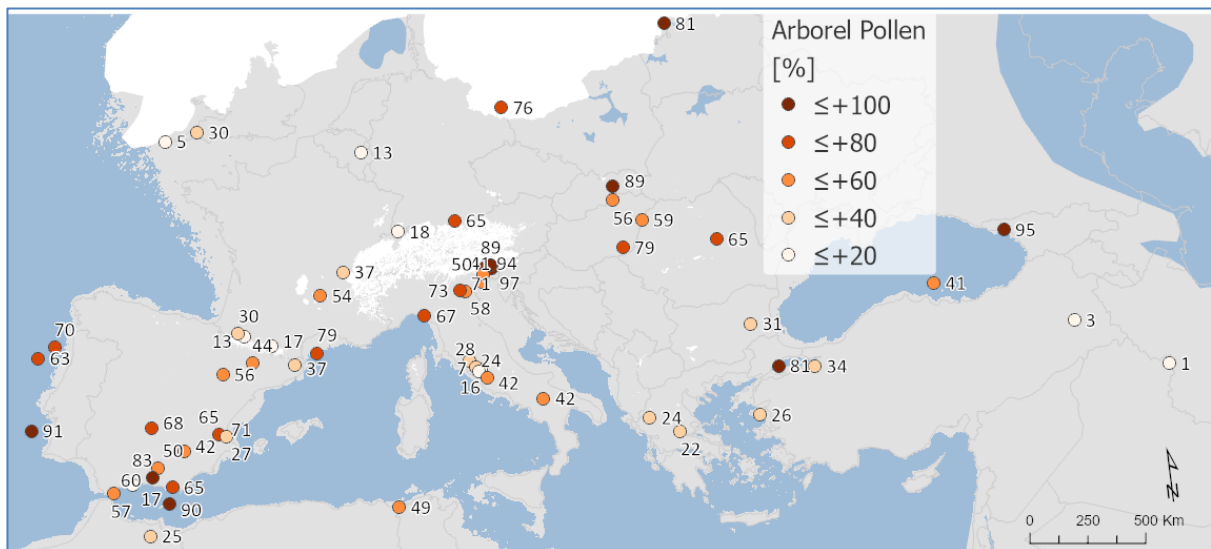
2165  
2166  
2167 **Figure 1. Site locations and archives (Site numbers are as shown in Table 1)**  
2168  
2169  
2170

2171



2172  
2173  
2174  
2175  
2176

Figure 2. Pollen biomes

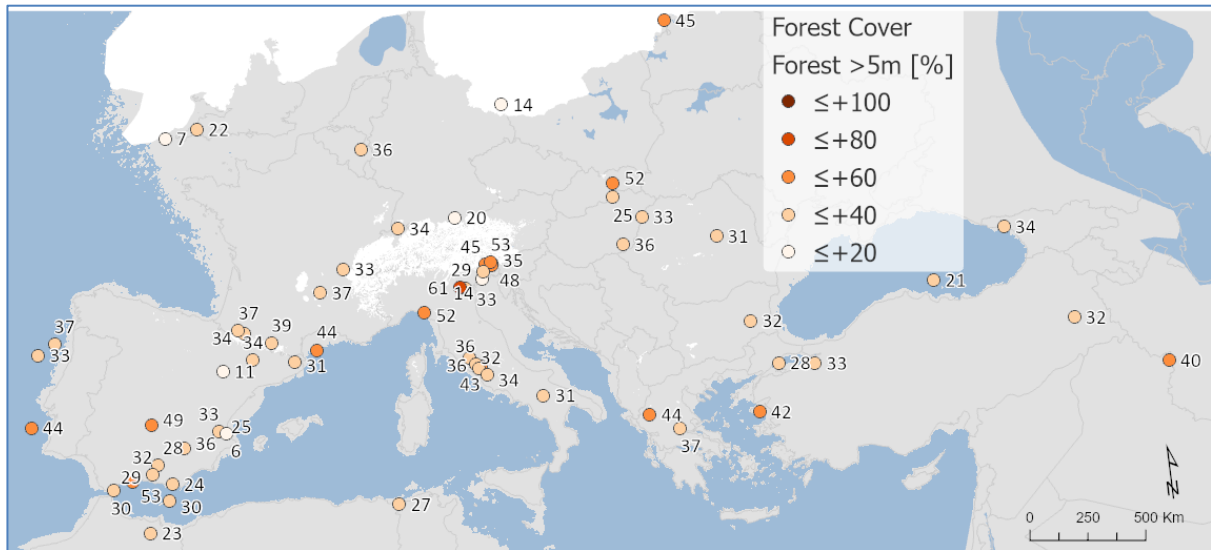


2177  
2178  
2179  
2180  
2181

Figure 3. Arboreal Pollen (AP) % forest cover



2182



2183

2184

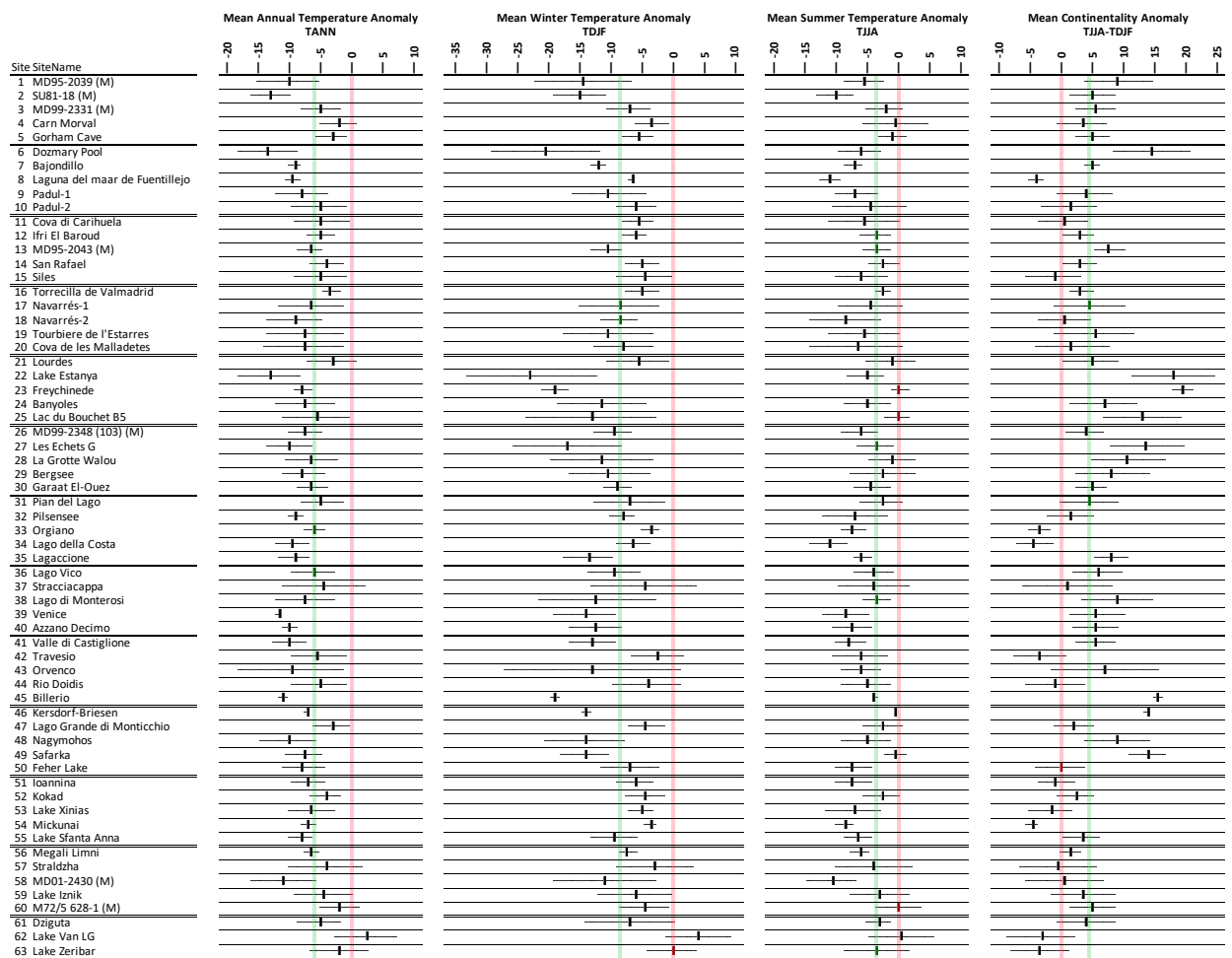
2185

2186

2187

Figure 4. Modern Analogue Technique (MAT) % forest cover

2188  
2189

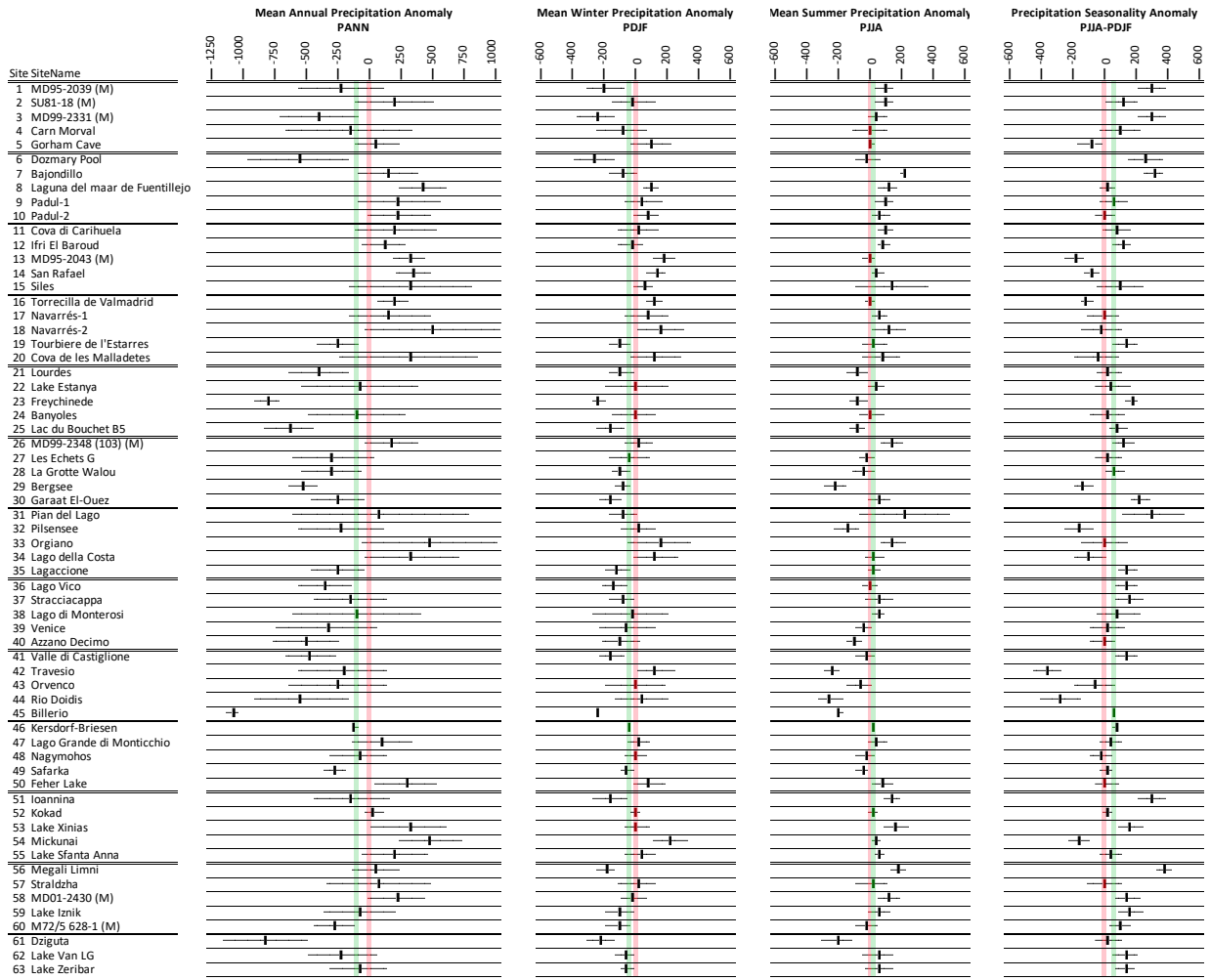


2190  
2191  
2192  
2193  
2194  
2195  
2196  
2197  
2198  
2199

Figure 5. Pollen-based MAT reconstructions for LGM annual, winter and summer temperature anomalies (uncertainties represent one standard deviation). Continentality represents the difference in temperature between summer and winter, with positive anomalies indicating an increase in the temperature difference between summer and winter. All values are expressed as anomalies compared with the present day. The green line indicates the mean for all the sites.



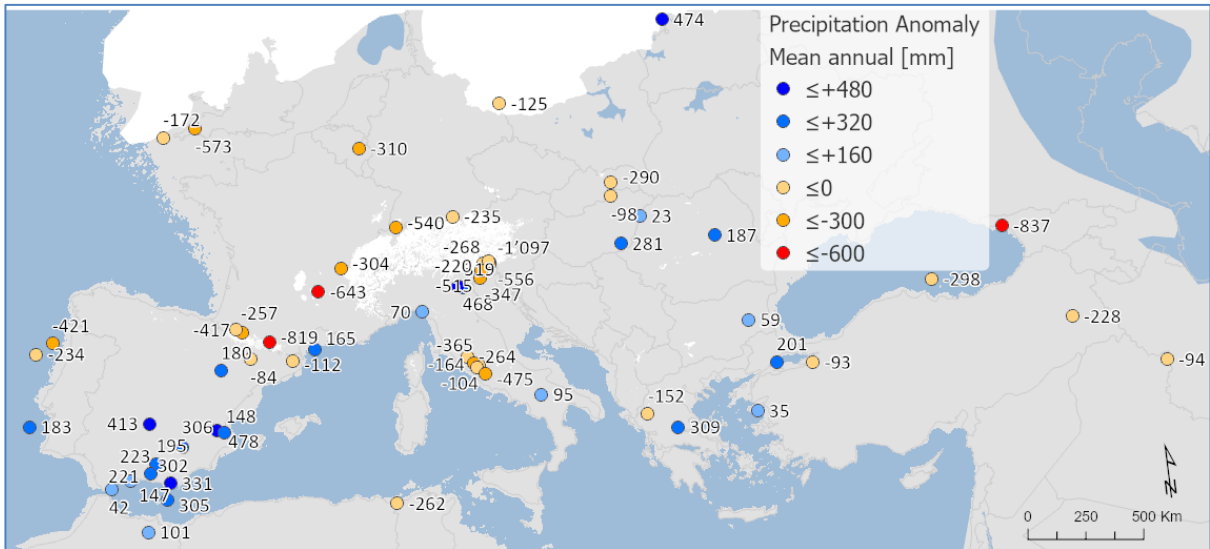




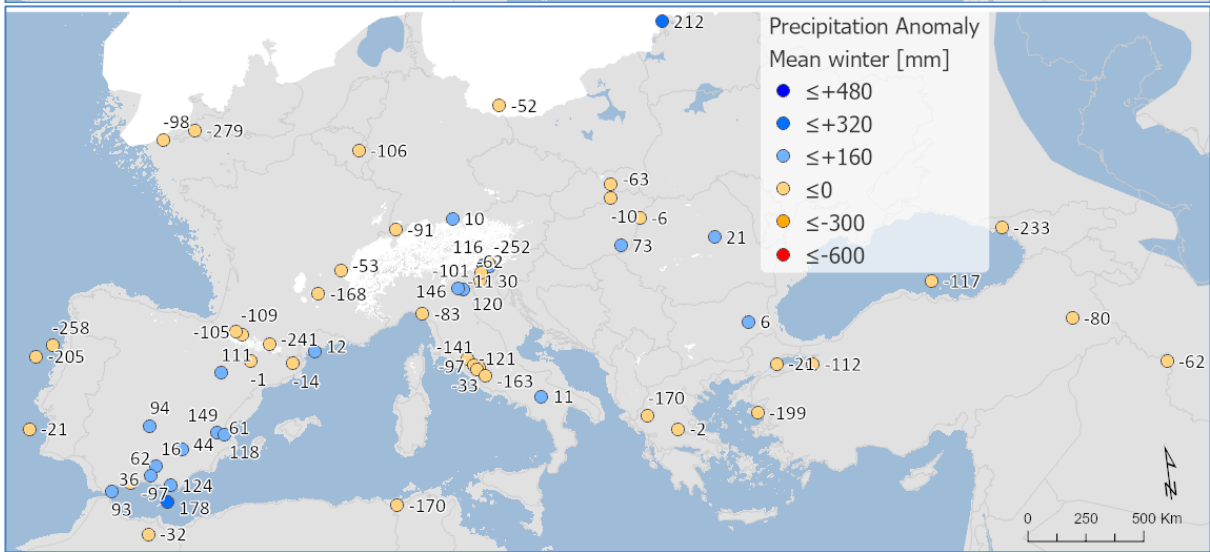
2212  
 2213  
 2214  
 2215  
 2216  
 2217  
 2218  
 2219

Figure 7. Pollen-based MAT reconstructions for LGM annual, winter and summer precipitation anomalies (uncertainties represent one standard deviation). Seasonality represents the difference in precipitation between summer and winter, with positive anomalies indicating an increase in summer precipitation compared to winter. All values are expressed as anomalies compared with the present day. The green line indicates the mean for all the sites.

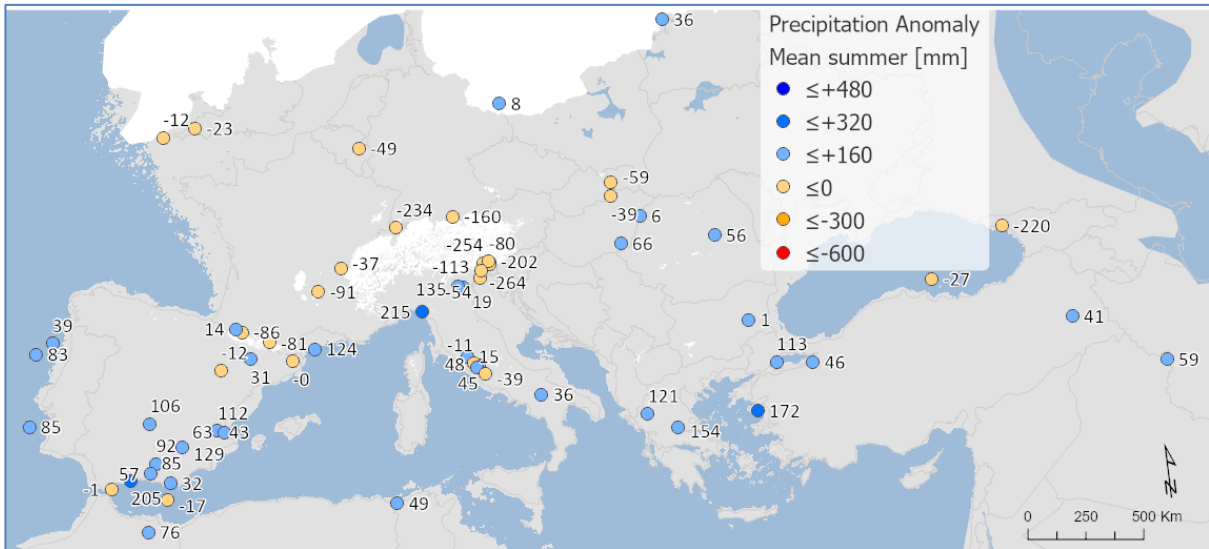
2220



2221



2222



2223

2224

2225

2226

2227

2228

2229

2230

2231

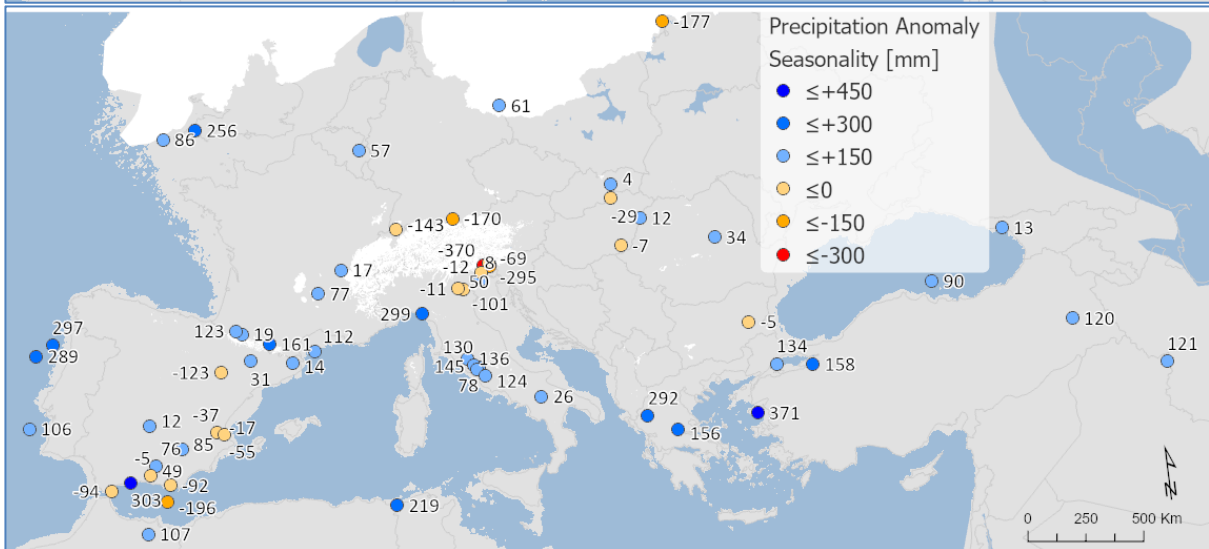
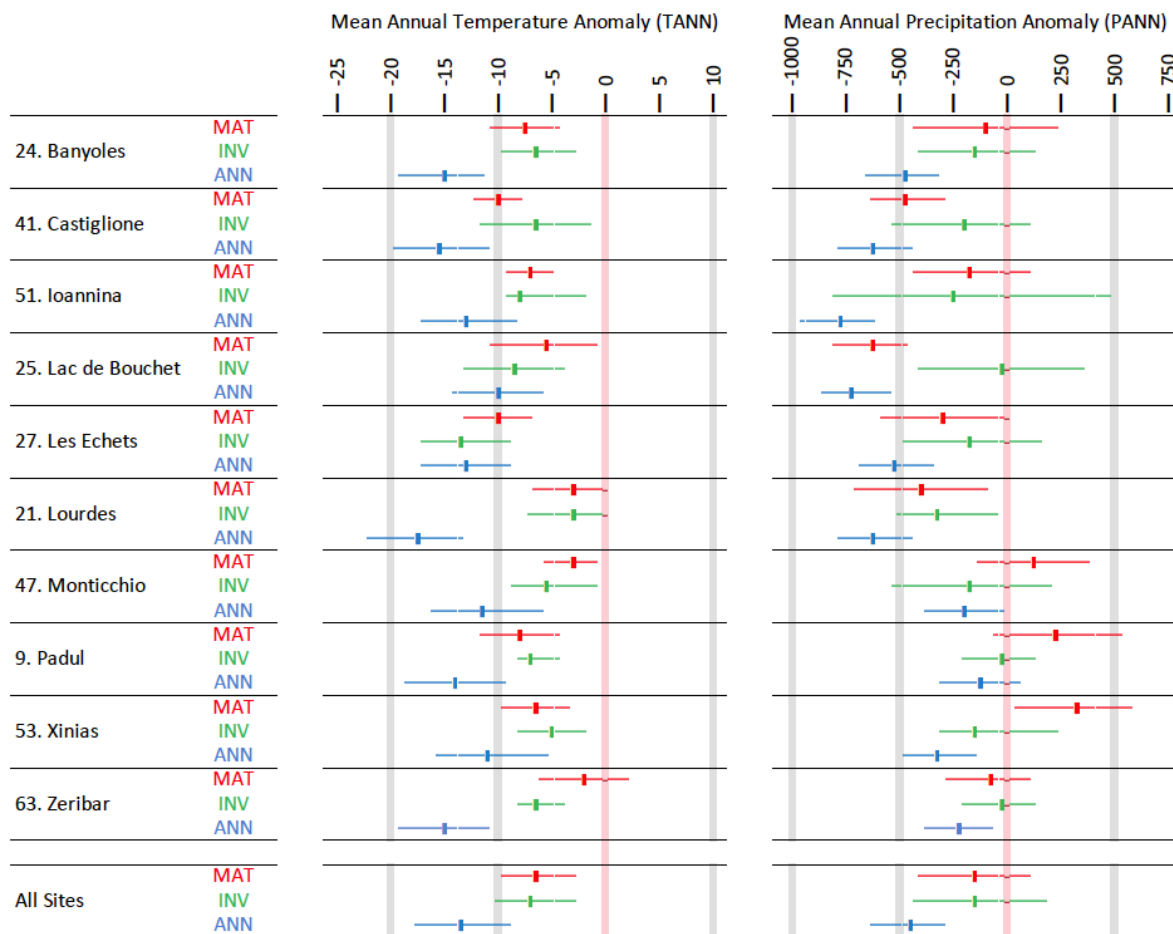


Figure 8. Maps of pollen-based MAT reconstructions for LGM annual, winter and summer precipitation anomalies (as shown in figure 11). Seasonality represents the difference in precipitation between summer and winter, with positive anomalies indicating an increase in summer precipitation compared to winter. All values are expressed as anomalies compared with the present day.

2232



2233

2234

2235

2236

2237

2238

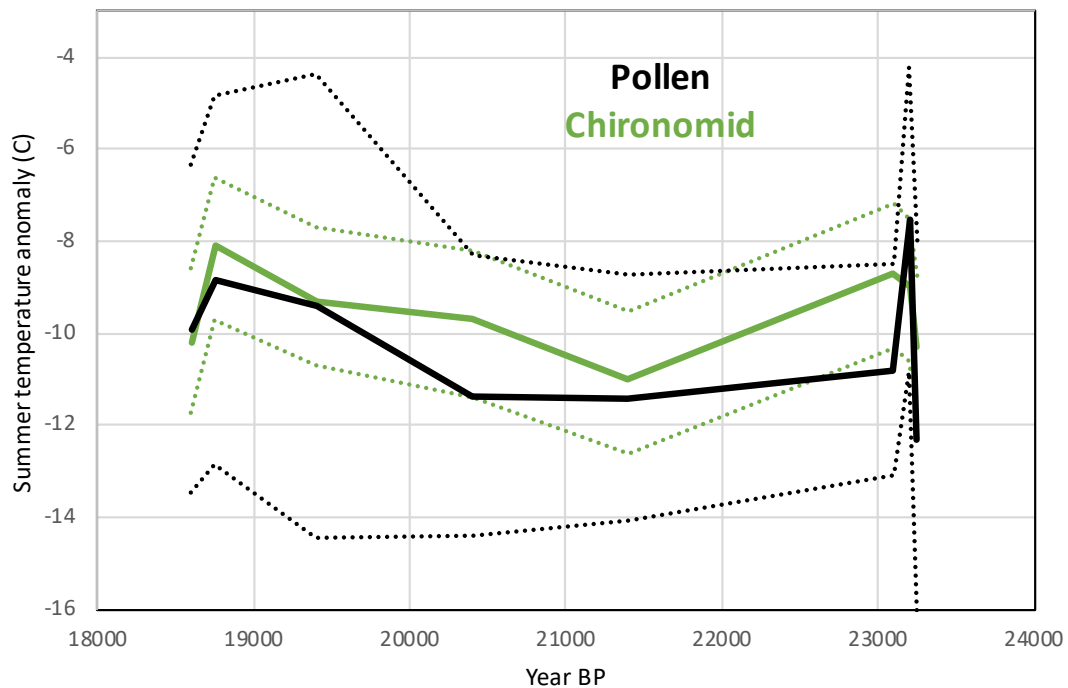
2239

2240

Figure 9. A site-by-site comparison between LGM pollen-climate reconstructions based on Modern Analogue Technique MAT (this study), neural-networks ANN (Peyron et al., 1998), and Inverse Modelling INV (Wu et al., 2007). The results show that MAT and INV give similar climate reconstructions, but ANN is significantly cooler/drier.



2241  
2242  
2243



2244  
2245  
2246  
2247  
2248  
2249  
2250

Figure 10. Comparison between LGM pollen-climate MAT and chironomid summer temperature reconstructions at Lago della Costa, Italy (chironomid reconstruction and pollen data from Samartin et al., 2016). Dash lines show uncertainties.

2251  
2252  
2253

# Appendix

Site	Site Name	COHMAP Quality	COHMAP													Upper 14C	Upper Cal. BP	Lower 14C	Lower Cal. BP
			< 17k	18k	19k	20k	21k	22k	23k	24k	25k >								
1	MD95-2039 (M)	3C													14830±80	18166±269	19950±210	23883±374	
2	SU81-18 (M)	2C													17510±270	20952±404	21250±280	25420±441	
3	MD99-2331 (M)	2C													16170±130	19325±303	19770±170	23682±336	
4	Carr Morval	4C														18600±3700	21500±890/800	25867±1127	
5	Gorham Cave	4D															18440±160	22055±341	
6	Dozmary Pool	2C													14568±129	17569±523	18325±216	21769±602	
7	Bajondillo	1C														18701±2154			
8	Laguna del maar de Fuentillejo	5D													16540±90	19847±308			
9	Padul-1	3D													18300±300	21821±412	19100±160	22922±308	
10	Padul-2	1D														17450±539		21082±539	
11	Cova di Carihuela	2C													15700±220	18958±280	21430±130	25659±226	
12	Ifri El Baroud	2D													17296±87	20761±293			
13	MD95-2043 (M)	2C													15440±90	18533±294	18260±120	21951±335	
14	San Rafael	3D													9980±60	11464±133	16860±120	20083±292	
15	Siles	2D													17030±80	20345±351			
16	Torreçilla de Valmadríd	2D													17100±85	20456±366			
17	Navarrés-1	4D													18360±195	22001±353	20700±295	24664±411	
18	Navarrés-2	5D													5150±50	5881±85	16000±	19144±	
19	Tourbiere de l'Estarres	1C													17150±250	20522±470	18970±160	22847±317	
20	Cova de les Malladetes	5D													16300±1500	19686±1723			
21	Lourdes	4D													18510±130	22112±130	20025±175	23952±355	
22	Lake Estanya	5D														9498±50		19184±251	
23	Freychinède	3C													14800±800	17912±856	21300±760	25615±1030	
24	Banyoles	4C														19878±100		27862±3000	
25	Lac du Bouchet B5	2C													15350±350	18513±435	19200±300	23006±384	
26	MD99-2348 (103) (M)	1D													17660±60	21065±310	19350±90	23111±271	
27	Les Echets G	4C													17530±270	20970±407	18030±250	21704±473	
28	La Grotte Walou	1D																21200±700	
29	Bergsee	2D															17780±90	21244±306	
30	Garaat El-Ouez	2C													16010±320	19200±801			
31	Pian del Lago	2D																21260±320	
32	Pilsensee	6D													15860±250	19073±290			
33	Orgiano	2D													17760±160	21221±373	19290±520	23141±621	
34	Lago della Costa	2C													15400±150	18484±330	19285±160	23052±302	
35	Lagaccione	2C													16080±450	19369±527	20615±940	24746±1201	
36	Lago Vico	3C													14385±140	17541±272	20500±230	24430±376	
37	Stracciaccappa	4C													12060±130	14093±281	19745±820	22675±955	
38	Lago di Monterosi	2D													17040±350	20398±544			
39	Venice	5D															18640±100	22277±336	
40	Azzano Decimo	2D													18000±300	21637±529	21025±245	25179±449	
41	Valle di Castiglione	3C													14220±145	17443±270	20300±700	24266±842	
42	Travesio	5D															18780±200	22483±406	
43	Orvenco	2D													17760±160	21221±373	19290±520	23141±621	
44	Rio Doidis	5D															18860±190	22390±373	
45	Billerio	3D															18165±200	21872±382	
46	Kersdorf-Briesen	1D															17622±94	21183±356	
47	Lago Grande di Monticchio	2C														20204±		24014±	
48	Nagymohos	2C													14246±144	17361±425	18159±247	21735±622	
49	Safarka	3D															18287±1512	21912±1781	
50	Feher Lake	1D													17715±250	21190±463	19911±81	23841±313	
51	Ioannina	3C													15330±140	18420±312	20760±230	24748±330	
52	Kokad	5D													14326±63	17433±443	16280±90	19685±538	
53	Lake Xinias	6C													11150±130	13049±160	21390±430	25671±648	
54	Mickunai	1D														21000±2200			
55	Lake Sfanta Anna	1D													17626±96	20955±432			
56	Megali Limni	6D													19072±237	22906±340			
57	Straldzha	6C													14696±65	18022±364	23653±114	28580±390	
58	MD01-2430 (M)	4C													12050±75	14904±324	18310±380	21746±968	
59	Lake Iznik	7D													16910±100	19515±115			
60	M72/5 628-1 (M)	2C													16835±85	18490±	19495±90	21280±	
61	Dziguta	2C													12990±160	15839±483	20560±880	24666±1126	
62	Lake Van LG	4C														18590±62		23290±596	
63	Lake Zeribar	4C													13650±160	16610±399	22000±500	26462±880	

COHMAP chronological quality classification:  
 1C: Bracketing dates within 2000 14C (2360 Cal.) yr interval about the time being assessed  
 2C: Bracketing dates, one within 2000 14C (2360 Cal.) yr and the second within 4000 14C (4682 Cal.) yr of the time being assessed  
 3C: Bracketing dates within 4000 14C (4682 Cal.) yr interval about the time being assessed  
 4C: Bracketing dates, one being within 4000 14C (4682 Cal.) yr and the second being within 6000 14C (7490 Cal.) yr of the time being assessed  
 5C: Bracketing dates within 6000 14C (7490 Cal.) yr interval about the time being assessed  
 6C: Bracketing dates, one within 6000 14C (7490 Cal.) yr and the second within 8000 14C (9681 Cal.) yr of the time being assessed  
 7C: Poorly dated  
 1D: Date within 250 14C (206 Cal.) yr of the time being assessed  
 2D: Date within 500 14C (684 Cal.) yr of the time being assessed  
 3D: Date within 750 14C (975 Cal.) yr of the time being assessed  
 4D: Date within 1000 14C (1123 Cal.) yr of the time being assessed  
 5D: Date within 1500 14C (1881 Cal.) yr of the time being assessed  
 6D: Date within 2000 14C (2360 Cal.) yr of the time being assessed  
 7D: Poorly dated

2254  
2255  
2256  
2257  
2258  
2259  
2260  
2261  
2262  
2263  
2264  
2265  
2266  
2267  
2268  
2269  
2270  
2271  
2272  
2273

**Table A1. Chronological control**

2274  
2275

Site Number	Site Name	Site Type	TANN	TDJF	TJJA	PANN	PDJF	PJJA
1	MD95-2039 (M)	Marine	15.7	10.7	20.8	1047	427	70
2	SU81-18 (M)	Marine	20.8	15.3	26.5	629	282	25
3	MD99-2331 (M)	Marine	14.6	9.8	19.4	1239	507	88
4	Carn Morval	Lake	12.5	8.7	16.9	1183	392	206
5	Gorham Cave	Cave	18.3	13.4	23.7	740	336	25
6	Dozmary Pool	Lake	10.3	6.0	15.2	1271	422	236
7	Bajondillo	Cave	16.6	10.5	23.4	542	223	27
8	Laguna del maar de Fuentillejo	Lake	16.1	8.1	25.4	474	156	47
9	Padul-1	Peat Bog	16.6	9.6	24.9	417	157	23
10	Padul-2	Peat Bog	16.6	9.6	24.9	417	157	23
11	Cova di Carihuela	Cave	15.7	8.1	25.1	551	187	57
12	Ifri El Baroud	Cave	16.9	10.7	24.0	457	184	22
13	MD95-2043 (M)	Marine	17.9	12.4	24.0	214.2	37	72
14	San Rafael	Peat Bog	18.1	11.9	24.9	243	87	14
15	Siles	Lake	14.4	6.8	23.4	658	195	92
16	Torreçilla de Valmadrid	Colluvium	14.2	6.6	22.5	390	75	82
17	Navarrés-1	Peat Bog	17.0	10.9	23.8	421	96	51
18	Navarrés-2	Peat Bog	17.0	10.9	23.8	421	96	51
19	Tourbiere de l'Estarres	Lake	13.0	6.1	20.4	1045	272	217
20	Cova de les Malladetes	Cave	18.1	12.1	24.8	478	117	60
21	Lourdes	Lake	12.6	5.5	20.1	1002	256	212
22	Lake Estanya	Lake	12.8	5.1	21.0	641	125	152
23	Freychinede	Lake	10.8	3.9	19.0	1128	257	277
24	Banyoles	Lake	14.3	7.7	21.9	698	157	139
25	Lac du Bouchet B5	Lake	8.2	1.3	15.9	1070	251	221
26	MD99-2348 (103) (M)	Marine	14.6	8.0	21.9	618	158	95
27	Les Echets G	Peat Bog	11.4	3.6	19.6	876	175	215
28	La Grotte Walou	Cave	10.3	3.2	17.0	903	215	249
29	Bergsee	Lake	9.6	1.4	17.6	1048	189	387
30	Garaat El-Ouez	Peat Bog	17.3	11.0	24.3	830	360	33
31	Pian del Lago	Lake	12.4	5.1	20.0	995	266	149
32	Pilsensee	Lake	9.3	0.6	17.7	947	151	374
33	Orgiano	Peat Bog	13.0	3.3	22.3	907	200	228
34	Lago della Costa	Lake	12.9	3.3	22.1	888	196	224
35	Lagaccione	Lake	14.2	7.2	21.7	705	203	109
36	Lago Vico	Lake	13.7	6.4	21.5	870	258	132
37	Stracciacappa	Lake	14.6	7.3	22.4	867	266	115
38	Lago di Monterosi	Lake	15.0	7.7	22.9	837	248	115
39	Venice	Peat Bog	13.4	4.5	22.1	1050	221	277
40	Azzano Decimo	Alluvial Fan	13.3	4.4	22.1	1170	241	311
41	Valle di Castiglione	Lake	16.3	9.1	24.0	988	294	144
42	Travesio	Lake	12.6	3.7	21.3	1415	281	375
43	Orvenco	Alluvial Fan	13.0	3.3	22.3	907	200	228
44	Rio Doidis	Lake	12.8	4.1	21.2	1529	315	392
45	Billerio	Lake	12.8	4.1	21.2	1529	315	392
46	Kersdorf-Briesen	Lake	8.8	-1.0	17.9	538	110	175
47	Lago Grande di Monticchio	Lake	11.5	4.1	19.8	518	154	76
48	Nagymohos	Peat Bog	9.5	-1.5	19.1	616	103	230
49	Safarka	Peat Bog	7.0	-3.2	16.0	755	119	280
50	Feher Lake	Lake	11.0	-0.1	20.7	546	112	185
51	Ioannina	Peat Bog	14.7	6.5	23.3	1000	364	98
52	Kokad	Peat Bog	10.2	-0.9	19.8	601	130	204
53	Lake Xinias	Lake	15.6	7.5	24.1	563	211	47
54	Mickunai	Lake	6.0	-5.0	16.3	682	131	230
55	Lake Sfanta Anna	Lake	11.6	5.2	18.4	867	253	172
56	Megali Limni	Lake	15.5	8.2	23.4	684	357	28
57	Straldzha	Peat Bog	12.5	2.6	21.8	591	158	135
58	MD01-2430 (M)	Marine	18.0	8.7	27.5	595	219	75
59	Lake Iznik	Lake	13.9	6.1	21.8	677	250	85
60	M72/5 628-1 (M)	Marine	14.5	8.0	21.6	857	251	156
61	Dziguta	Peat Bog	14.1	6.6	21.7	1549	409	373
62	Lake Van LG	Lake	12.0	0.9	23.1	635	201	34
63	Lake Zeribar	Lake	17.1	5.0	29.0	427	167	6

2276  
2277  
2278  
2279  
2280

**Table A2.** Modern climate values for each site used in the calculation of anomalies (taken from WorldClim 2, Fick & Hijmans 2017)

2281  
2282  
2283

Biome	Change in Biome compared to the Control								
	Control	0 Pinaceae	+5% Pinaceae	+10% Pinaceae	+20% Pinaceae	+50% Pinaceae	+100% Pinaceae	+200% Pinaceae	+400% Pinaceae
CLDE	25	454	0	0	0	-1	-1	-4	-4
TAIG	1489	-1430	16	38	74	192	337	554	914
CLMX	70	108	1	2	3	-6	-4	4	6
COCO	388	-388	0	-1	3	6	25	50	74
TEDE	33	16	1	1	1	-1	-2	-8	-5
COMX	2952	-761	1	8	14	-4	-42	-101	-284
WAMX	418	-28	-1	0	-1	-6	-11	-29	-62
XERO	699	-323	3	4	12	45	68	113	180
DESE	0	0	0	0	0	0	0	0	0
STEP	1752	1388	-14	-39	-83	-173	-296	-468	-663
TUND	387	964	-7	-13	-23	-52	-74	-111	-156
<b>Total</b>	<b>8213</b>	<b>5860</b>	<b>44</b>	<b>106</b>	<b>214</b>	<b>486</b>	<b>860</b>	<b>1442</b>	<b>2348</b>

2284  
2285

2286

2287

2288

2289

2290

2291

2292

2293

2294

2295

2296

2297

2298

2299

2300

2301

2302

2303

2304

**Table A3.** This shows the results of experiment to test the sensitivity of pollen Biomes to changes in the amount of Pinaceae in the pollen assemblage using 8213 modern pollen samples from the EMPD2. Pinaceae can be over-represented in marine samples, and it has been proposed that removing all Pinaceae from these samples is better than leaving the Pinaceae in the pollen assemblage. The 'Control' column on the left shows the number of samples that were classified for each Biome without changing the amount of Pinaceae (ie using the original pollen assemblage). The other 8 columns to the right show the number of samples where the Biome changed relative to the number shown in the control column as a result of either removal of all Pinaceae ('0 Pinaceae'), or by artificially increasing the amount of Pinaceae respectively from 5 to 400% of the original count ('+5% Pinaceae' to '+400% Pinaceae'). For instance, for the CLDE (Cold Deciduous) Biome, 25 pollen samples were classified as CLDE without any change in Pinaceae ('Control'), but 454 more samples were classified as CLDE when all Pinaceae was removed ('0 Pinaceae') compared to 4 fewer samples that were classified as CLDE when Pinaceae was increased by as much as 400% ('+400% Pinaceae'). The totals along the bottom show that out of the 8213 pollen samples included in the experiment, 5860 biomes changed when all Pinaceae was removed, compared to up to 2348 when Pinaceae was artificially increased by up to 400%.

2305

Temperature Anomlay

Site Name	Site Number	TANN delta		TDJF delta		TJJA delta		PANN delta		PDJF delta		PJJA delta	
		Pinaceae	No Pinaceae	Pinaceae	No Pinaceae	Pinaceae	No Pinaceae	Pinaceae	No Pinaceae	Pinaceae	No Pinaceae	Pinaceae	No Pinaceae
MD95-2039 (M)	1	-10.5	-12.3	-14.6	-17.9	-5.7	-5.9	-234.3	-236.3	-205.4	-196.4	83.1	63.0
SU81-18 (M)	2	-13.3	-21.4	-15.2	-23.0	-10.4	-17.7	183.3	703.2	-21.1	124.4	85.1	167.7
MD99-2331 (M)	3	-5.3	-4.8	-7.5	-7.0	-2.3	-1.4	-420.6	-435.6	-257.7	-251.1	39.4	19.0
MD95-2043 (M)	13	-7.0	-6.0	-11.0	-9.9	-3.6	-2.7	304.6	332.5	178.4	201.9	-17.3	-22.9
MD99-2348 (103) (M)	26	-7.8	-8.8	-10.0	-11.5	-6.5	-7.3	164.7	218.0	12.1	7.6	124.0	179.5
MD01-2430 (M)	58	-11.1	-13.5	-11.3	-14.5	-11.0	-12.8	200.6	349.1	-20.8	31.4	113.1	127.9
M72/5 628-1 (M)	60	-2.3	-0.5	-4.9	-3.0	-0.2	1.7	-298.0	-311.1	-116.8	-100.1	-27.0	-51.7
Site Average		-8.2	-9.6	-10.6	-12.4	-5.7	-6.6	-14.2	88.5	-61.6	-26.0	57.2	68.9

Standard Deviation

Site Name	Site Number	TANN STDEV		TDJF STDEV		TJJA STDEV		PANN STDEV		PDJF STDEV		PJJA STDEV	
		Pinaceae	No Pinaceae	Pinaceae	No Pinaceae	Pinaceae	No Pinaceae	Pinaceae	No Pinaceae	Pinaceae	No Pinaceae	Pinaceae	No Pinaceae
MD95-2039 (M)	1	4.6	3.7	7.5	4.0	2.9	4.0	330.6	268.9	110.5	96.7	53.6	55.6
SU81-18 (M)	2	3.1	4.0	4.0	3.4	2.8	4.8	297.1	149.3	126.6	58.0	47.3	28.4
MD99-2331 (M)	3	2.9	4.0	3.4	3.8	2.8	5.0	302.6	368.6	103.5	134.2	57.6	64.3
MD95-2043 (M)	13	2.0	4.7	2.4	5.6	2.1	4.1	115.9	121.5	59.3	72.1	36.2	25.2
MD99-2348 (103) (M)	26	2.4	3.8	3.0	4.2	2.7	4.6	192.7	242.9	75.8	68.2	58.9	52.1
MD01-2430 (M)	58	5.1	2.3	8.1	2.0	3.9	2.8	218.7	182.8	78.9	58.3	53.4	45.0
M72/5 628-1 (M)	60	3.2	3.9	3.8	4.0	3.5	4.6	149.0	171.9	67.1	48.2	56.5	61.8
Site Average		3.3	3.8	4.6	3.9	3.0	4.3	229.5	215.1	88.8	76.5	51.9	47.5

2306  
2307  
2308  
2309  
2310  
2311  
2312  
2313  
2314  
2315  
2316  
2317  
2318  
2319

**Table A4.** A comparison of the LGM reconstructed climate for marine sites showing the effect of excluding Pinaceae (shaded) from the pollen assemblage, compared to the results of including Pinaceae (unshaded, also presented in Figures 6-8). It has been proposed that because of the potential for over-representation of Pinaceae in marine pollen samples, it is better to exclude Pinaceae completely from marine pollen samples. Comparing the two approaches, temperatures are generally 1-2C cooler, and precipitation slightly higher when Pinaceae is excluded. The differences for both temperature and precipitation are significantly less than the standard deviation of their uncertainties.

	All surface samples		Steppe only	
	RMSE	R2	RMSE	R2
TANN	2.28	0.9	2.51	0.87
TDJF	3.35	0.91	3.26	0.88
TJJA	2.21	0.81	2.49	0.82
PANN	224.94	0.69	185.7	0.71
PDJF	78.51	0.69	66.5	0.66
PJJA	52.49	0.75	43.8	0.79

2320  
2321  
2322  
2323  
2324  
2325  
2326  
2327  
2328  
2329  
2330

**Table A5.** A comparison of MAT performance statistics based on the modern pollen sample training set using all surface samples from the EMPD2 used in the LGM reconstruction (as shown in Table 3), and a subset of 1588 samples from the EMPD2 that were classified as steppe. The results show little difference between the two different types of samples. The table includes Mean Annual Temperature and Precipitation (TANN and PANN), Mean Winter Temperature and Precipitation (TDJF and PDJF) and Mean Summer Temperature and Precipitation (TJJA and PJJA).

Site Name	Site#	Pollen Biome	Modern Analogue Biome	Modern Analogue Ecoregion
MD95-2039	1	XERO	Mediterranean Forests, woodlands and scrubs	Iberian conifer forests
SU81-18	2	COMX	Mediterranean Forests, woodlands and scrubs	Iberian conifer forests
MD99-2331	3	STEP	Mediterranean Forests, woodlands and scrubs	Alps conifer and mixed forests
Carn Morval	4	STEP	Temperate broadleaf and mixed forests	North Atlantic moist mixed forests
Gorham Cave	5	STEP	Mediterranean Forests, woodlands and scrubs	Cyprus Mediterranean forests
Dozmary Pool	6	STEP	Temperate Coniferous Forest	Alps conifer and mixed forests
Bajondillo	7	STEP	Temperate broadleaf and mixed forests	Central European mixed forests
Laguna del maar de Fuentillejo	8	COMX	Mediterranean Forests, woodlands and scrubs	Northwest Iberian montane forests
Padul	9	STEP	Mediterranean Forests, woodlands and scrubs	Central Anatolian steppe
Padul-15-05	10	WAMX	Mediterranean Forests, woodlands and scrubs	Iberian sclerophyllous and semi-deciduous forests
Cova di Carhuela	11	STEP	Deserts and xeric shrublands	Azerbaijan shrub desert and steppe
Ifri El Baroud	12	STEP	Mediterranean Forests, woodlands and scrubs	Iberian sclerophyllous and semi-deciduous forests
MD95-2043	13	CLMX	Mediterranean Forests, woodlands and scrubs	Southern Anatolian montane conifer and deciduous forests
San Rafael	14	XERO	Mediterranean Forests, woodlands and scrubs	Tyrrhenian-Adriatic Sclerophyllous and mixed forests
Siles	15	XERO	Mediterranean Forests, woodlands and scrubs	Northwest Iberian montane forests
Torreçilla de Valmadríd	16	STEP	Mediterranean Forests, woodlands and scrubs	Southern Anatolian montane conifer and deciduous forests
Navarres	17	XERO	Mediterranean Forests, woodlands and scrubs	Iberian sclerophyllous and semi-deciduous forests
Navarres	18	STEP	Temperate broadleaf and mixed forests	Pyrenees conifer and mixed forests
Tourbiere de Istarres	19	STEP	Temperate grasslands, savannas and shrublands	Eastern Anatolian montane steppe
Cova de les Malladetes	20	XERO	Mediterranean Forests, woodlands and scrubs	Pyrenees conifer and mixed forests
Lourdes	21	STEP	Temperate broadleaf and mixed forests	Gissaro-Alai open woodlands
Estanya	22	XERO	Temperate broadleaf and mixed forests	Western Siberian hemiboreal forests
Freychinede	23	STEP	Temperate grasslands, savannas and shrublands	Mongolian-Manchurian grassland
Lake Banyoles	24	STEP	Temperate grasslands, savannas and shrublands	Gissaro-Alai open woodlands
Lac du Bouchet B5	25	STEP	Temperate grasslands, savannas and shrublands	Gissaro-Alai open woodlands
MD99-2348-103	26	COMX	Temperate broadleaf and mixed forests	Rodope montane mixed forests
Les Echets G - DIGI	27	STEP	Temperate broadleaf and mixed forests	Western Siberian hemiboreal forests
La Grotte Walou	28	STEP	Temperate broadleaf and mixed forests	Kazakh forest steppe
Bergsee	29	STEP	Temperate broadleaf and mixed forests	Kazakh forest steppe
Garaat El-Ouez	30	STEP	Mediterranean Forests, woodlands and scrubs	Anatolian conifer and deciduous mixed forests
Pian del Lago	31	COMX	Temperate broadleaf and mixed forests	Western European broadleaf forests
Pilsensee	32	TAIG	Tundra	Kola Peninsula tundra
Orgiano	33	COMX	Temperate broadleaf and mixed forests	Western European broadleaf forests
Lago della Costa	34	COMX	Temperate Coniferous Forest	Alps conifer and mixed forests
Lagaccione	35	STEP	Temperate grasslands, savannas and shrublands	Gissaro-Alai open woodlands
Lago Vico	36	STEP	Temperate grasslands, savannas and shrublands	Gissaro-Alai open woodlands
Stracciaccia	37	STEP	Mediterranean Forests, woodlands and scrubs	Western European broadleaf forests
Lago di Monterosi	38	STEP	Temperate grasslands, savannas and shrublands	Northwest Iberian montane forests
Venice	39	XERO	Tundra	Scandinavian Montane Birch forest and grasslands
Azzano Decimo	40	XERO	Temperate broadleaf and mixed forests	Scandinavian Montane Birch forest and grasslands
Valle di Castiglione	41	STEP	Temperate broadleaf and mixed forests	Tian Shan montane steppe and meadows
Travesio	42	XERO	Mediterranean Forests, woodlands and scrubs	Iberian conifer forests
Orvenco	43	TAIG	Temperate broadleaf and mixed forests	Western Siberian hemiboreal forests
Rio Doidis	44	XERO	Mediterranean Forests, woodlands and scrubs	Cyprus Mediterranean forests
Billerio	45	TAIG	Temperate broadleaf and mixed forests	Western Siberian hemiboreal forests
Kersdorf-Briesen	46	TAIG	Temperate broadleaf and mixed forests	Western Siberian hemiboreal forests
Lago Grande di Monticchio	47	STEP	Temperate broadleaf and mixed forests	Tian Shan montane steppe and meadows
Nagymohos Pleistocene	48	STEP	Tundra	Sarmatic mixed forests
Safarka	49	TAIG	Boreal forests / Taiga	Ural montane forests and tundra
Feher-to	50	COMX	Temperate Coniferous Forest	Alps conifer and mixed forests
Ioannina	51	STEP	Temperate broadleaf and mixed forests	Central European mixed forests
Kokad	52	STEP	Temperate broadleaf and mixed forests	East European forest steppe
Lake Xinias	53	STEP	Temperate broadleaf and mixed forests	Western European broadleaf forests
Mickunai	54	COCO	Tundra	Scandinavian Montane Birch forest and grasslands
Lake Sfanta Anna	55	COMX	Temperate Coniferous Forest	Alps conifer and mixed forests
Lesvos ML01 Megali Limni	56	STEP	Temperate broadleaf and mixed forests	Rodope montane mixed forests
Straldzha	57	STEP	Temperate broadleaf and mixed forests	Aegean and Western Turkey sclerophyllous and mixed forests
MD01-2430	58	STEP	Temperate broadleaf and mixed forests	Euxine-Colchic broadleaf forests
Lake Iznik	59	STEP	Temperate broadleaf and mixed forests	Tian Shan montane steppe and meadows
M72/5 628-1	60	STEP	Deserts and xeric shrublands	Azerbaijan shrub desert and steppe
Dziguta Core 1	61	CLMX	Temperate broadleaf and mixed forests	Northeastern Spain and Southern France Mediterranean forests
Lake Van LG	62	STEP	Mediterranean Forests, woodlands and scrubs	Aegean and Western Turkey sclerophyllous and mixed forests
Lake Zeribar	63	STEP	Temperate grasslands, savannas and shrublands	Pontic steppe

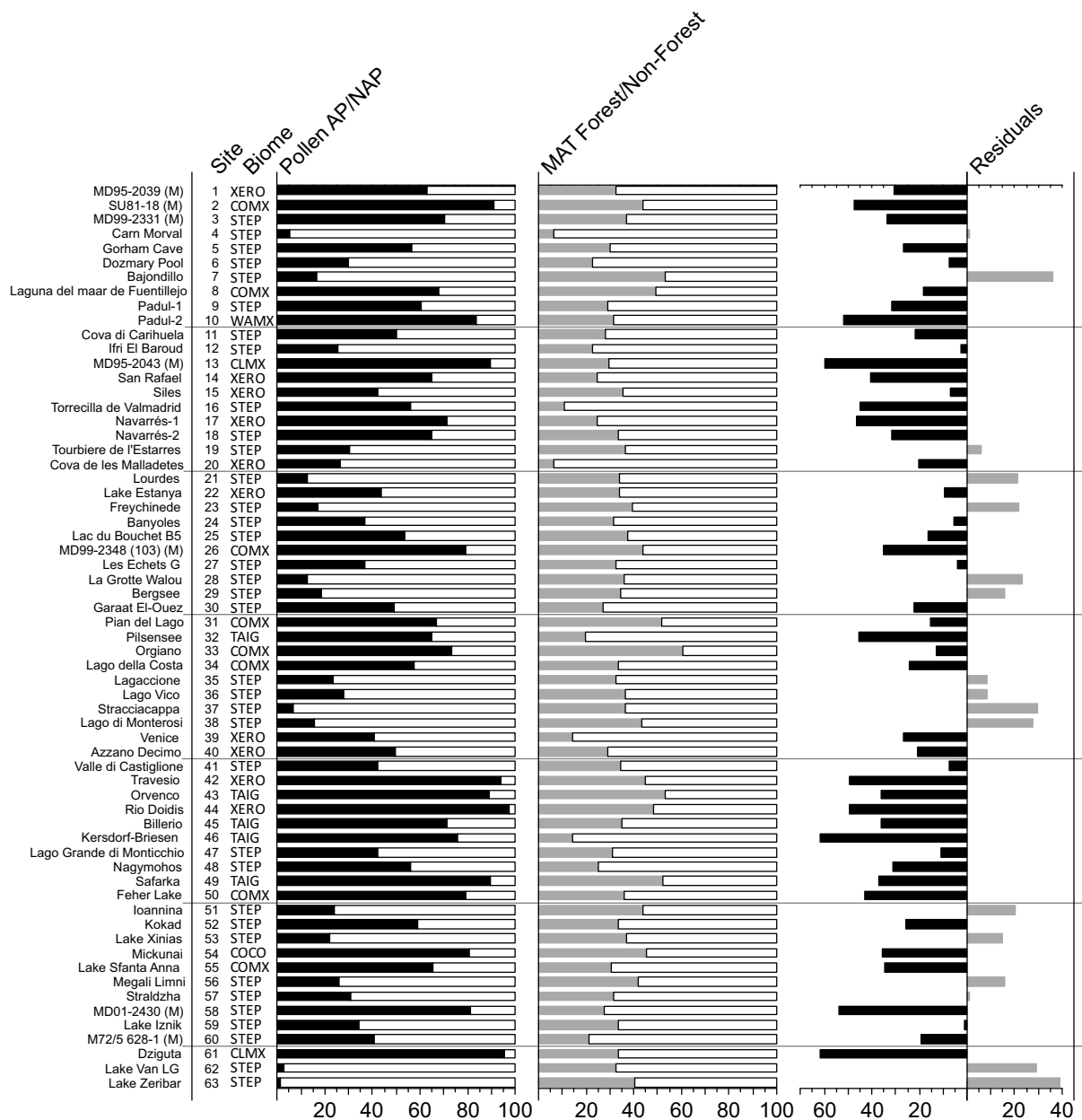
Notes: Modern analogue Biomes and Ecoregions were calculated as the most commonly occurring amongst all 6 best modern analogue pollen samples in all LGM samples for each pollen site/record. These are taken from the EMPD2 (Davis et al 2020), using the classification of Olsen et al 2001.

2331  
2332  
2333  
2334  
2335  
2336  
2337  
2338

**Table A6.** The biome and ecoregion of the modern surface samples used as analogues in the pollen-climate reconstructions.

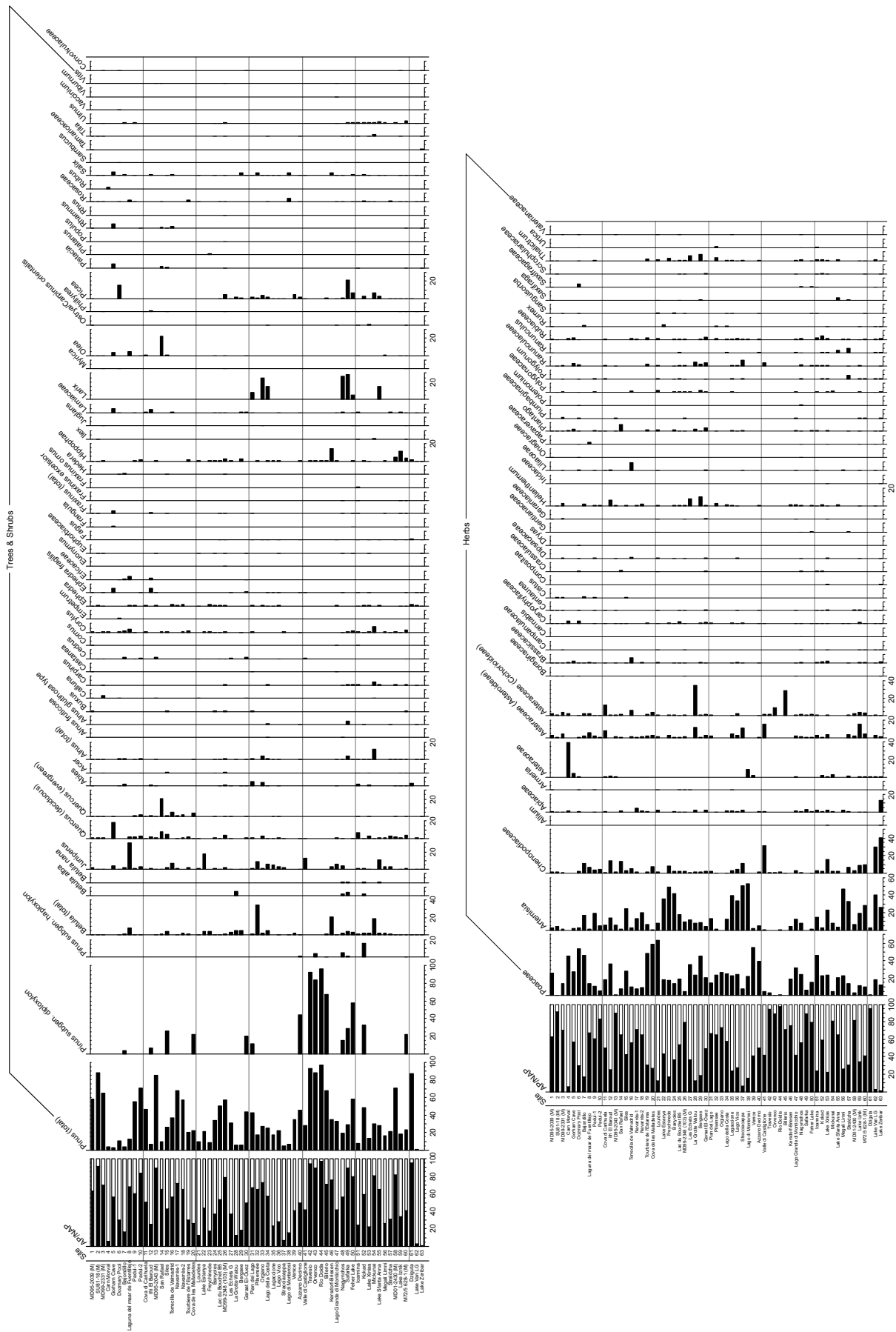
2339  
 2340  
 2341  
 2342  
 2343

**Figures**



2344  
 2345  
 2346  
 2347  
 2348

Figure A1. Pollen biomes (see figure 2 for key), Arboreal Pollen (AP) % forest cover, MAT % forest cover and residuals (AP % compared to MAT Forest %)

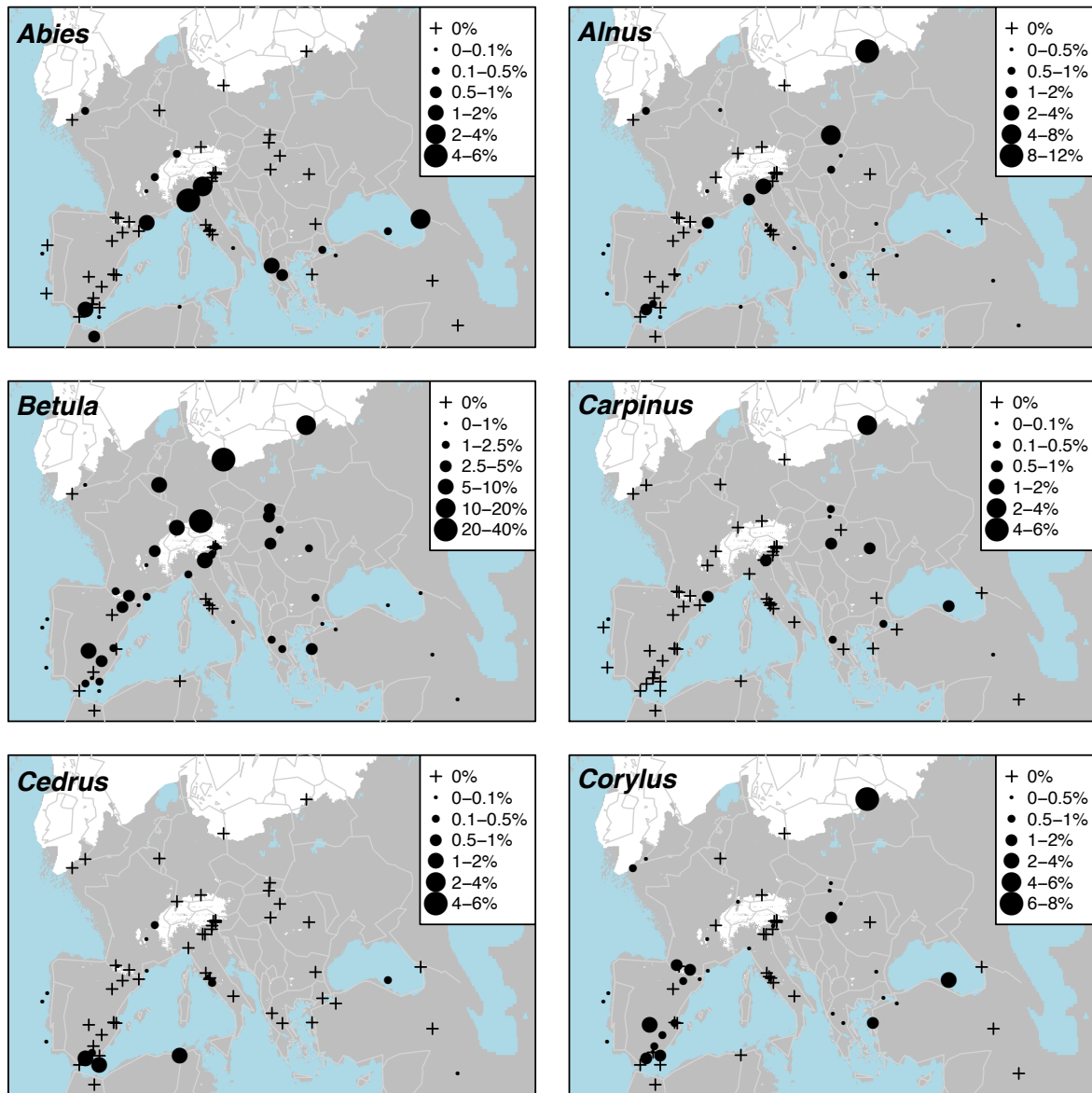


2349  
2350

Figure A2. Pollen taxa percentages for all LGM sites/records

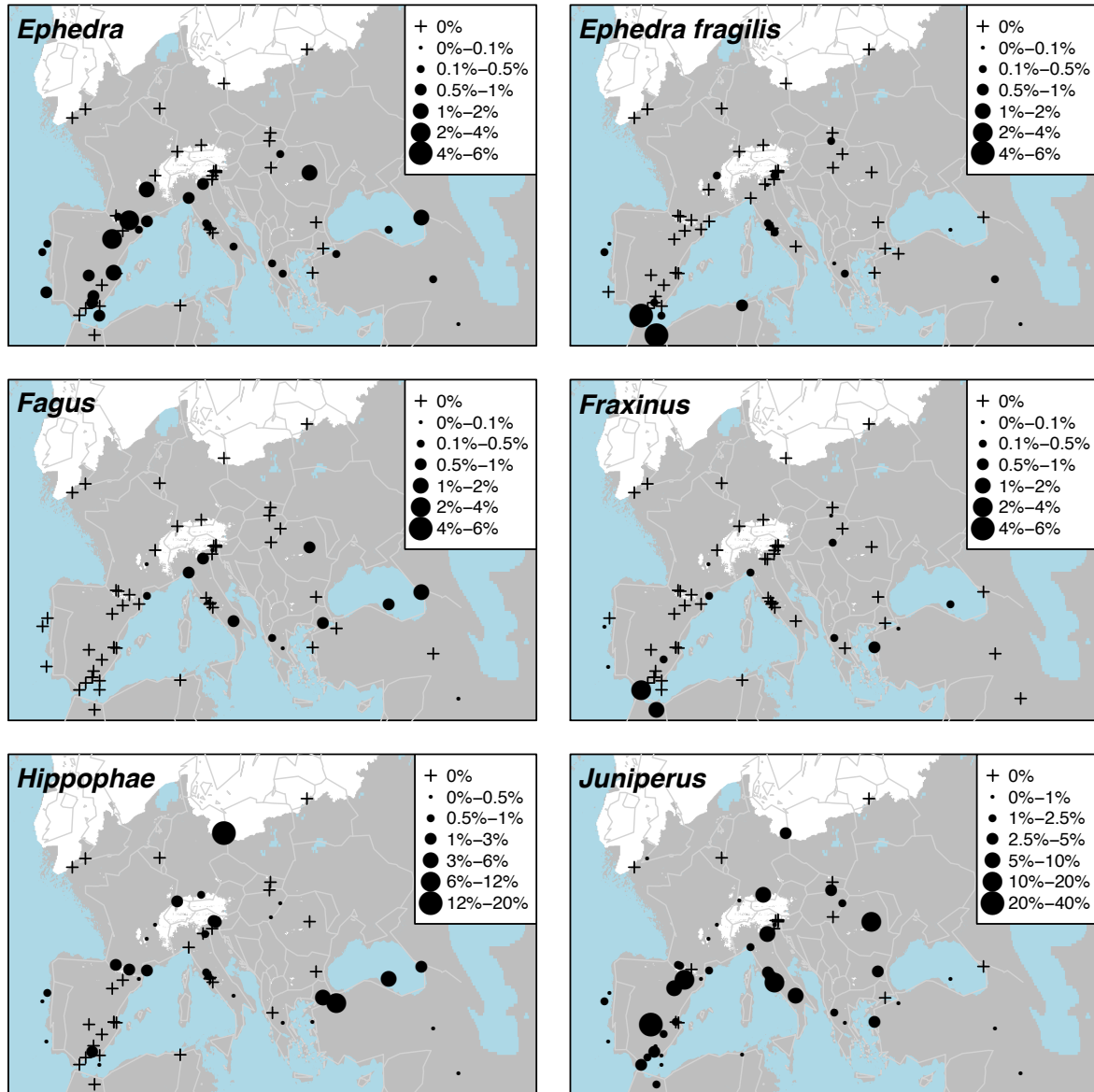


2351  
2352  
2353  
2354



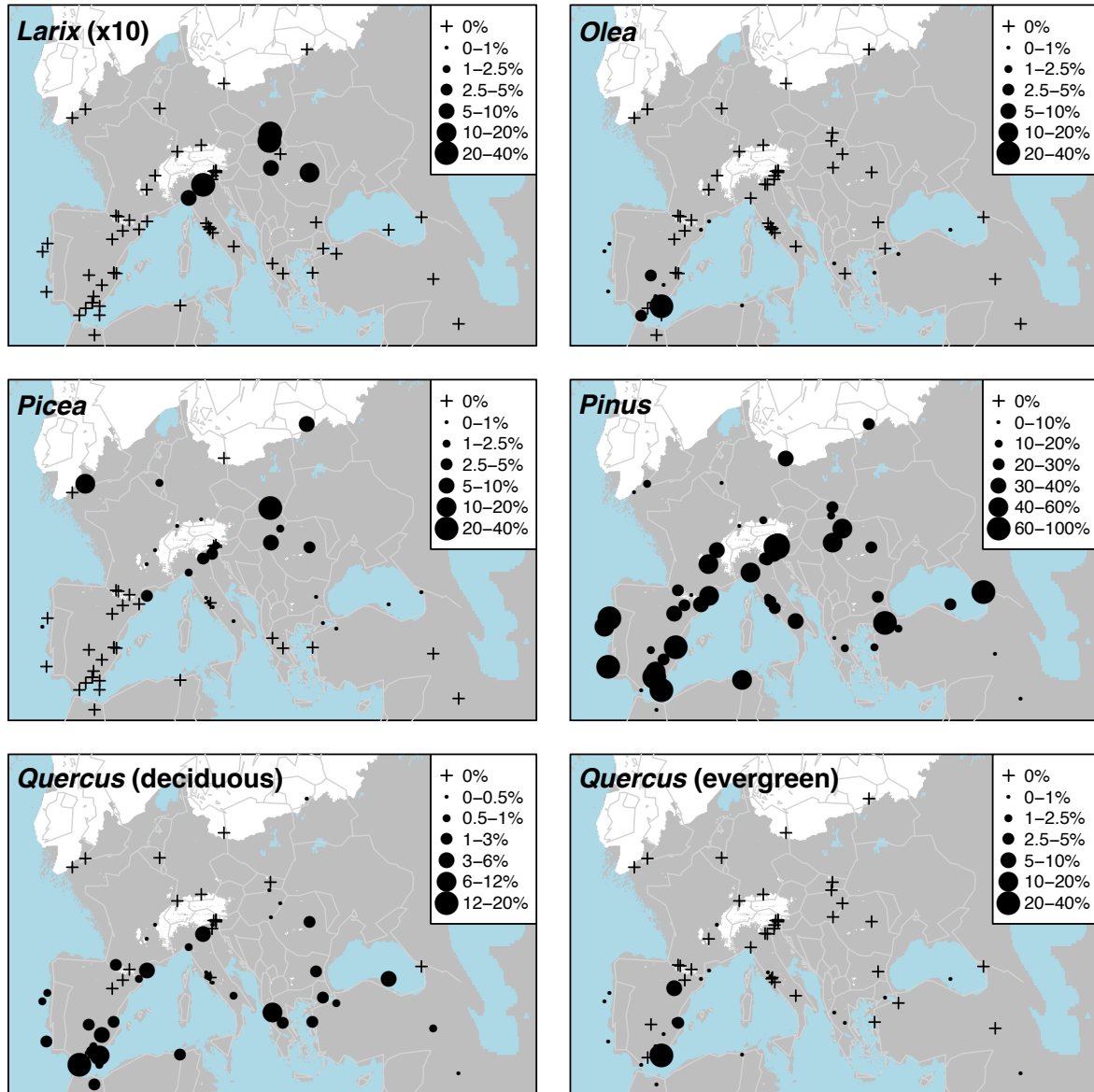
2355  
2356  
2357  
2358

Figure A3a. Percentage maps of *Abies*, *Alnus*, *Betula*, *CarPinus*, *Cedrus* and *Corylus*



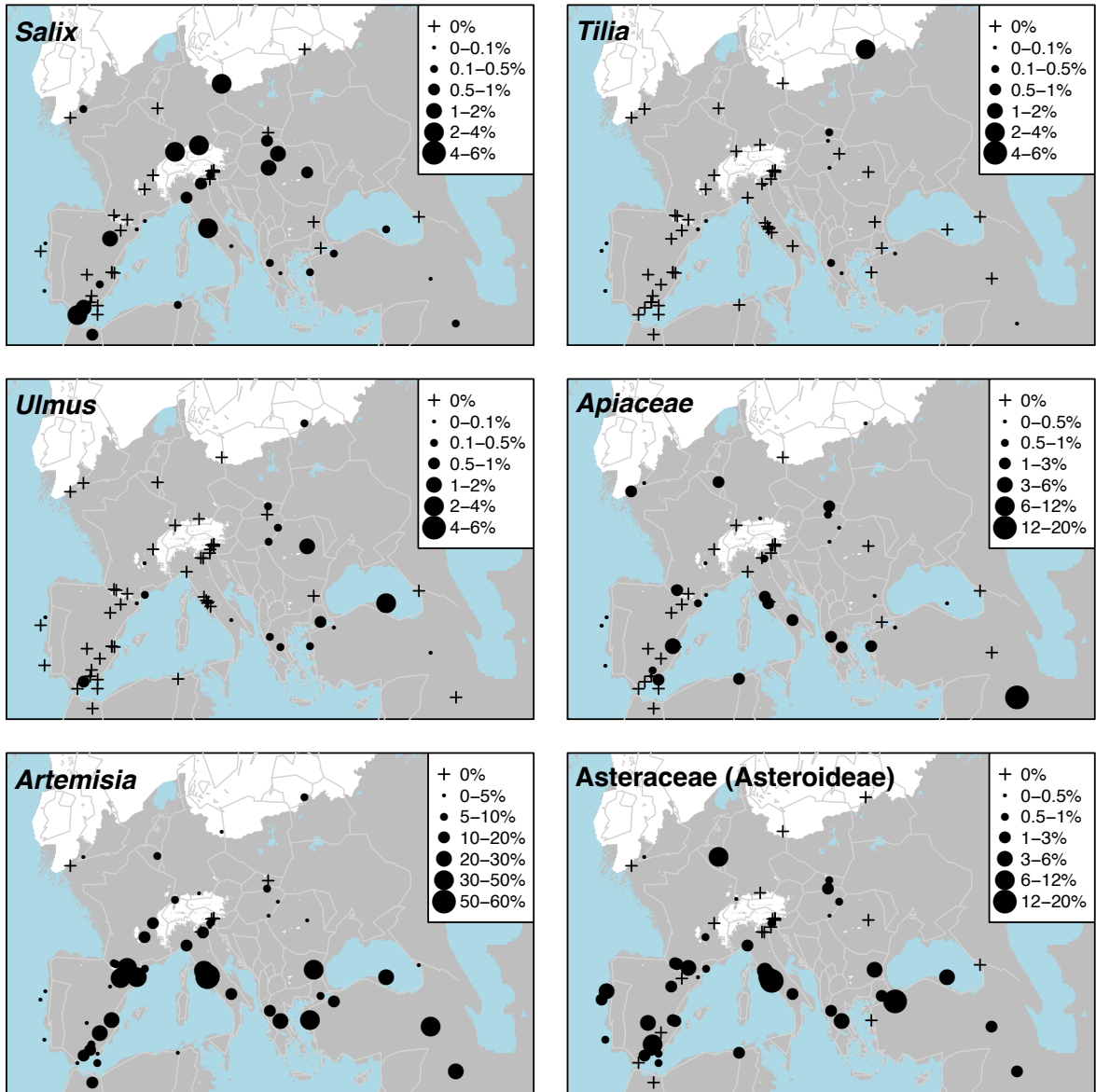
2359  
 2360  
 2361  
 2362  
 2363

Figure A3b. Percentage maps of *Ephedra*, *Ephedra fragilis*, *Fagus*, *Fraxinus*, *Hippophae* and *Juniperus*



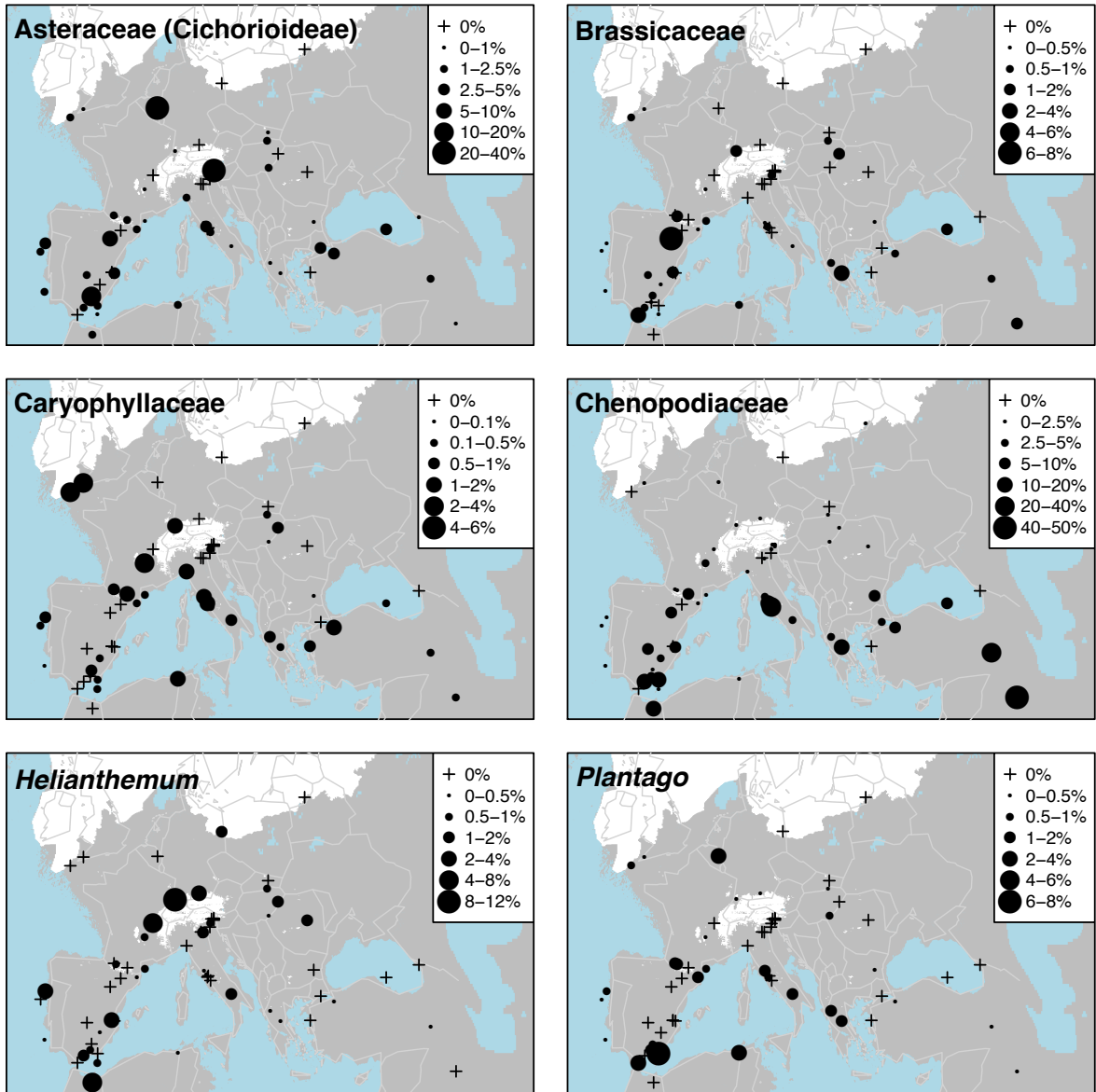
2364  
 2365  
 2366  
 2367  
 2368

Figure A3c. Percentage maps of *Larix* (x10 exaggeration), *Olea*, *Picea*, *Pinus*, *Quercus* (deciduous) and *Quercus* (evergreen)



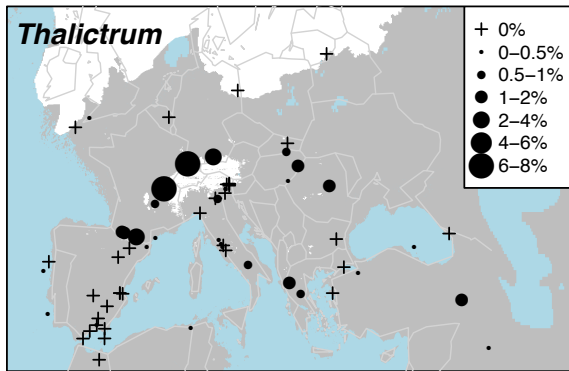
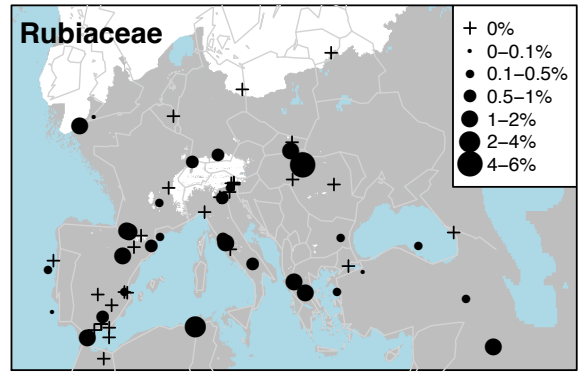
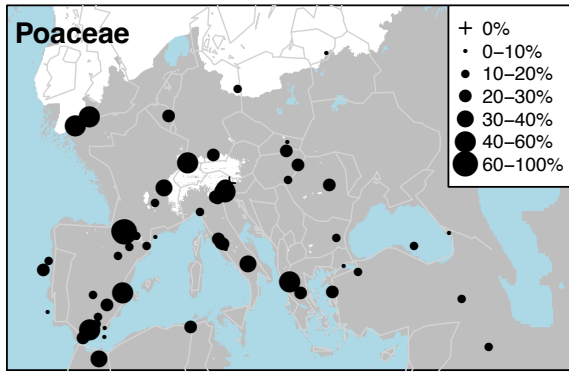
2369  
 2370  
 2371  
 2372

Figure A3d. Percentage maps of *Salix*, *Tilia*, *Ulmus*, *Apiaceae*, *Artemisia* and *Asteraceae* (*Asteroideae*)



2373  
 2374  
 2375  
 2376  
 2377

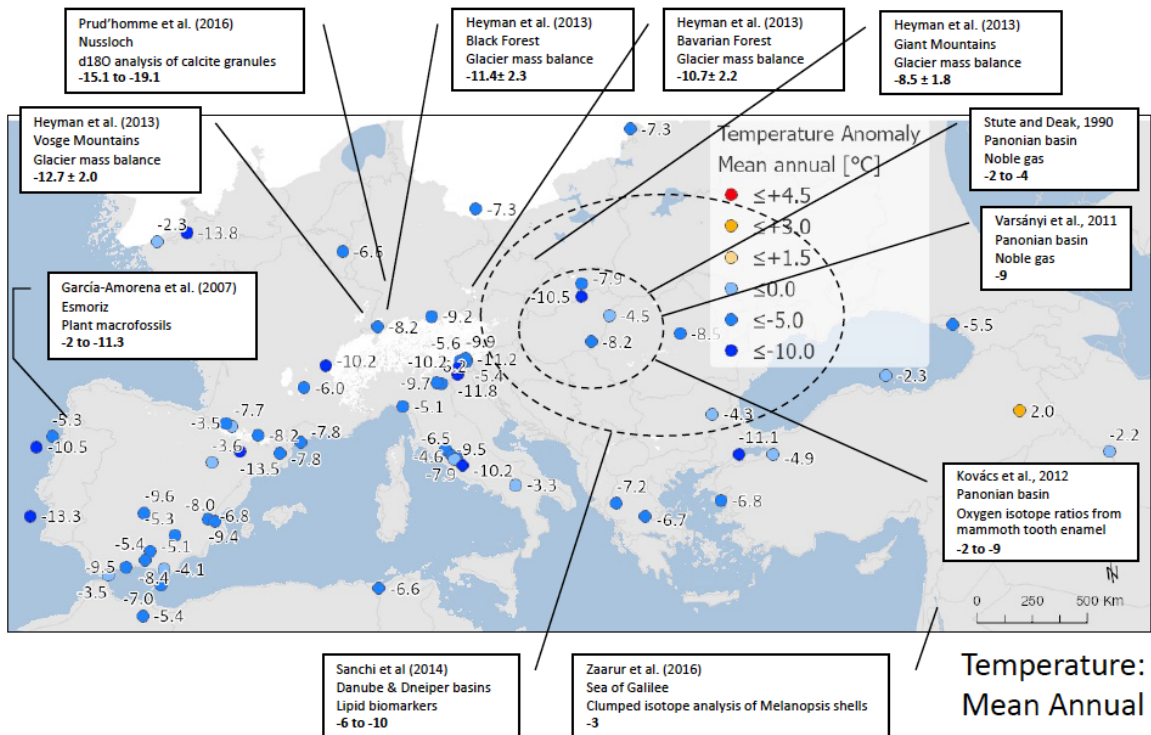
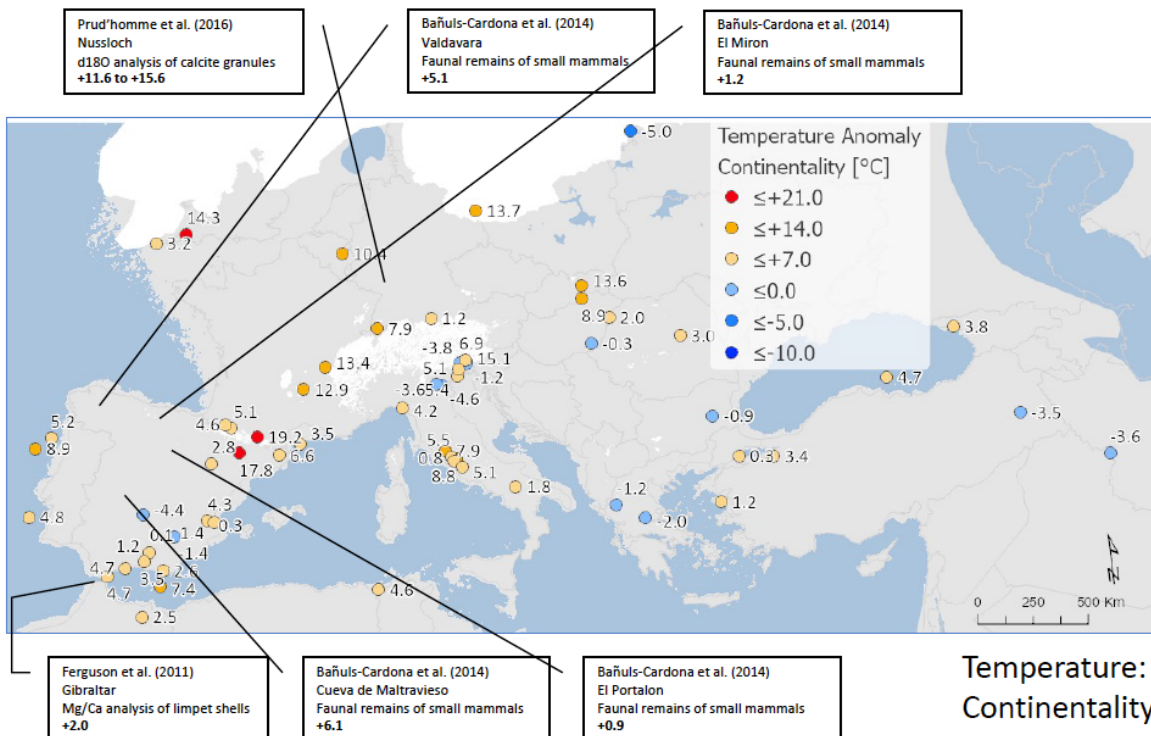
Figure A3e. Percentage maps of Asteraceae (Cichorioideae), Brassicaceae, Caryophyllaceae, Chenopodiaceae, Helianthemum and *Plantago*

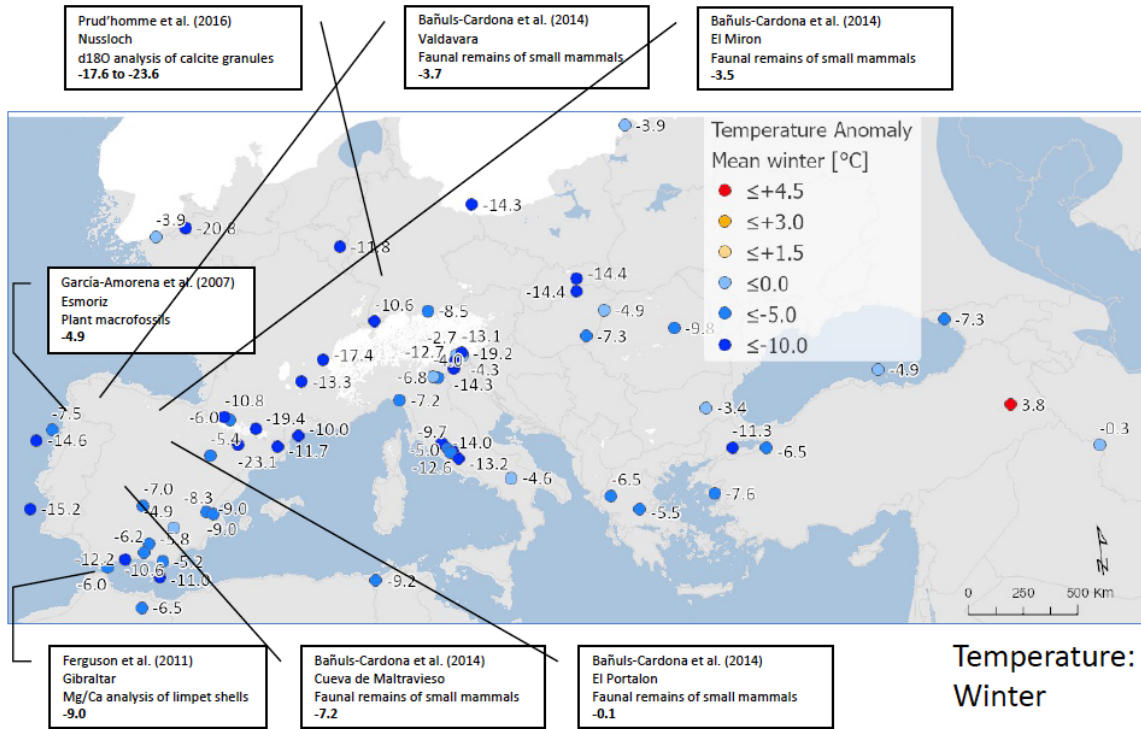


2378  
 2379  
 2380  
 2381  
 2382  
 2383  
 2384  
 2385  
 2386

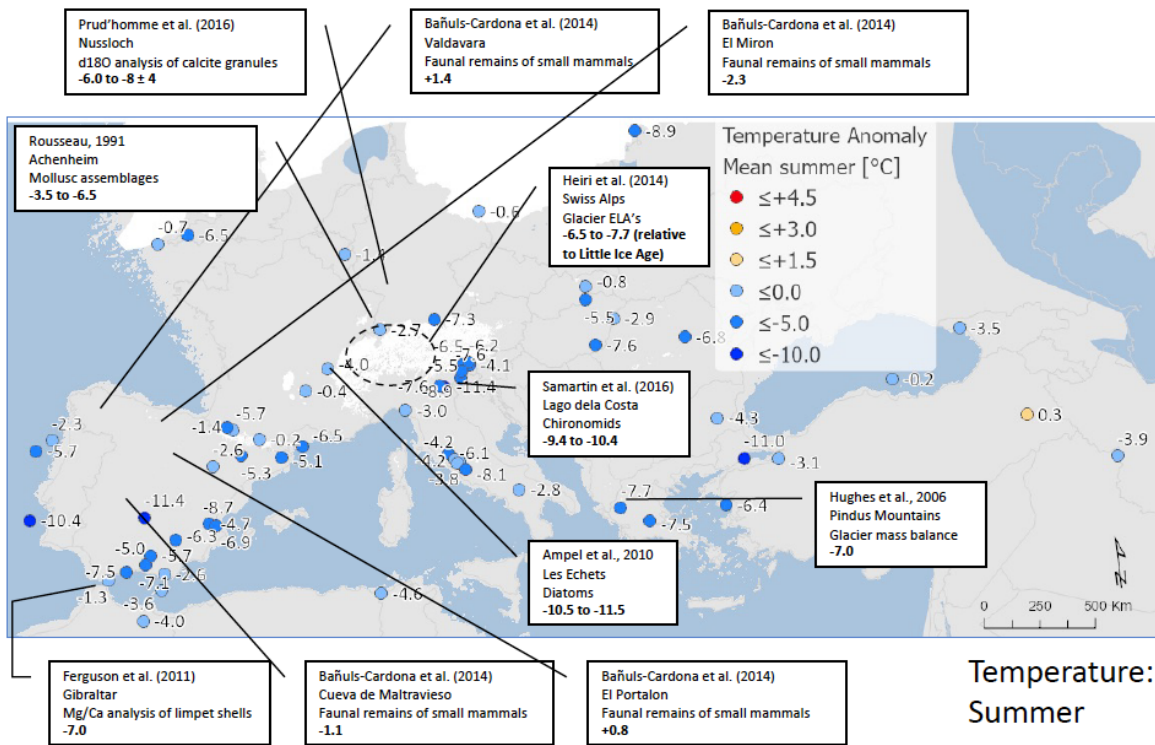
Figure A3f. Percentage maps of Poaceae, Rubiaceae and *Thalictrum*







Temperature:  
Winter



Temperature:  
Summer

2393  
2394

2395  
2396

2397 Figure A4. Maps of pollen-based MAT reconstructions for LGM annual, winter and summer  
2398 temperature anomalies (as shown in figure 10), shown together with the results of other  
2399 published studies. Continentality represents the difference in temperature between summer  
2400 and winter, with positive anomalies indicating an increase in the temperature difference  
2401 between summer and winter. All values are expressed as anomalies compared with the  
2402 present day unless otherwise indicated.





2410  
2411